UNIVERSITÀ
DI TORINO

UNIVERSITY OF TURIN

Department of Molecular Biotechnology and Health Sciences

Doctoral School in Molecular Medicine – XXXIV cycle

PhD Thesis

Untangling the immune suppressive network to accelerate the roadmap for a cure in human myeloma

PhD candidate: Claudia Giannotta

Supervisor: Prof. Massimo Massaia

Academic year 2022/2023

Index

Overview

Multiple Myeloma (MM) is a paradigm disease in which genetic/epigenetic alterations of myeloma cells and alterations in the tumor microenvironment (TME) are mutually supportive to promote the disease progression leading to devastating clinical consequences.

Myeloma cells originate from antigen-experienced B cells that take advantage of a time-limited and unique opportunity to operate DNA rearrangements during differentiation in the secondary lymphoid organs. This opportunity can occasionally results in genetic alterations conferring proliferative and survival advantages when these germinal center or post-germinal-center B cells settle down in the bone marrow (BM) (1). The BM is a very sophisticated ecosystem which is physiologically organized to accommodate approximately 5-10% of polyclonal plasma cells. When the BM is colonized by a limited number of genetically altered plasma cells, it can still handle a harmless cohabitation for many years (or even lifetime) as attested by the great majority of monoclonal gammopathy of undetermined significance (MGUS) that never progress to MM. Interestingly, plasma cells isolated from MGUS individuals already harbor many of the genetic and epigenetic alterations found in MM patients, indicating that tumor-extrinsic factors play a critical role in keeping clonal plasma cells under control (2,3). When the BM plasma cell infiltration exceeds 10%, the BM ecosystem becomes dysfunctional with a series of negative chain reactions involving bystander cells, including osteoclasts (OC), osteoblasts (OB), endothelial cells (EC), stromal cells (BMSC), and immune cells. The result is a progressive TME switch from tumor-inimical to tumor-permissive, tumor-friendly, and protumor conditions (4). This switch is orchestrated by myeloma cells which establish an intensive cross-talk mediated by soluble factors and cell-to-cell interactions to re-educate bystander cells to support tumor progression, drug resistance and immune evasion (5). One major mechanism to promote immune escape is the highly redundant expression of multiple immune checkpoints/immune checkpoint- ligands (ICP/ICP-L) that allows myeloma cells to hinder mechanisms of physiological regulation and to hamper antitumor immune responses in the TME. Immune dysfunctions are also induced by the TME metabolic reset and the different capacity of myeloma cells, immune suppressor cells, and immune effector cells to compete for nutrients, resist to hypoxia, and face other energetic challenges. The high metabolic demand of myeloma cells is fueled by aerobic glycolysis, and the increased utilization of amino acids. The prosurvival changes in myeloma cells are detrimental to the metabolic requirements of immune effector cells (6) which are further penalized by the progressive accumulation of suppressive metabolites in the TME. Thus, the ICP/ICP-L circuitry and metabolic checkpoints jointly operate in the TME to produce early and persistent impairment of immune effector cells like conventional T cells, NK cells and γδ T cells.

Based on these data, it is clear that targeting myeloma cells only with conventional treatments is not sufficient to go back to the initial antitumor TME immune contexture and reinstate the best conditions to eradicate the disease or to prevent the regrowth of residual myeloma cells. The clinical results obtained by immunomodulatory drugs (IMiDs) like thalidomide, lenalidomide, and pomalidomie have confirmed the importance to target the immune system as anticipated by the clinical results of allo-transplanted MM patients (7) and patients treated with idiotype vaccines (8).

More recently, the discovery of ICP and other mechanisms of immune suppression and/or immune escape have paved the way to the development of more effective immune-based interventions, from passive immunotherapy with monoclonal antibodies (mAb) to Chimeric Antigen Receptor (CAR)-T cells. Anti-CD38 mAb have significantly improved the clinical outcome of newly diagnosed or relapsed/refractory MM after incorporating in drug combinations with IMiDs or proteasome inhibitors (PI). However, even patients treated with triple-drug combinations continue to experience disease relapse, sometimes after a very prolonged period of disease-free survival times (DFS).

Therapeutic resistance is defined as primary in patients who never respond and acquired in patients who relapse after an initial response. Both primary and acquired resistance are dependent on tumor-intrinsic and extrinsic factors (9).

The TME is a critical player of therapeutic resistance (10,11), but its immune and metabolic alterations represent a target opportunity for immune-based interventions.

The present dissertation is aimed at providing a mechanistic insight into immune suppressive network operating in MM patients and to deepen our understanding of how immunotherapeutic approaches such as ICP inhibitors (ICP-I) and CD38-targeted therapy can be exploited to recover anti-myeloma immune responses and develop individually tailored immune interventions.

In the first study, we have used Vγ9Vδ2 T cells as investigative tools to decipher the immune suppressive TME network in MM. Vγ9Vδ2 T cells resent very early of immune suppressive commitment of the TME and combine phenotypic and functional alterations not fully rescued by single PD-1 blockade, reflecting the disappointing results of ICP-I in MM. Our data indicate that single or multiple anti-ICP treatment should take into account the disease status to overcome (diagnosis, remission) or mitigate (relapse) the immune suppression operated by the ICP/ICP-L network on BM MM Vγ9Vδ2 T cells.

The second work extensively reviews the pros and cons of Vγ9Vδ2 T cells as therapeutic immune effector cells in hematological cancers. Intriguingly, Vγ9Vδ2 T cells have unique antitumor properties, but therapeutic applications in cancer immunotherapy have so far failed to meet clinical expectations. (12). However, the great advances in the knowledge of immune escape mechanisms,

molecular biology and genetic engineering has opened new perspectives including the possibility to build on Vγ9Vδ2 T cells autologous or allogenic immune-based interventions.

The third work reports the short- and long-term effects of Daratumumab (Dara) treatment in CD38+ immune cells in the peripheral blood (PB) and BM of relapsed/refractory MM patients (RRMM) enrolled in the NCT03848676 study. Significant changes have been observed during the first 3-6 months of treatment and up to 4 years of follow-up. Some baseline immune features related to CD38 expression have been correlated with the clinical outcome. Further analyses and clinical correlations are ongoing with myeloma cell genetic alterations to strengthen the prognostic significance of tumor cell/TME interactions in MM.

The fourth work is a comprehensive overview about the role played by myeloid-derived suppressor cells (MDSC) in the establishment of immune suppressive TME contexture in MM patients and possible therapeutic applications targeting these cells.

Bibliography

1. Johnsen HE, Bøgsted M, Schmitz A, Bødker JS, El-Galaly TC, Johansen P, et al. The myeloma stem cell concept, revisited: From phenomenology to operational terms. *Haematologica* (2016) 101:1451–1459. doi: 10.3324/haematol.2015.138826

2. Bailur JK, McCachren SS, Doxie DB, Shrestha M, Pendleton K, Nooka AK, et al. Early alterations in stem-like/marrow-resident T cells and innate and myeloid cells in preneoplastic gammopathy. *JCI Insight* (2019) 4: doi: 10.1172/jci.insight.127807

3. Zavidij O, Haradhvala NJ, Mouhieddine TH, Sklavenitis-Pistofidis R, Cai S, Reidy M, et al. Single-cell RNA sequencing reveals compromised immune microenvironment in precursor stages of multiple myeloma. *Nat Cancer* (2020) 1:493–506. doi: 10.1038/s43018-020-0053-3

4. Leone P, Solimando AG, Malerba E, Fasano R, Buonavoglia A, Pappagallo F, et al. Actors on the scene: Immune cells in the myeloma niche. *Front Oncol* (2020) 10:1–15. doi: 10.3389/fonc.2020.599098

5. Holthof LC, Mutis T. Challenges for immunotherapy in multiple myeloma: Bone marrow microenvironment-mediated immune suppression and immune resistance. *Cancers (Basel)* (2020) 12: doi: 10.3390/cancers12040988

6. Castella B, Riganti C, Massaia M. Metabolic approaches to rescue antitumor Vγ9Vδ2 T-cell functions in myeloma. *Frontiers in Bioscience - Landmark* (2020) 25:69–105. doi: 10.2741/4795

7. Rosenblatt J, Avigan D. Role of immune therapies for myeloma. *JNCCN Journal of the National Comprehensive Cancer Network* (2015) 13:1440–1447. doi: 10.6004/jnccn.2015.0168

8. Massaia M, Borrione P, Battaglio S, Mariani S, Beggiato E, Napoli P, et al. Idiotype Vaccination in Human Myeloma: Generation of Tumor-Specific Immune Responses After High-Dose Chemotherapy. *Blood* (1999) 94:673–683. doi: 10.1182/blood.v94.2.673

9. Padmanee Sharma, Siwen Hu-Lieskovan, Jennifer A. Wargo AR. Primary, Adaptive, and Acquired Resistance to Cancer Immunotherapy. *Cell* (2017)707–723.

10. Encinas J, Castellano E. The Role of Tumor Microenvironment in Multiple Myeloma. *Cancers (Basel)* (2021)1–22.

11. Solimando AG, Malerba E, Leone P, Prete M, Terragna C, Cavo M, et al. Drug resistance in multiple myeloma: Soldiers and weapons in the bone marrow niche. *Front Oncol* (2022) 12: doi: 10.3389/fonc.2022.973836

12. Saura-Esteller J, de Jong M, King LA, Ensing E, Winograd B, de Gruijl TD, et al. Gamma Delta T-Cell Based Cancer Immunotherapy: Past-Present-Future. *Front Immunol* (2022) 13: doi: 10.3389/fimmu.2022.915837

Immune dysfunctions affecting bone marrow Vγ9Vδ2 T cells in multiple myeloma: role of immune and metabolic checkpoints

ABSTRACT

Bone marrow (BM) Vγ9Vδ2 T cells are intrinsically predisposed to sense the immune fitness of the tumor microenvironment (TME) in multiple myeloma (MM) and monoclonal gammopathy of undetermined significance (MGUS). In this work, we have used BM Vγ9Vδ2 T cells to interrogate the role of the immune checkpoint/immune checkpoint-ligand (ICP/ICP-L) network in the TME immune suppressive contexture of MM patients. PD-1+ BM MM Vγ9Vδ2 T cells combine phenotypic, functional, and TCR-associated alterations consistent with chronic exhaustion and immune senescence. When challenged by zoledronic acid (ZA) as a surrogate assay to interrogate the reactivity to their natural ligands, BM MM Vγ9Vδ2 T cells further up-regulate PD-1 and TIM-3 and worsen TCR-associated alterations. BM MM Vγ9Vδ2 T cells up-regulate TIM-3 after stimulation with ZA in combination with anti-PD-1, whereas PD-1 is not up-regulated after ZA stimulation with anti-TIM-3, indicating a hierarchical regulation of inducible ICP expression. Dual anti-PD-1/anti-TIM-3 blockade improves the immune functions of BM Vγ9Vδ2 T cells in MM at diagnosis (MM-dia), whereas single PD-1 blockade is sufficient to rescue BM Vγ9Vδ2 T cells in MM in remission (MM-rem). By contrast, ZA stimulation induces LAG-3 up-regulation in BM Vγ9Vδ2 T cells from MM in relapse (MM-rel) and dual PD-1/LAG-3 blockade is the most effective combination in this setting. These data indicate that: 1) inappropriate immune interventions can exacerbate Vγ9Vδ2 T-cell dysfunction 2) ICP blockade should be tailored to the disease status to get the most of its beneficial effect.

GRAPHICAL ABSTRACT

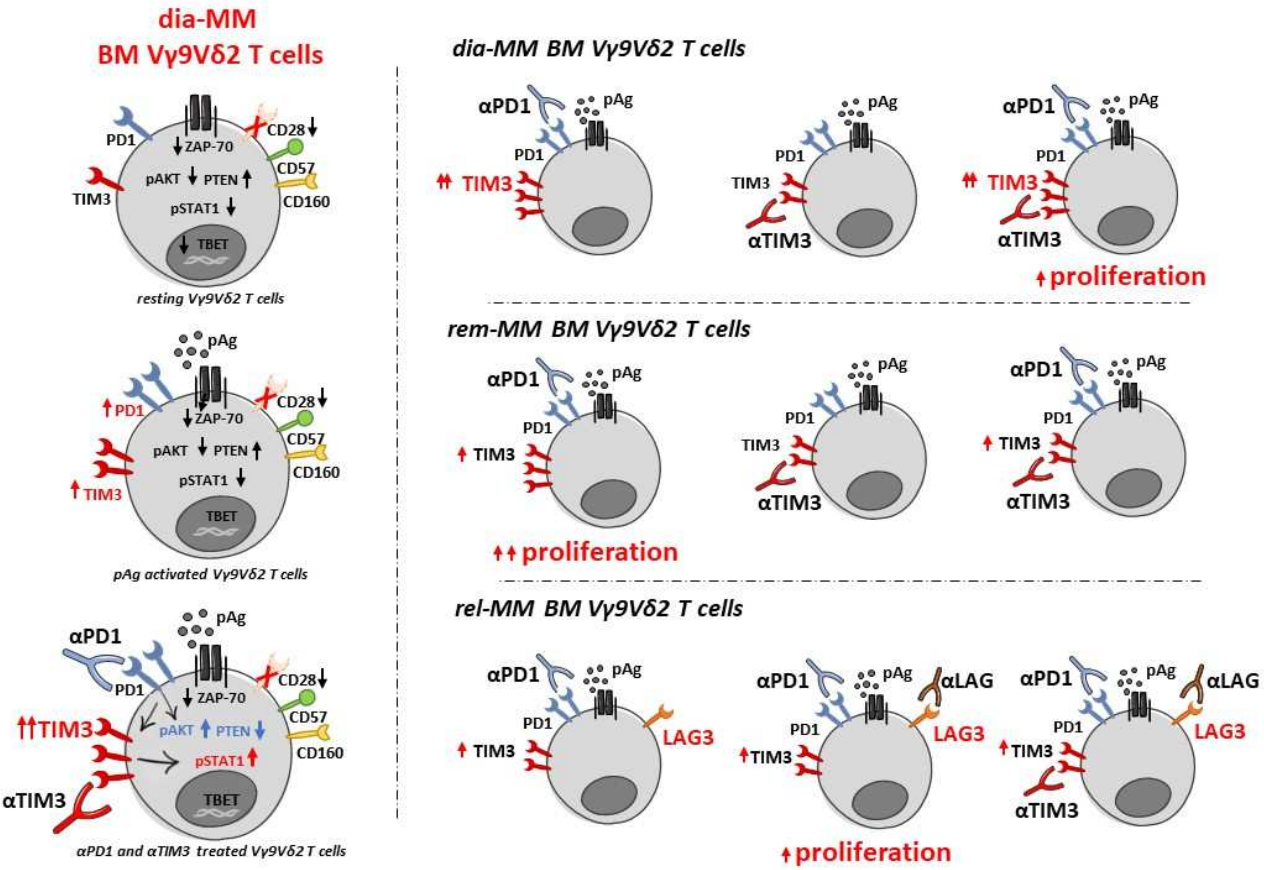

Decoding the bone marrow immune checkpoint network in multiple myeloma with Vγ9Vδ2 T cells. Bone marrow Vγ9Vδ2 T cells combine phenotypic, functional, and TCR-associated alterations consistent with chronic exhaustion and immune senescence. Tailoring immune checkpoint blockade to the disease status partially mitigates resistance to single PD1 blockade and could improve efficacy of ICP-inhibitors.

INTRODUCTION

The discovery of immune checkpoints (ICP) and their role as therapeutic targets has revitalized immunotherapy in cancer (1). However, clinical results have been discontinuous with major achievements in some diseases and negligible or disappointing results in others (2–5). Both primary and acquired resistance have been reported to hamper the efficacy of ICP blockade, but the underlying mechanisms have only partially been elucidated. Multiple myeloma (MM) is a paradigm disease in which the immune system and the tumor microenvironment (TME) play a major role in the disease progression (6–8). Several phenotypic and functional alterations have been reported in innate and adaptive immune effector cells, including the expression of ICP/ICP ligands in myeloma cells and bystander cells in the TME (9–11). Despite these favourable premises, single anti-PD-1 treatment has fallen short of clinical expectations in MM, whereas clinical studies of anti-PD-1 in combination with immunomodulatory drugs (IMiDs) have been terminated ahead of time because of unexpected toxicity in the experimental arm. These unsuccessfully immune interventions have led to the premature termination of alternative studies targeting the ICP/ICP-L network and generated some reluctance in further pursuing this approach due to the complexity of the tumor-host interactions in MM (12).

Vγ9Vδ2 T cells from the bone marrow (BM) are excellent tools to monitor the immune suppressive commitment and decode the ICP/ICP-L network in MM patients (13). Vγ9Vδ2 T cells are non-conventional T cells half-way between adaptive and innate immunity resenting early of immune suppressive commitment of TME. These cells have a leading role in immune surveillance and share many qualities with both αβ T cells and NK cells, as suggested by Vγ9 T cell gene signature that overlaps those from both αβ cells and NK cells (14). High-throughput single-cell RNA sequencing analysis deepened these data by revealing that Vδ2 T lymphocytes mapped next to the mature CD8 T cells, whereas the Vδ1 T lymphocytes were closer to the NK cells (15).

Vγ9Vδ2 T cells are activated via HLA-indipendent and TCR mediated system by phosphoantigens (pAgs) generated in the mevalonate (Mev) pathway (16), whose dysregulation has been reported in many types of cancer cells (17). Moreover, Vγ9Vδ2 T cells are endowed with a wide array of receptors though which they recognize stress- inducible MHC class-I-related molecules (16). Isopentenyl pyrophosphate (IPP) is the prototypic Mev metabolite recognized by Vγ9Vδ2 T cells via the combination of two immunoglobulin superfamily members, butyrophilin 2A1 (BTN2A1) and BTN3A1. The former directly binds the Vγ9+ domain of the T cell receptor (TCR), whereas the latter binds the Vδ2 and γ-chain regions on the opposite side of the TCR (18–21). By sensing homeostatic alterations of cancer cells, Vγ9Vδ2 T cells are activated and exert a broad variety of anti-tumor

effector functions i.e., TNFα and IFNγ production and cytotoxic activity (22,23). In addition, Vγ9Vδ2 T cells can orchestrate immune responses by behaving as professional antigen-presenting cells, by collaborating with B cells to produce antibodies and by inducing DC maturation and consequent boost of αβ T cell priming and MHC-restricted antigen-specific T-cell responses (24). Multifaceted array of direct and indirect anti-tumor functions is summarized in Image 1 (23).

Vγ9Vδ2 T cell reactivity to pAg can be evaluated *in vitro* using synthetic compounds, such as bromohydrin pyrophosphate (BrHPP), monoethyl pyrophosphate (EtPP) and 2-methyl-3-butenyl-1-pyrophosphate (2M3B1-PP), or through indirect stimulation with aminobiphosphonates (NBP). Zoledronic acid (ZA), modulating pAg intracellular levels in tumor cells, monocytes and dendritic cells, boosts pAg-release via ATP-binding cassette transporter A1 (ABCA1), a plasma-membrane associated transporter involved in efflux of cholesterol and phospholipids, and the consequent activation of Vγ9Vδ2 T lymphocytes (25,26).

Vγ9Vδ2 T cells recognize and kill a variety of solid tumor and leukemia and lymphoma cells, although tumor cells of B cell origin are mostly immunogenic to activate unprimed Vγ9Vδ2 T cells (16). Lipid metabolism reprogramming through Mev-pathway dysregulation together with the expression of stress-induced proteins make myeloma cells privileged target of Vγ9Vδ2 T cells *in vitro*. However, by interrogating the reactivity of BM MM Vγ9Vδ2 T cells to IPP generated by monocytes or dendritic cells (DC) after stimulation with ZA, we have revealed a very early and long-lasting dysfunction of BM Vγ9Vδ2 T cells which is already detectable in monoclonal gammopathy of undetermined significance (MGUS) and not fully reverted in clinical remission after autologous stem cell transplantation (9). Multiple cell subsets [myeloma cells, myeloid-derived suppressor cells (MDSC), regulatory T cells (Tregs), BM-derived stromal cells (BMSC)] are involved in Vγ9Vδ2 T-cell inhibition via several immune suppressive mechanisms including PD-1/PD-L1 expression (9,10). Previous work from our lab has shown that single PD-1 blockade improved ZA-induced proliferation of BM MM Vγ9Vδ2 T cells from MM at diagnosis (MM-dia). PD-1 blockade also increased CD107 expression suggesting improved effector functions, but both proliferation and CD107 expression remained far from standard values observed in BM Vγ9Vδ2 T cells from controls (Ctrl) (9).

Recently, it has been reported that the expression of additional ICP on immune effector cells can be involved in acquired resistance to single ICP blockade. PD-1 and TIM-3 co-expression has been reported in conventional T cells from patients with solid cancers (27–30), acute myeloid leukemia (AML) (31), and MM (32–34). PD-1 and TIM-3 co-expression has also been reported in Vγ9Vδ2 T cells chronically exposed to infectious agents (35) or cancer cells in solid (36,37) and blood tumors (38). Exhaustion and senescence are other T-cell dysfunctions which can potentially contribute to resistance to ICP blockade (39–42).

The aim of this work was to investigate the contribution of ICP expression, exhaustion, and senescence to the immune dysfunction of BM Vγ9Vδ2 T cells and to envisage possible interventions, correlated with the disease status, to overcome the immune suppressive commitment operated by the ICP/ICP-L network in the TME of MM patients.

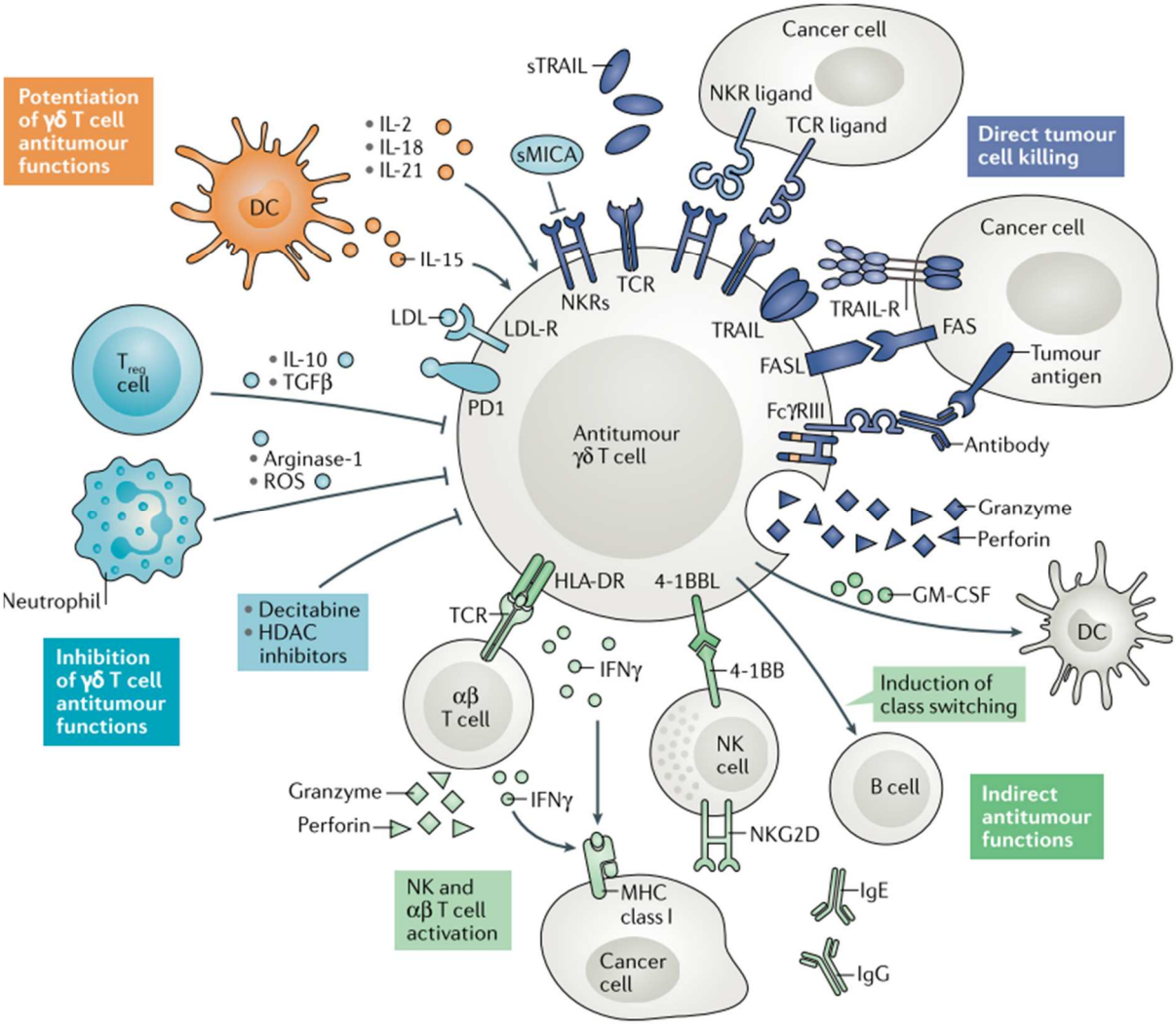

Image 1 Antitumour γδ T cell functions and their regulation. *B. Silva-Santos et al., Nature Reviews Cancer 19.7 (2019): 392-404.*

METHODS

Samples collection

Bone marrow mononuclear cells (BMMC) obtained from routine BM aspirates and autologous peripheral blood mononuclear cells (PBMC) from MGUS and MM patients at different stages of disease (diagnosis: MM-dia; remission: MM-rem; relapse: MM-rel) were used for the study. All experiments have been performed with BM Vγ9Vδ2 T cells from MM-dia unless otherwise specified, as in the experiments comparing different disease settings. BMMC obtained from BM aspirates from patients with different hematological malignancies in molecular remissions, frozen human normal BMMC purchased from Stem Cell Technologies, and PBMC from healthy blood donors attending at the local Blood Bank were used as control (Ctrl). Samples have been collected after informed consent and study approval by institutional regulatory boards (n.176-19 - December 11, 2019).

Cell surface and intracellular flow cytometry

Cells were washed once with a solution containing PBS and 1% FBS before staining. For membrane immunofluorescence, the cells were incubated with their respective anti-human monoclonal antibodies (mAbs) at 4 ° C in the dark for 30 minutes. Afterward, the cells were washed twice and fixed with para-formaldehyde-PBS 1% before the cytofluorimetric acquisition. Cell surface proteins were targeted with fluorescinated isocyanine (FITC), r-phycoerythrin (PE), chlorophyll protein peridine (Per-CP) or allophycocyanin (APC), conjugated with mAb, according to the list in Supplemental Table 1.

Vγ9Vδ2 T cells were identified with αTCR Vγ9 mAb conjugated with the appropriate fluorochrome (FITC, PE, APC) depending on the multicolor staining combination (see Supplemental Table 1). We have intentionally focused on Vγ9Vδ2 T cells because this is the only γδ T-cell subset directly activated by pAgs or indirectly activated by ZA stimulation (43–45). Moreover, Vδ2 chain is the only one to combine with the Vγ9 chain confirming that αTCR Vγ9 mAbs are reliable tools to identify Vγ9Vδ2 T cells (46).

For intracellular staining (ZAP-70, CD3-ζ chain and Tbet), cells were fixed with Fixation Buffer in the dark for 20 minutes at room temperature and then centrifuged at 350xg for 5 minutes. After discarding supernatant, cells were permeabilized with Staining Perm Wash Buffer and centrifuged at 350xg for 10 minutes. Finally, cells were incubated with the appropriate mAbs or controls for 20

minutes in the dark at room temperature and washed twice with Intracellular Staining Perm Wash Buffer before the cytofluorimetric acquisition.

IFN-γ, TNF-α and IL-17 detection, and CD107 expression were evaluated in cell samples after washing with staining buffer (PBS with 1% FCS and 0.1% sodium azide) and incubation for 30 min at 4°C with anti-CD3 and anti-TCR Vγ9. After extensive washing, cells were fixed with 4% p-formaldehyde for 20 min at room temperature, washed twice with permeabilization buffer and incubated with anti-IFN-γ, TNF-α and anti-IL17. Intracellular cytokine staining and CD107 expression were evaluated by multiparametric flow cytometry.

Cytofluorimetric analyses were performed with FACS Calibur Cell Sorter and FlowJo software (Becton Dickinson, Mountain View, CA).

The mAbs used in the study are listed in Supplemental Table 1.

Vγ9Vδ2 T-cell proliferation, cytokine release and degranulation activity

After isolation on Ficoll-Hypaque density gradients, PB and BM Vγ9Vδ2 T cells from MM patients and Ctrl were tested for their proliferative response to 1 μM ZA+10 IU/ml IL2 in the presence or absence of anti-PD1 (10 μg/ml) and/or anti-TIM-3 (10 μg/ml) and/or anti-LAG-3 (10 μg/ml) and or anti-CD38 (10 μg/ml) neutralizing mAb. Cryopreserved or freshly isolated PBMC or BMMC were cultured at $1x10^6$/ml in RPMI 1640, containing 10% FCS in round bottomed 96 wells plate. To evaluate proliferation, total counts of viable Vγ9Vδ2 T cells were calculated on day 7 with the trypan blue staining assay and flow cytometry after gating for CD3 in combination with appropriate αVγ9 mAb. To analyse cytokines secretion (IFN-γ, TNFα) and degranulation activity (CD107 expression), PBMC and BMMC on day 7 were incubated with brefeldin (500 ng/ml) and anti-CD107 mAb for 4 hours at 37°C and 5% CO2 and stained as reported in the above section. To analyse IL-17 production in resting condition, BMMC were stimulated with PMA (50 ng/ml)/Ionomycin (1 μg/ml) for 4 hours at 37°C and 5% CO2. After 1 hour, brefeldin (500 ng/ml) was added. After incubation, BMMC were stained as reported in the above section.

BMSC generation and co-culture experiments

BMSC were generated from MM and Ctrl samples by seeding 1 x 10^6 BMMC/well in 24-well plates in DMEM medium supplemented with 10% FCS and replacing fresh medium every 3 days. After 4 days, non-adherent cells were washed off and adherent cells, predominantly fibroblast-like cells, were grown in DMEM medium with 10% FCS until confluence (2-3 weeks). BMSC phenotype

was determined by cytofluorimetric analysis evaluating CD44 and CD105 expression as previously reported (26).

In co-colture experiments, $1x10^6$ Ctrl PBMC were cultured in 24-well plates and stimulated with 1 μM ZA+10 IU/ml IL2 in presence or absence of $1x10^5$ MM BMSC for 7 days. For the transwell (TW) group experiments the same procedure was carried out in 0.4 μm 24-well transwell plates (Corning, USA) and PBMC were cultured at the bottom of the transwell plates.

In selected experiments, anti-PDL-1 (10 μg/ml) or anti-TIM-3 (10 μg/ml) or anti-CD38 (10 μg/ml) were added.

Conventional T-cell proliferation

Conventional T cell proliferation was measured by carboxyfluorescein-diacetate-succinimidyl-ester (CFSE) dilution assay. BMMC were suspended in warmed PBS at a concentration of 10×10^6 cells/ml and labeled with 1 μM CFSE at 37°C for 15 min in the dark. After quenching with FCS for 10 minutes in dark at 37°C and washing with RPMI medium, cells were seeded at 1×10^6 cells/ml in 96-well flat-bottom plate and stimulated with anti-CD3 (1 μg/ml - BioLegend) and anti-CD28 (2 μg/ml - BioLegend) antibodies for 72 h at 37°C. After 3 days, cells where harvested and labeled with anti-CD8 and anti-CD4 and then analyzed by flow cytometry. In selected experiments, the proliferation of BM CD4+ and CD8+ T cells with anti-CD3 + anti-CD28 was performed in the presence (BMMC) or absence of γδ T cells T cells (BMMC- γδ depleted). Depletion was performed by immune magnetic separation using Anti-pan-γδ-conjugated magnetic microbeads (Miltenyi Biotec, Germany #130-050-701).

BMSC metabolic analysis

BMSC were cultured as previously reported. After 48h, BMSC were washed in PBS and detached by using trypsin-EDTA. BMSC and culture medium were collected for metabolic analysis, as previously reported (47).

Lactate. Extracellular lactate content was determined by using the L-Lactate Assay Kit (Sigma-Aldrich MAK064), according manufacturer instructions.

The Pentose Phosphate Pathway (PPP) and Tricarboxylic Acid (TCA) Cycle. BMSC were resuspended in 1 mL Hepes buffer (145 mmol/LNaCl, 5 mmol/L KCl, 1 mmol/L MgSO4, 10 mmol/L Hepes, 10 mmol/L glucose,1 mmol/LCaCl2, pH 7.4) (47). 50μL were taken up, sonicated and used to measure the protein content. In each remaining sample, 2 μCi of [6-^{14}C] glucose (55 mCi/mmol,

PerkinElmer) or 2μCiof [1-^{14}C] glucose (58 mCi/mmol, PerkinElmer) were added (47). The labelled cell suspension was incubated for 1 h in a closed tube to trap the $^{14}CO_2$ produced from the [^{14}C] glucose. After this incubation time, the metabolic flux was interrupted by adding 0.5 mL 0.8 NHClO4 (47). [1-^{14}C] glucose metabolized through PPP or TCA and [6-^{14}C] glucose metabolized through the TCE only produced ^{14}CO2. The amount of glucose producing CO_2 through the PPP was obtained by subtracting the amount of [6-^{14}C] glucose (TCA cycle) from [1-^{14}C] glucose (TCA + PPP cycles), as described. Results were expressed as nmolCO2/h/mg cell proteins (47).

Mitochondrial Respiratory Chain Measurement. Cells were rinsed twice in ice-cold PBS, lysed with 0.5 mL buffer A (50 mmol/L Tris, 100 mmol/L KCl, 5 mmol/L MgCl2, 1.8 mmol/L ATP, 1 mmol/L EDTA, pH 7.2) containing the protease inhibitor cocktail III [100 mmol/L AEBSF, 80 mmol/L aprotinin, 5 mmol/L bestatin, 1.5 mmol/L E-64, 2 mmol/L leupeptin and 1 mmol/L pepstatin (MerckMillipore, Milan, Italy) 1 mmol/L PMSF, 250 mmol/L NaF]. Samples were centrifuged at 650× g for 3 min at 4 ◦C, supernatants were transferred into a new tube series and centrifuged at 13,000× g for 5 min at 4 ◦C. The supernatants were discarded, the pellets containing mitochondria, after a washing step with 0.5 mL buffer A, were re-suspended in 0.25 mL buffer B (250 mmol/L sucrose, 15 μmol/L K2HPO4, 2 mmol/L MgCl2, 0.5 mmol/L EDTA, 5% w/v BSA). 50 μL were sonicated and used for protein quantification. The activity of mitochondria respiration complexes was evaluated according to [18]. Results were expressed as nmol red cit c/min/mg mitochondrial proteins (47).

Fatty Acid β-Oxidation. BMSC were centrifuged at 13,000×g for 5 min. Protein quantification was performed on 50μL of the sample after sonication. The remaining samples were resuspended in culture medium containing 0.24 mmol/L fatty acid-free bovine serum albumin (BSA), 0.5 mmol/LL-carnitine, 20 mmol/L Hepes, 2μCi [1-14C] palmitic acid (3.3 mCi/mmol, PerkinElmer) (47) and transferred into tightly closed tubes. For each experiment, a negative control was performed on cells incubated with the carnitine palmitoyltransferase inhibitor etomoxir (1μmol/L) for 30 min, a positive control was performed on cells incubated with the AMP-kinase activator 5-aminoimidazole-4-carboxamide ribonucleotide AICAR (1 mmol/L) for30 min. Samples were incubated 2 h at 37◦C, 1:1 v/v phenylethylamine/methanol (0.3 mL) and 0.8 N HClO4. (0.3 mL) were added. Samples were incubated for an additional 1 h at room temperature, then centrifuged at 13,000×gfor 10 min. The supernatants, containing ^{14}CO2, and the precipitates, containing ^{14}C-acid soluble metabolites (ASM), were subjected to liquid scintillation count. Results were expressed as pmol of [^{14}CO2] or^{14}C-ASM/h/mg cell proteins (47).

Glutamine Catabolism. Cells were rinsed with PBS, detached, centrifuged at 13,000× g for 5 min at 4 ◦C, re- suspended in 250 µL of buffer A (150 mmol/LKH2PO4, 63 mmol/L Tris/HCl, 0.25 mmol/L EDTA; pH 8.6) and sonicated to measure the protein content. In the first sample series, 100 µL of each lysate were incubated at 37 ◦C for 30 min in 850 µL of buffer B (80 mmol/L Tris/HCl, 20 mmol/L NAD+, 20 mmol/L ADP, 3% v/v H2O2; pH 9.4) and 50 µL of 20 mmol/L L-glutamine. NADH absorbance at 340 nm was followed with a Lambda 3 spectrophotometer (PerkinElmer) and was linear during the whole assay. Results, ex- pressed as µmol NADH/min/mg cell proteins, corresponded to the activity of glutaminase (GLS) plus L-glutamic dehydrogenase. In the second sample series, 20 µL of the GLS inhibitor bis-2-(5-phenylacetamido-1,3,4-thiadiazol-2-yl)ethyl sulfide BTPES (30 µmol/L, i.e., a concentration that inhibited GLS activity at 100%, data not shown), was added after 15 min and NADH absorbance was followed for 15 min. Results, expressed as µmol NADH/min/mg cell proteins, indicated the L-glutamic dehydrogenase activity. GLS activity was obtained by subtracting the rate of NADH production in second assay from the rate of the first assay.]

Isopentenyl pyrophosphate (IPP) extracellular release

0.5 x 106 cells were incubated 24 h with 1 µCi [3H]acetate (3600 mCi/mmol; Amersham International, Bucks, U.K.). The extracellular IPP neosynthesized by [3H]acetate was measured as reported previously (26). 300 µl culture supernatant was diluted 1:2 into an ice-cold acetonitrile solution containing 100 mM NaVO4 and centrifuged at 1200 x g for 5 min at 4˚C. After lyophilization under vacuum, samples were resuspended in 20 µl dimethylhexylamine and separated by thin layer chromatography (TLC). After exposing the plates to an iodine-saturated atmosphere for 2 h, the spot corresponding to IPP, according to the standard solution of 1 mg/ml IPP, run in the same experimental condition, was isolated, and radioactivity uptake was measured by liquid scintillation counting (Ultima Gold; Perkin Elmer). The titration curve was performed using three serial dilutions of [3H]IPP (Perkin Elmer). The counts per minutes (cpm) were normalized to the number of cells and expressed as. pmoles/10^6 cells.

Western blots

For Western blot experiments, γδ T cells were purified by immune magnetic separation using Anti-pan-γδ-conjugated magnetic microbeads (Miltenyi Biotec, Germany #130-050-701). Purity was always > 90% by FITC-conjugated-Hapten MicroBeads staining (Miltenyi Biotec, Germany #130-050-701). Both Vδ1 and Vγ9Vδ2 cells are represented in freshly purified γδ T cells (day 0). After ZA stimulation, Vγ9Vδ2 T cells were the predominant population also in MM patients who did not respond to ZA stimulation (Supplemental Figure 1). Cells were lysed in a MLB buffer (125 mM Tris-

HCl, 750 mM NaCl, 1% v/v NP40, 10% v/v glycerol, 50 mM MgCl2, 5 mM EDTA, 25 mM NaF, 1 mM NaVO4, 10 μg/ml leupeptin, 10 μg/ml pepstatin, 10 μg/ml aprotinin, 1 mM phenylmethylsulphonyl fluoride, pH 7.5), sonicated and centrifuged at 13,000 × g for 10 min at 4°C. Twenty μg of proteins from cell lysates were subjected to Western blotting and probed with the antibodies listed in Supplemental Table 2. The proteins were detected by enhanced chemiluminescence (Bio-Rad Laboratories). The band density analysis was performed using the ImageJ software (https://imagej.nih.gov/ij/) and expressed as arbitrary units. The ratio band density of each protein/band density of tubulin (as housekeeping protein) was calculated in each experimental condition. For untreated/baseline/unstimulated cells, the band density ratio was considered 1. For the other experimental conditions, the ratio was expressed as proportion towards the ratio obtained in untreated cells.

ELISA

Cell supernatants (S/N) obtained from 7-day stimulation of Ctrl and MM BMMC with 10 IU/ml IL2, 1 μM ZA+10 IU/ml IL2 in the presence or absence of anti-PD1 were collected and stored at -80°C. The concentration of human IL27 was quantified in cell S/N by enzyme-linked immunosorbent assay technology (ELISA) through IL-27 Human ELISA kit (Invitrogen; Catalogue number: # BMS2085) according manufacturer instructions.

Statistical analysis

The results are expressed as mean ± SE. Differences between the groups have been evaluated with a one-way analysis of variance, a Wilcoxon–Mann–Whitney non-parametric test for paired or unpaired samples as appropriate and considered to be statistically significant for P values <0.05. The GraphPad software has been used for the statistical analyses.

RESULTS

Dual PD-1/TIM-3 expression, functional exhaustion, and immune senescence are intertwined in BM MM Vγ9Vδ2 T cells

Figure 1A shows PD-1, TIM-3, LAG-3 and CTLA-4 expression in resting PB and BM Vγ9Vδ2 T cells from Ctrl and MM patients. PD-1 and TIM-3 expression was significantly higher in BM of MM patients than in Ctrl samples. After ZA stimulation, BM MM Vγ9Vγ2 T cells further increased PD-1 (9) and TIM-3 expression (Figure 1B), while the increase in BM Ctrl Vγ9Vδ2 T cells was limited and significantly lower (Figure 1B). Cytofluorimetric analysis from one representative MM shows that PD-1 and TIM-3 are co-expressed by approximately 60% of BM MM Vγ9Vδ2 T cells after ZA stimulation (Figure 1C). In freshly isolated Vγ9Vδ2 T cells we have previously shown that central memory (CM) Vγ9Vδ2 T cells display the highest PD-1 expression (9). After ZA stimulation, TIM-3 up-regulation was documented in all Vγ9Vδ2 T-cell subsets with CM and naïve Vγ9Vδ2 T cells showing slightly higher levels than effector memory (EM) and terminally differentiated effector memory (TEMRA) Vγ9Vδ2 T cells (Figure 1D). The gating strategy used to investigate TIM-3 expression in Vγ9Vδ2 T-cell subsets is shown in Supplemental Figure 2.

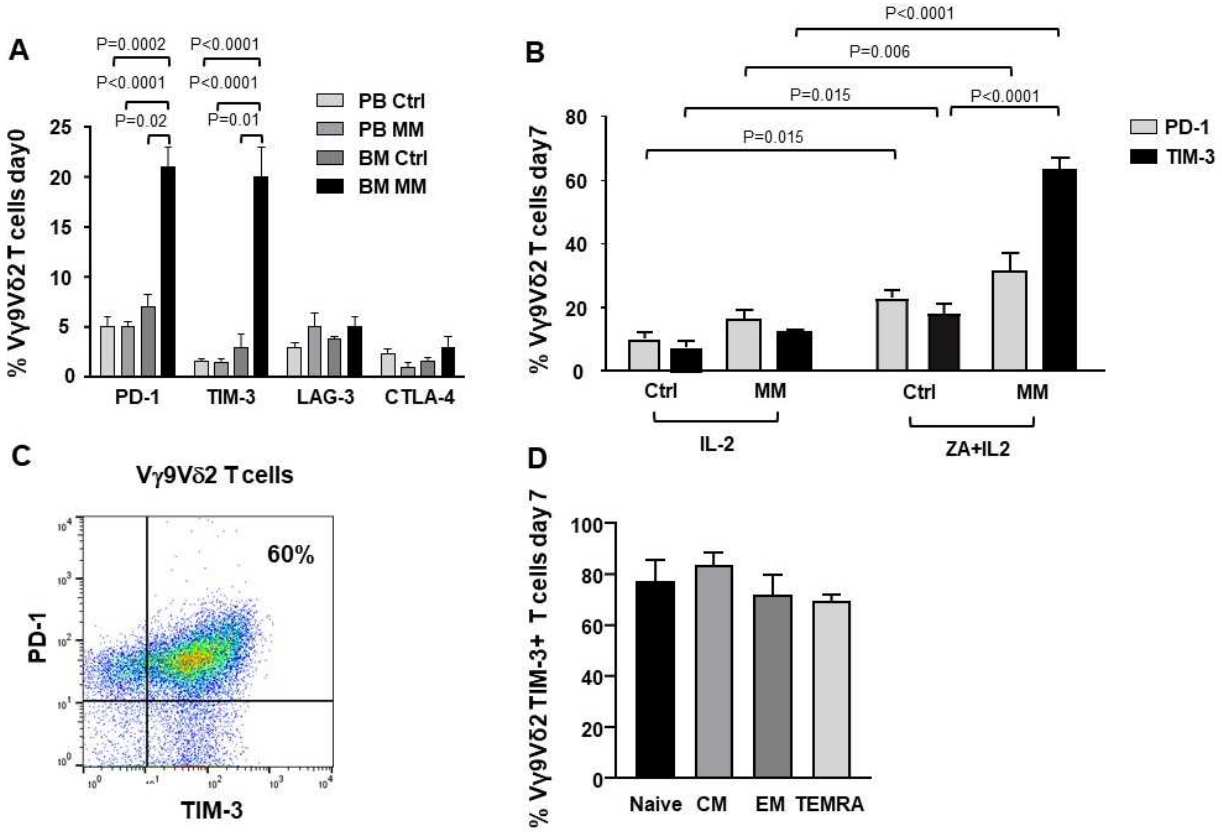

Figure 1. **ICP expression and subset distribution in resting and ZA-stimulated BM MM Vγ9Vδ2 T cells. A**) PD-1, TIM-3, LAG-3 and CTLA-4 expression in resting PB and BM Vγ9Vδ2 T cells from healthy subjects (Ctrl) and MM at diagnosis. Bars represent mean values

± SE from 5 (BM Ctrl) to 30 (BM MM) experiments. **B**) PD-1 and TIM-3 expression are significantly increased after ZA stimulation in MM BM Vγ9Vδ2 T cells. Bars represent mean values ± SE from 7 (BM Ctrl) to 30 (BM MM) experiments; **C**) Cytofluorimetric analysis of PD-1 and TIM-3 co-expression in BM MM Vγ9Vδ2 T cells from one representative MM after ZA stimulation. **D**) TIM-3 expression in naive (CD27+ CD45RA+), central memory (CM) (CD27+ CD45RA-), effector memory (EM) (CD27- CD45RA-), and terminally differentiated effector memory (TEMRA) (CD27- CD45RA+) BM MM Vg9Vd2 T cells after ZA stimulation. Bars represent mean values ± SE from 3 experiments.

Figure 2A compares the expression of immune senescence markers (40,48,49) in BM Ctrl and MM Vγ9Vδ2 T cells. BM MM Vγ9Vδ2 T cells showed significantly higher CD57 and CD160, and lower CD28 expression than BM Vγ9Vδ2 T cells, even if differences were not statistically significant. The highest CD160 expression was observed in CM BM Vγ9Vδ2 T cells which is the cell subset with the highest PD-1(9) and TIM-3 expression (Figure 2B). Cytofluorimetric analysis of CD160 and PD-1 co-expression in BM MM Vγ9Vδ2 T cells from one representative sample is shown in Figure 2B (right panel).

Phosphorylated-γH2AX (p-γH2AX) is an early marker of immune senescence-associated DNA damage (50). p-γH2AX expression in BM Ctrl and MM-dia γδ T cells is shown in Figure 2C (one representative experiment) and Figure 2D (pooled data). These experiments were performed on purified γδ T cells. Both Vδ1 and Vγ9Vδ2 subsets can be represented in variable proportions in freshly purified γδ T cells (day 0), whereas after ZA stimulation Vγ9Vδ2 T cells become predominant (Supplemental Figure 1) and any change should be referred to these because they are the only γδ T-cell subset sensitive to ZA stimulation. In freshly isolated BM γδ T cells, p-γH2AX expression was slightly higher in MM than Ctrl, but the difference was not statistically significant. After ZA stimulation, p-γH2AX significantly increased only in BM MM Vγ9Vδ2 T cells (Figure 2C, 2D).
IL-7 has been reported to mitigate the induction of immune senescence induced by the incubation of conventional T cells with tumor cells (51,52). We have investigated whether IL-7 could relieve the immune dysfunction of BM MM Vγ9Vδ2 T cells, but we have not observed any beneficial effect in ZA-stimulated Vγ9Vδ2 T cells (data not shown).

Accumulating evidences indicate that Vγ9Vδ2 T cells can exert different functions depending on the local microenvironment, including the ability to promote tumor progression *via* the acquisition of regulatory or pro-tumoral functions (53–55). Figure 2E shows the expression of CD38, CD39, and CD73 in BM Vγ9Vδ2 T cells from Ctrl and MM patients. These molecules cooperate in the induction of the immune suppressive TME in MM via adenosine production (56). Only CD38 was significantly up-regulated in MM compared with Ctrl, whereas no differences were observed in CD39 and CD73 expression. The adenosine circuitry operated by CD38, CD39, and CD73 is well known to contribute

to the establishment of the immune suppressive contexture in the TME of MM (56), but our data indicate that Vγ9Vδ2 T cells are not key players in this circuitry.

Lastly, BM MM Vγ9Vδ2 T cells did not show any phenotypic and/or functional features consistent with suppressor and/or pro-tumoral functions. The proliferation of CD4+ and CD8+ T cells after αCD3+αCD28 stimulation was similar in the presence or absence of γδ T cells (Figure 2F). Supplementary Figure 3A shows that proliferation of BM MM CD4+ and CD8+ cells was similar or even better compared with PB Ctrl CD4+ and CD8+ cells. Unlike BM Vγ9Vδ2 T cells, CD4+ and CD8+ cell proliferation was not influenced by the disease status (Supplementary Figure 3B), confirming the unique BM MM Vγ9Vδ2 T-cell susceptibility to the immune suppressive TME contexture.

The expression of PD-L1, GAL-9 and IL-17 characterizes Vγ9Vδ2 T cells with pro-tumoral functions in the TME (57–60). A shown in Figure 2G-H, the expression of GAL-9 and cytoplasmic IL-17 was similar in BM Ctrl and MM Vγ9Vδ2 T cells except for PD-L1 expression, which was slightly increased in the former, but the difference was not statistically significant. Representative dot plots of IL-17 expression in BM MM and Ctrl Vγ9Vδ2 T cells are shown in Supplemental Figure 4.

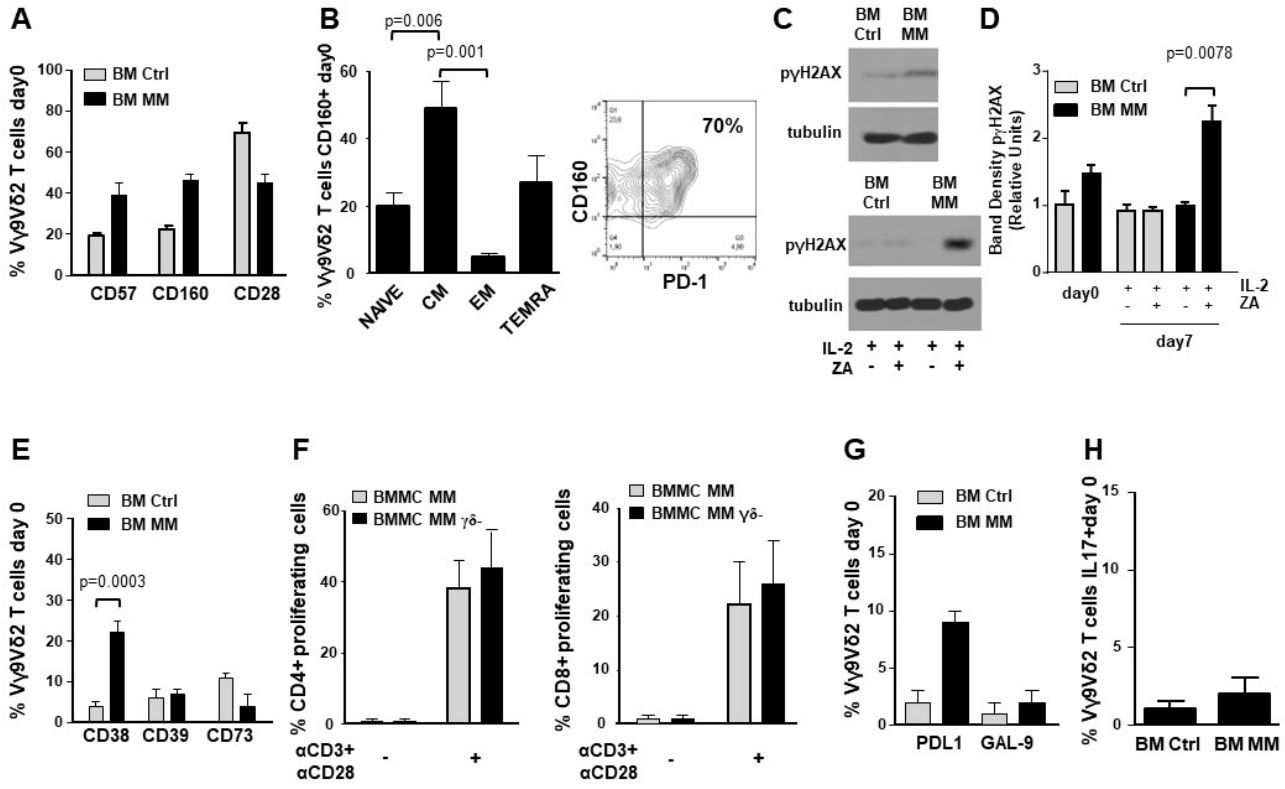

Figure 2 **ICP expression in BM MM Vγ9Vδ2 T cells is associated with chronic exhaustion and immune senescence markers. A**) CD57, CD160, and CD28 expression in BM Ctrl and BM MM Vγ9Vδ2 T cells. Bars represent mean values ± SE from 3 (BM Ctrl) to 50 (BM MM)

experiments. **B**) *left:* CM is the BM MM Vγ9Vδ2 T-cell subset with the highest CD160 expression. Bars represent mean values ± SE of 8 experiments; *right:* cytofluorimetric analysis of CD160 and PD-1 co-expression in BM MM Vγ9Vδ2 T cells from one representative sample. **C**) Western blot analysis of p-γH2AX expression in resting (upper panel) and ZA-stimulated (lower panel) γδ T cells from one representative PB Ctrl and BM MM sample. Tubulin expression is shown to confirm equal protein loading per lane. **D**) Densitometric analysis of pooled p-γH2AX expression data in resting (day 0) and ZA-stimulated (day 7) BM Ctrl and MM γδ T cells. Bars represent mean values ± SE from 1 (BM Ctrl and BM MM d0) to 4 (BM MM) experiments. **E**) CD38, CD39, and CD73 expression in resting BM Ctrl and BM MM Vγ9Vδ2 T cells. Bars represent mean values ± SE from 8 (BM Ctrl) to 40 (BM MM) experiments. **F**) CFSE-based analysis of BM MM CD4+ and CD8+ T-cell proliferation after 72-hour stimulation with αCD3 + αCD28 in the presence (BMMC) or absence (BMMC- γδ T-cell depleted) of γδ T cells. **G**) PD-L1 and GAL-9 expression in resting BM Ctrl and MM Vγ9Vδ2 T cells. **H**) Intracellular IL-17 expression in resting BM Ctrl and MM Vγ9Vδ2 T cells

Key drivers of TME-induced Vγ9Vδ2 T-cell immune dysfunction: immune and metabolic checkpoints

TME contribution to Vγ9Vδ2 T cell immune dysfunction was evaluated by analysing immunomodulatory functions of MM BMSC and by performing co-colture experiments with fully competent Ctrl PB Vγ9Vδ2 T cells.

Since chronic antigen stimulation of TCR promote functional exhaustion state of immune effector cells (61), IPP secretion by BMSC derived from Ctrl, MGUS and MM in different stage of disease was assessed. Unexpectedly, the highest amounts of IPP were released by BMSC isolated from MGUS individuals (Figure 3A). These data indicate that the TME is saturated very early by supra-physiological IPP concentrations that are released mainly by BMSC (26). This early and persistent exposure of BM Vγ9Vδ2 T cells can contribute to their chronic activation and functional exhaustion. The high extracellular IPP concentrations released by BMSC after that myeloma cells have been eliminated by treatment can also contribute to the persistent anergy of BM Vγ9Vδ2 T cells in MM-rem (9).

Figure 3 B shows ICP/ICP-L expression in BMSC from BM niche of MM patients and Ctrl. Cytofluorimetric analysis revealed that PDL-1 and GAL-9 are significantly upregulated by MM BMSC compared to Ctrl. ICP/ICP-L expression in myeloma cells, MDSC and EC shown in Supplementary Figure 5 confirms that the widespread expression of ICP-L in TME (9,11) may hold in check BM-resident Vγ9Vδ2 T cells expressing cognate receptors.

MM cells are extremely dependent on the BM niche and drive a metabolic reset finalized to meet their own energetic needs to the detriment of bystander cells. Metabolic analysis of BMSC isolated from the BM of Ctrl and MM at different stages of the disease (MGUS, diagnosis: dia-MM, remission: MM-rem; relapse: MM-rel) shown in Figure 3 C-G identified metabolic alterations of MM BMSC. Data of each metabolic pathway are represented as heat maps. BMSC from dia-MM patients

showed a trend of increase in PPP activity (Figure 3C) and mostly in lactate production (Figure 3D) compared to Ctrl. In addition, TCA cycle (Figure 3E) and electron transport chain (ETC) activity (Figure 3F) were significantly reduced in dia-MM BMSC compared to Ctrl, whereas no significant differences were observed by analysing glutaminolysis, fatty acid oxidation (FAO) and lipoperoxidation (Supplemental Figure 6). Interestingly, BMSC from one MGUS patient analysed showed a metabolic profile similar to dia-MM patients, BMSC from patients achieving remission phase restored their metabolic profile while rel-MM BMSC metabolic alterations were close to dia-MM BMSC, suggesting a metabolic regulation tightly controlled by interactions with myeloma cells. This acidic and nutritionally deficient TME may contribute to the strengthening of immune dysfunction and to relapse.

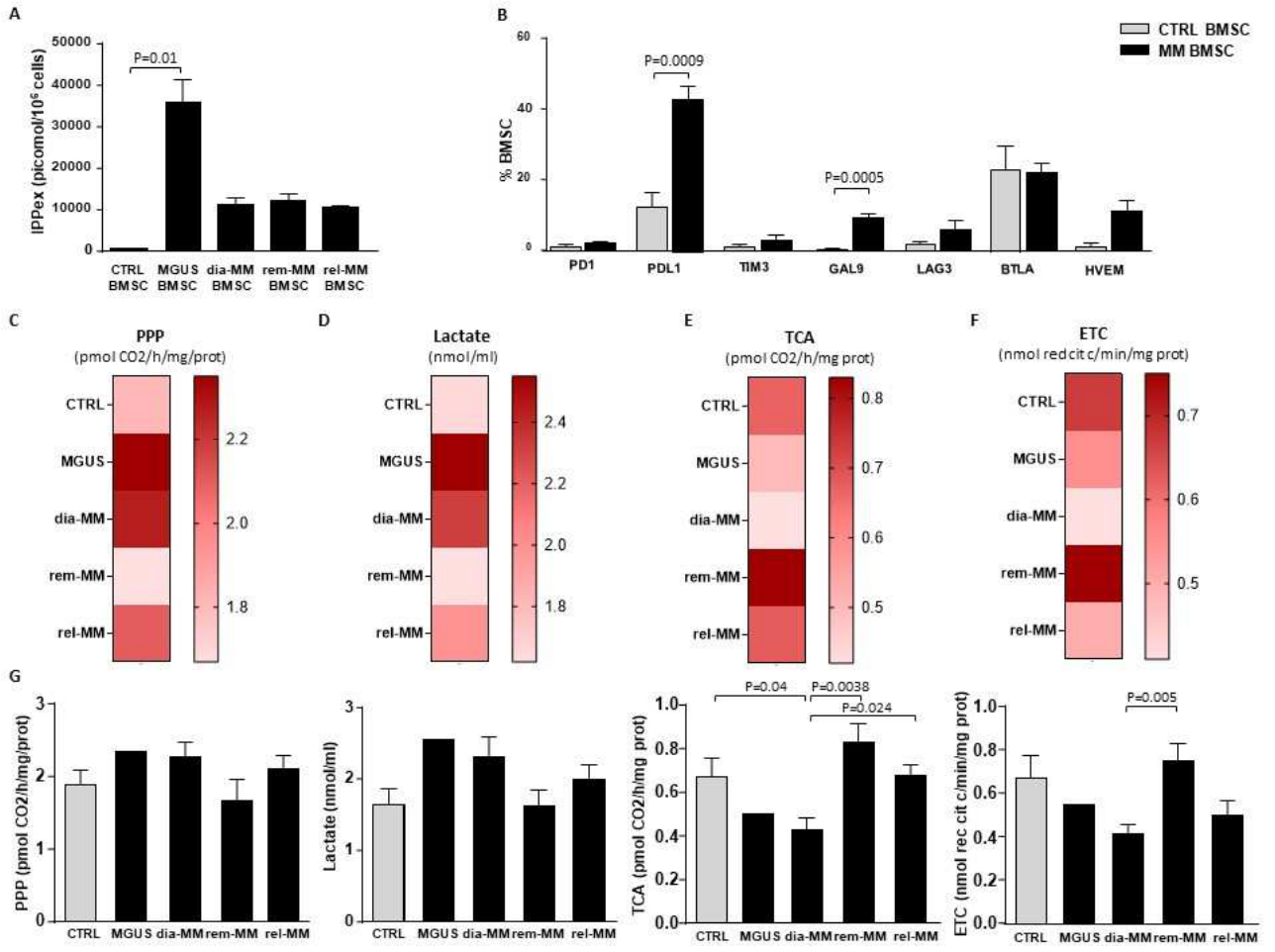

Figure 3 **MM BMSC show phenotypic and metabolic alterations. A**) Extracellular IPP levels (IPPex) in BMSC from Ctrl and MM patients at different stages of disease. Bars represent mean values ± SE from 2 (MM-rel) to 8 (Ctrl) experiments; **B**) PD-1, PDL-1, TIM-3, Gal-9, LAG-3, BTLA, and HVEM expression in Ctrl and MM BMSC. Bars represent mean values ± SE from 2 (HVEM on Ctrl) to 28 (BTLA on MM) experiments; (**C**-**F**) Heat maps and (**G**) relative bar graphs representing **C**) quantification of lactate levels, **D**) analysis of Pentose Phosphate Pathway (PPP) flux, **E**) analysis Tricarboxylic Acid (TCA) cycle flux, and **F**) analysis of mitochondria electron transport chain activity. Bars represent mean values ± SE from 1 (MGUS) to 7 (rem-MM) experiments.

Immune fitness of fully competent Vγ9Vδ2 T cells from Ctrl was evaluated in the presence of MM BMSC. A sharp reduction of the absolute number of ZA-stimulated Ctrl PB Vγ9Vδ2 T cells in presence of MM BMSC was observed (Figure 4A). Moreover, TIM-3 and TIGIT expression were significantly increased when ZA-treated Vγ9Vδ2 T cells and MM BMSC were co-cultured (Figure 4B). BMSC induced immune dysfunction of Vγ9Vδ2 T cells was observed in presence or absence of transwell (TW) and was not reverted by single ICP blockade (Supplemental Figure 7), suggesting that both soluble factors and cell-to-cell contacts are involved.

We analysed degranulation activity (CD107 expression) (Figure 4C) and cytokine production (IFN-γ) (Figure 4D) of Ctrl PB Vγ9Vδ2 T cells after ZA stimulation in the presence of MM BMSC. Our results suggested that CD107 and cytoplasmatic IFNγ expressions were not modulated by MM BMSC. Additionally, the expression of TBET, a transcription factor that controls IFNγ expression in conventional T cells (62), was not to affected (Figure 4E).

Impaired immunomodulatory functions of MM BMSC promote senescence of conventional T cells through pAKT signaling pathway (63). However, MM BMSC did not show a significant senescence-stimulating effect on ZA-treated Vγ9Vδ2 T-cells from Ctrl, as shown in Figure 4F.

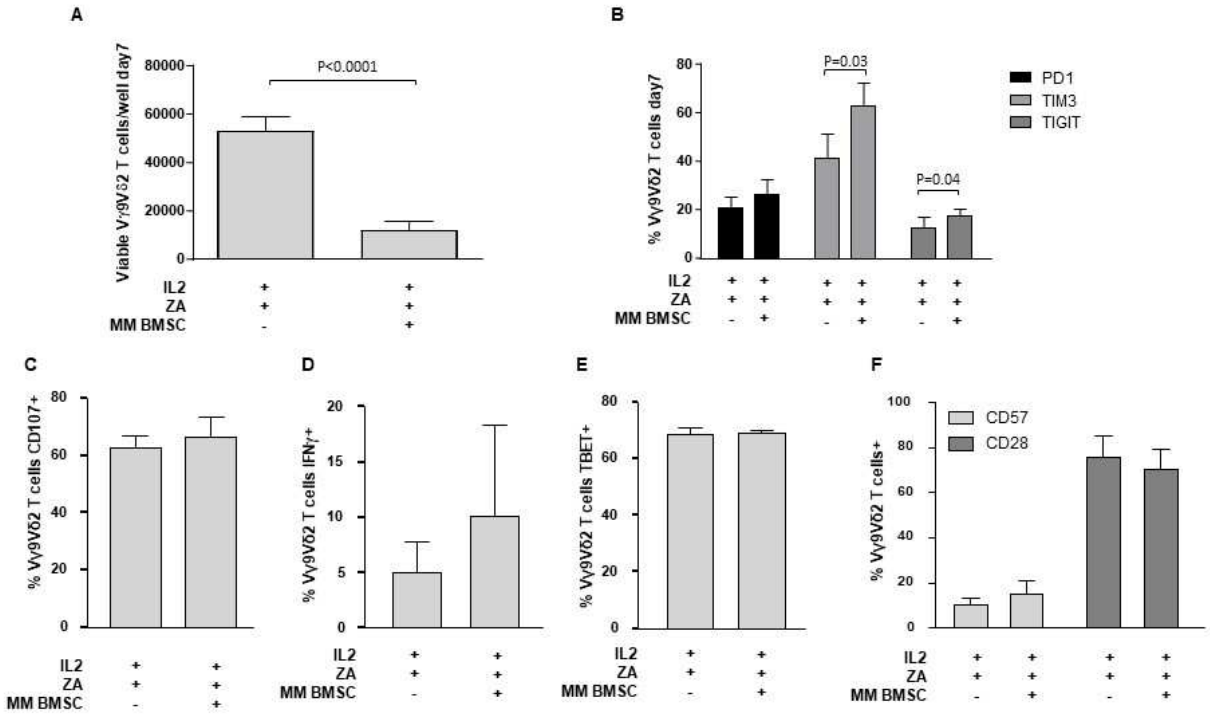

Figure 4 **MM BMSC phenotypic and metabolic alterations may contribute to Vγ9Vδ2 T cell dysfunction. A**) Total counts of viable Ctrl PB Vγ9Vδ2 T cells after 7-day ZA stimulation in the presence or absence of MM BMSC. Bars represent mean values ± SE from 19 experiments; **B**) PD-1, TIM-3, and TIGIT expression on Ctrl PB Vγ9Vδ2 T cells after 7-day ZA stimulation in the presence or absence of MM BMSC. Bars represent mean values ± SE from 11 (PD1 analysis) to 7 (TIGIT analysis) experiments; **C**) CD107 expression in ZA-stimulated Ctrl PB Vγ9Vδ2 T cells in presence or absence of MM BMSC. Bars represent mean values ± SE from 3 experiments. **D**)

Intracellular IFN-γ production and (**E**) TBET expression on ZA-stimulated Ctrl PB Vγ9Vδ2 T cells in presence or absence of MM BMSC. Bars represent mean values ± SE from 3 experiments. **F**) CD57 and CD28 expression in ZA-stimulated Ctrl PB Vγ9Vδ2 T cells in presence or absence of MM BMSC. Bars represent mean values ± SE from 3 experiments.

Altered expression of TCR-associated molecules in BM MM Vγ9Vδ2 T cells

ICP expression and immune senescence in T cells are associated with defective intracellular TCR signaling (64,65). Figure 5A shows the expression of selected TCR-associated molecules in in purified BM γδ T cells from one representative Ctrl and MM patient on day 0 and after ZA-stimulation (day 7). As reported above, both Vδ1 and Vγ9Vδ2 cells are represented in freshly purified γδ T cells (day 0), whereas Vγ9Vδ2 T cells are predominant on day 7 and they are the only γδ T-cell subset engaged by ZA (Supplemental Figure 1). Pooled data are shown in Figure 3B. BM MM Vγ9Vδ2 T cells showed significantly lower pAKT, and pSTAT-1 expression, and significantly higher PTEN expression than BM Ctrl Vγ9Vδ2 T cells on day 7; SHP-2 expression was similar on day 0 and day7, while pJAK1 was slightly lower on day 0.

ZAP-70 and CD3-ζ chain are other TCR-associated molecules defectively expressed in T cells from the TME of mice and humans (66–68). ZAP-70 expression was significantly lower in resting BM MM Vγ9Vδ2 T cells compared with PB and BM Ctrl Vγ9Vδ2 T cells, but also with PB MM Vγ9Vδ2 T cells (Figure 3C), further confirming the striking difference between circulating *vs* TME-resident Vγ9Vδ2 T cells. Representative dot plots are shown in Figure 5D. Paired analyses of Vγ9Vδ2+ and CD3+ Vγ9Vδ2- cells showed that the mean ZAP-70 expression was also significantly down-regulated in BM CD3+ Vγ9Vδ2- T cells of MM patients with a wide range of expression in individual samples (Supplemental Figure 8). A slight increase was observed after ZA stimulation in Vγ9Vδ2 T cells from 3 MM patients with low ZAP-70 expression at baseline, but values remained inferior to Ctrl values (Figure 5E). Unlike ZAP-70, the proportion and MFI of CD3-ζ chain expression were not different in PB and BM Ctrl and MM Vγ9Vδ2 T cells (Supplemental Figure 9).

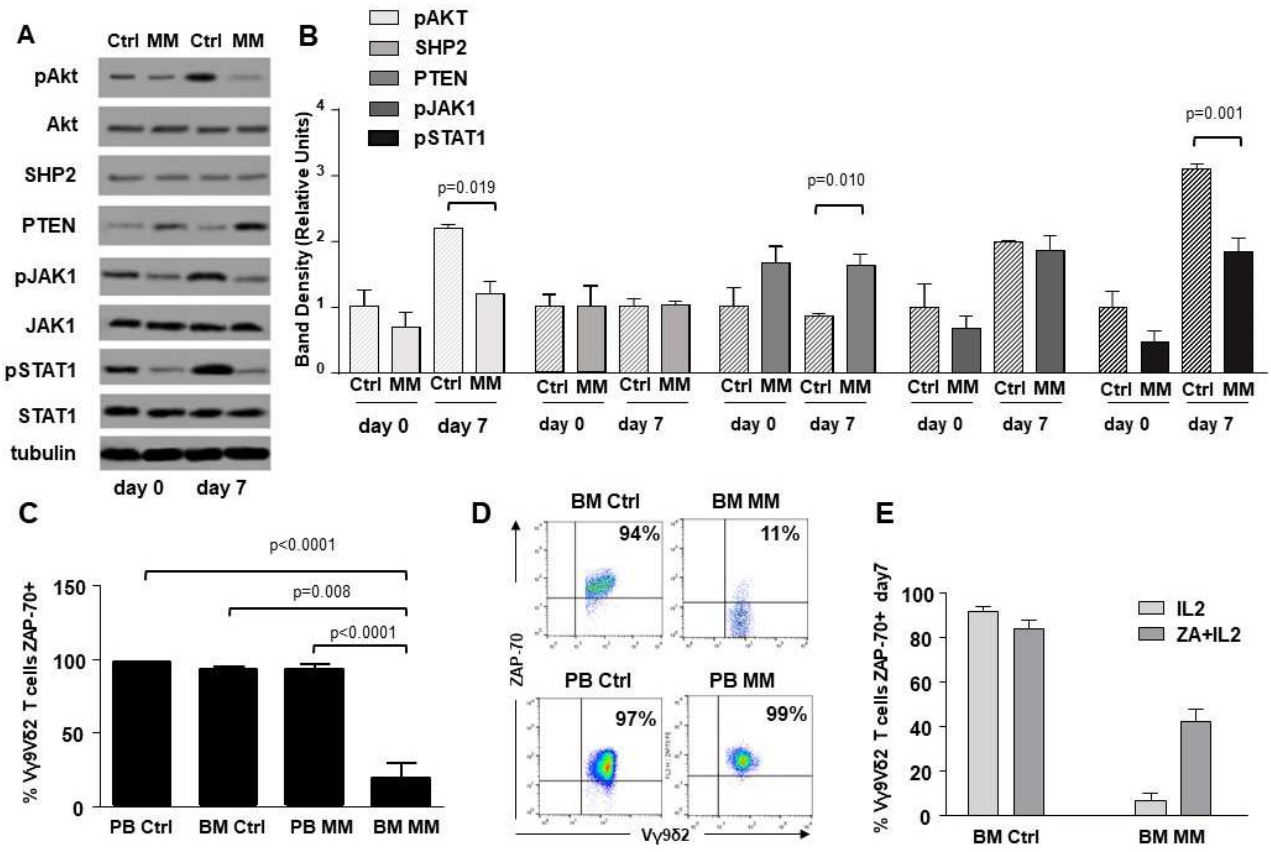

Figure 5 **Alterations of TCR-associated molecules in BM MM Vγ9Vδ2 T cells**. **A**) Western blot analysis of selected TCR-associated molecules (pAKT, AKT, SHP2, PTEN, pJAK-1, JAK-1, pSTAT-1, STAT-1) in purified resting (day 0) and ZA-stimulated (day 7) BM γδ T cells from one representative Ctrl and MM. Tubulin expression is shown to confirm equal protein loading per lane. **B**) Densitometric analysis of pooled data from ZA-stimulated BM Ctrl and BM MM γδ T cells confirms lower expression of pAKT, and pSTAT1, and higher PTEN expression in BM MM Vγ9Vδ2 T cells *vs* BM Ctrl Vγ9Vδ2 T cells. Bars represent mean values ± SE from 1 (BM Ctrl d0 and BM MM d0) to 14 experiments (BM MM). **C**) ZAP-70 expression in resting PB and BM Vγ9Vδ2 T cells from Ctrl and MM patients. Bars represent mean values ± SE from 3 (BM Ctrl) to 25 experiments (BM MM). **D**) Cytofluorimetric analysis of ZAP-70 expression in Vγ9Vδ2 T cells in BM and PB Ctrl and MM. **E**) ZAP-70 expression after ZA stimulation in Ctrl and MM BM Vγ9Vδ2T cells. Bars represent mean values ± SE from 2 (BM Ctrl) to 3 experiments (BM MM).

PD-1/TIM-3 cross-talk in BM MM Vγ9Vδ2 T cells

It has been reported that TIM-3 up-regulation is involved in the acquired resistance to PD-1 blockade (38,69,70). Thus, we have investigated whether TIM-3 was involved in the incomplete recovery of BM MM Vγ9Vδ2 T cells after ZA stimulation in the presence of single PD-1 blockade. Figure 6A shows that both TIM-3 expression and MFI values were significantly up-regulated in BM MM Vγ9Vδ2 T cells in the presence of αPD-1, whereas PD-1 expression was slightly down-regulated after ZA stimulation in the presence of αTIM-3, but the decrease was not statistically significant. Representative cytofluorimetric analyses of increased TIM-3 up-regulation and PD-1 down-regulation are shown in Figure 6A (right panel) and Figure 6B (right panel).

Next, we investigated whether dual PD1-/TIM-3 blockade was more effective than single blockade. We evaluated the proliferation (Figure 6C), IFN-γ production (Figure 6D) and CD107 expression (Figure 6E) in BM MM Vγ9Vδ2 T cells after ZA stimulation in the presence of αPD-1, αTIM-3, and the combination thereof. Representative cytofluorimetric analyses of increased IFN-γ and CD107 expression in BM MMVγ9Vδ23 T cells after dual blockade are shown in Figure 6D (right panel) and Figure 6E (right panel).

Our results indicate that dual blockade PD-1/TIM-3 blockade is more effective than single PD-1 or TIM-3 blockade in MM-dia to mitigate BM MM Vγ9Vδ2 T-cell dysfunctions.

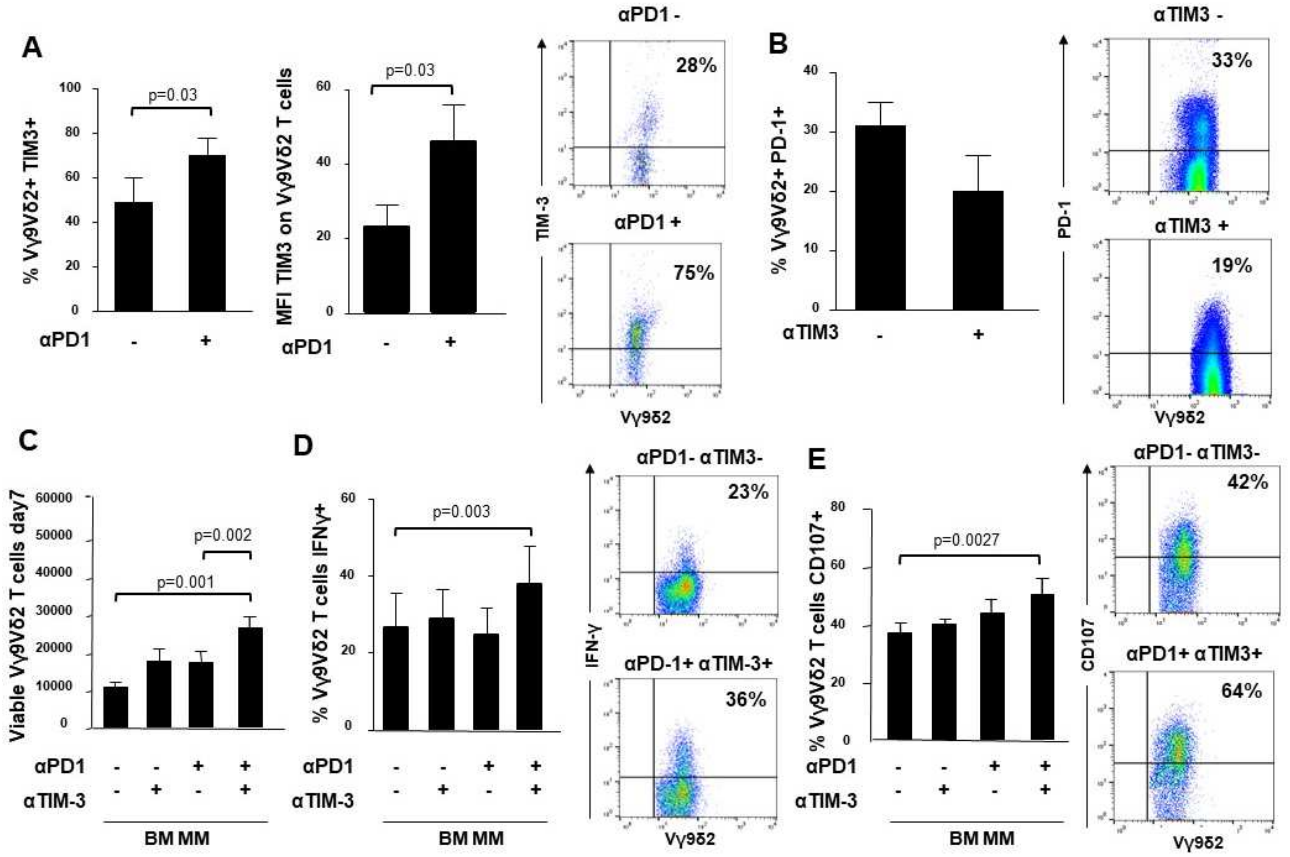

Figure 6 **Intracellular cross-talk between PD-1 and TIM-3 in BM MM Vγ9Vδ2 T cells**. **A**) *left:* Percentage and MFI of TIM-3+ cells are significantly up-regulated in BM MM Vγ9Vδ2 T cells after ZA stimulation in the presence of αPD1. Bars represent mean values ± SE of 6 experiments; *right:* cytofluorimetric analysis of TIM-3 expression after ZA stimulation in the absence (upper panel) or in the presence (lower panel) of αPD-1 in one representative experiment; **B**) *left:* PD-1 expression is down-regulated in BM MM Vγ9Vδ2 T cells after ZA stimulation in the presence of αTIM-3. PD-1 expression is significantly up-regulated after ZA stimulation as already reported in Figure 1B. Bars represent mean values ± SE of 5 experiments; *right:* cytofluorimetric analysis of PD-1 expression after ZA stimulation in the absence (upper panel) or in the presence (lower panel) of αTIM-3 in one representative experiment; **C**) ZA-induced BM MM Vγ9Vδ2 T cell proliferation in the absence or in the presence of αPD-1, αTIM-3 and the combination thereof: dual PD-1/TIM-3 blockade significantly improves ZA-induced proliferation compared with none or single PD-1 blockade. Bars represent mean values ± SEM of 5 experiments. **D**) *left:* intracellular IFN-γ production by ZA-stimulated BM MM Vγ9Vδ2 T cells in the absence or in the presence of αPD-1, αTIM-3 and the combination thereof. Dual PD-1/TIM-3 blockade significantly improves IFN-g production compared with none or single blockade. Bars represent mean values ± SEM of 4 experiments; *right:* cytofluorimetric analyses of IFN-

γ production in BM MM Vγ9Vδ2 T cells after ZA stimulation in the absence (upper panel) or in the presence (lower panel) of dual PD1/TIM-3 blockade. **E**) *left:* CD107 expression in ZA-stimulated BM MM Vγ9Vδ2 T cells in the absence or in the presence of αPD-1, αTIM-3, and the combination thereof. Dual PD-1/TIM-3 blockade significantly up-regulates CD107 expression compared with none or single blockade. Bars represent mean values ± SE of 6 experiments; *right:* cytofluorimetric analyses of CD107 expression in BM MM Vγ9Vδ2 T cells after ZA stimulation in the absence (upper panel) or in the presence (lower panel) of dual blockade PD1/TIM-3 blockade.

Dual PD-1/TIM-3 blockade was associated with a partial mitigation of TCR-associated alterations. Data from one representative Ctrl and MM sample are shown in Figure 7A, while pooled data from 2 paired experiments are shown in Figure 7B. αPD-1 partially normalized pAKT and PTEN expression, whereas αTIM-3 partially normalized pJAK1 and pSTAT1 expression. No antagonist, additive or synergistic effect was observed suggesting that αPD-1 and αTIM-3 target mutually exclusive TCR-associated molecules in BM MM Vγ9Vδ2 T cells. Supplementary Figure 10 shows pooled data from unpaired experiments after αPD-1 treatment only.

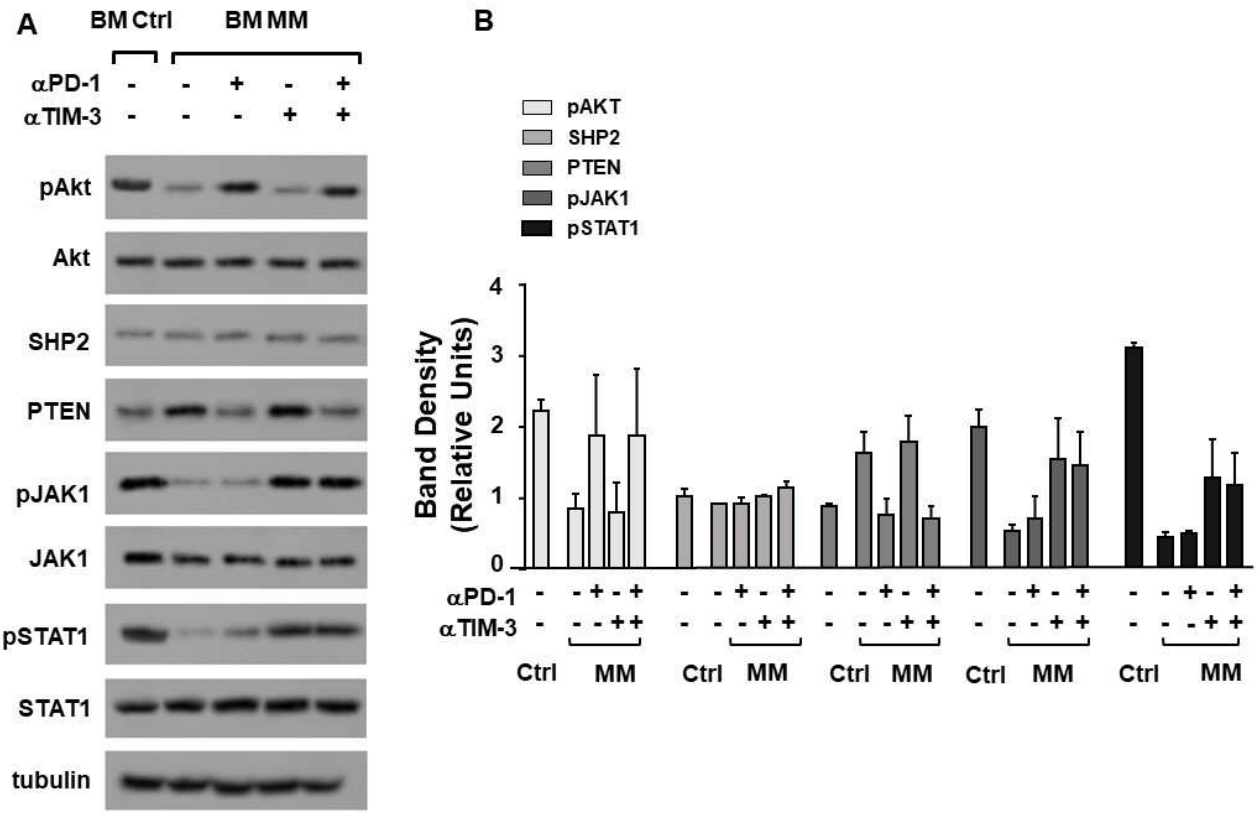

Figure **7 Alterations of TCR-associated molecules are mitigated by αPD-1 and/or αTIM-3**. **A**) Western blot analysis of pAKT, AKT, SHP2, PTEN, pJAK-1, JAK-1, pSTAT-1, and STAT-1 expression in BM Ctrl and BM MM γδ T cells from one representative experiment after ZA stimulation in the absence or in the presence of αPD1, αTIM-3, and the combination thereof. Tubulin expression is shown to confirm equal protein loading per lane. **B**) Densitometric analysis of pooled data. Bars represent mean values ± SE of 2 experiments.

Intracellular PD-1/TIM-3 cross-talk is not mediated by the IL-27/pSTAT1/T-bet or the PI3K-AKT pathways

Next, we looked for possible intersections between the intracellular pathways triggered by αPD-1 and αTIM-3. Previous work from Zhu C. et al. (71) has reported a cross-talk between TIM-3 and PD-1 mediated by the IL-27/pSTAT1/T-bet axis. BM MM Vγ9Vδ2 T cells showed the lowest T-bet (Figure 8A), and the highest IL-27R expression (Figure 8B). This pattern has recently been reported in severely exhausted T cells from the BM of patients with AML in relapse after allogeneic transplantation (72). αPD-1 treatment did not increase T-bet and/or IL-27R expression in ZA-stimulated BM Vγ9Vδ2 T cells (Figure 8C, 8D). Moreover, very small amounts of IL-27 were detected in the supernatants of BM MM Vγ9Vδ2 T cells which were unaffected by αPD-1 (Figure 8E).

The PI3K/Akt axis is another intracellular signalling pathway connecting PD-1 and TIM-3 in tumor-infiltrating lymphocytes from patients with head and neck cancer (70). In these cells, TIM-3 up-regulation induced by αPD-1 can be abrogated with LY294002, a broad PI3K inhibitor (52). Thus, we evaluated whether αPD-1-induced TIM-3 up-regulation in BM MM Vγ9Vδ2 T cells could be inhibited by single pSTAT-1 inhibition with fludarabine monophosphate (FAMP) (73), single PI3K inhibition with LY294002, or the combination thereof. Results shown in Figure 8F indicate that that

these pathways are not druggable to prevent αPD-1-induced TIM-3 up-regulation in BM MM Vγ9Vδ2 T cells.

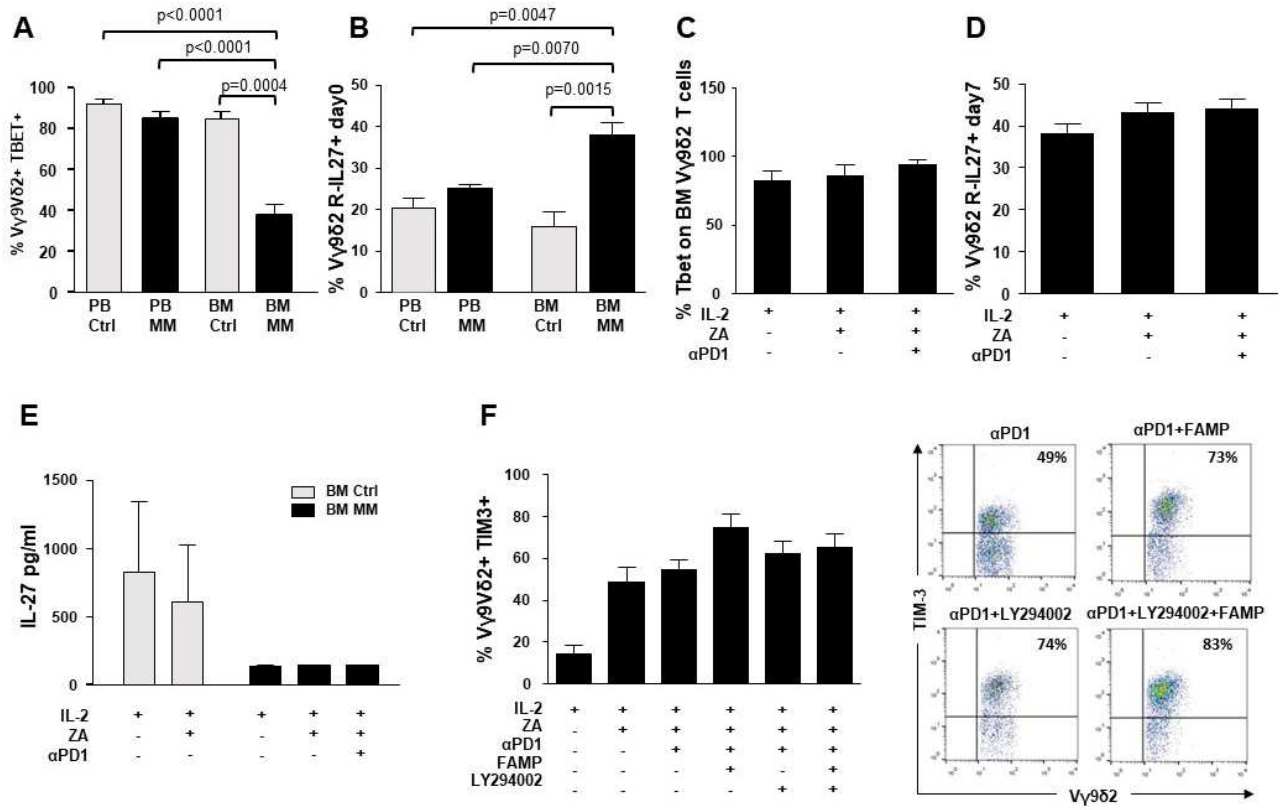

Figure 8 **Intracellular PD-1/TIM-3 cross-talk is not mediated by the IL-27/pSTAT1/T-bet or PI3K-AKT axes**. **A**) T-bet percentage and MFI expression in resting PB and BM Ctrl and MM Vγ9Vδ2 T cells. Bars represent the mean values ± from 6 (BM Ctrl) to 25 experiments (BM MM); **B**) IL-27R expression in resting PB and BM Ctrl and MM Vγ9Vδ2 T cells. Bars represent the mean values ± from 6 (BM Ctrl) to 25 experiments (BM MM). **C**) T-bet and **D**) IL-27R expression in ZA-stimulated BM MM Vγ9Vδ2 T cells with or without αPD1. **E**) IL-27 concentrations in the supernatants (S/N) of ZA-stimulated BMMC from Ctrl and MM patients. Bars represent the mean values ± from 3 (BM Ctrl) to 4 experiments (BM MM). **F**) Left: TIM-3 expression in ZA-stimulated BM MM Vγ9Vδ2 T cells without or with αPD1 in the presence of LY294002 (PI3K inhibitor), fludarabine monophosphate (FAMP) (p-STAT1 inhibitor), and the combination thereof. Bars represent the mean values ± of 7 experiments. Right: cytofluorimetric analysis of TIM-3 expression in ZA-stimulated BM MM Vg9Vd2 T cells without or with α-PD-1 and PI3K and/or pSTAT-1 inhibitors from one representative MM.

Shaping ICP blockade on the disease status

Next, we investigated whether the ICP/ICP-L immune suppressive circuitry was influenced by the disease status. PD-1 expression was significantly higher in MM-rel than in MM-dia, while MM-rem showed intermediate values. By contrast, no differences were observed in TIM-3 expression between MM-dia, MM-rem, and MM rel (Figure 9A). We investigated whether αPD-1 treatment induced TIM-3 up-regulation also in MM-rem and MM-rel. Figure 9B shows that TIM-3 was up-regulated in MM-dia only, but not in MM-rem and MM-rel.

The effect of single or dual PD-1/TIM-3 blockade on ZA-induced proliferation in BM MM Vγ9Vδ2 T cells in MM-dia, MM-rem and MM-rel is shown in Figure 9C. BM Vγ9Vδ2 T cells from MM-rem were the only ones to reach normal proliferation values (Supplemental Figure 11) with single PD-1 or TIM-3 blockade, the former being slightly more effective than the latter. Dual PD-1/TIM-3 blockade was not superior to single blockade in MM-rem. By contrast dual PD-1/TIM-3 blockade was more effective than single blockade in MM-dia, the only clinical setting in which αPD-1 induces TIM-3 up-regulation. BM Vγ9Vδ2 T cells from MM-rel showed the worst anergy to single and dual blockade, even if TIM-3 expression was similar to MM-dia and MM-rem and was not up-regulated by αPD-1 (Figure 9A, 9B).

These findings prompted us to investigate the expression of additional ICP on BM MM Vγ9Vδ2 T cells in MM-rel. Figure 7D shows that LAG-3 expression was similar in resting (day 0) BM Vγ9Vδ2 T cells from MM-dia, MM-rem, and MM-rel. After ZA stimulation, LAG-3 expression was slightly increased in MM-dia, unmodified in MM-rem, but increased in MM-rel, even if the differences was not statistically significant. Next, we determined which PD-1/TIM-3/LAG-3 combination was more effective to mitigate the anergy of BM Vγ9Vδ2 T cells in MM-rel. Results shown in Figure 9E indicate that dual PD-1/LAG-3 blockade was more effective than dual PD-1/TIM-3, dual TIM-3/LAG-3, and even triple PD-1/TIM-3/LAG-3 blockade, but still inferior to that reached in MM-rem after single PD-1 or TIM-3 blockade, or MM-dia after dual PD-1/TIM-3 blockade.

These data confirm that the relapse is the most challenging setting, and immune-based strategies should be delivered in remission, when the immune suppressive TME commitment is partially relieved.

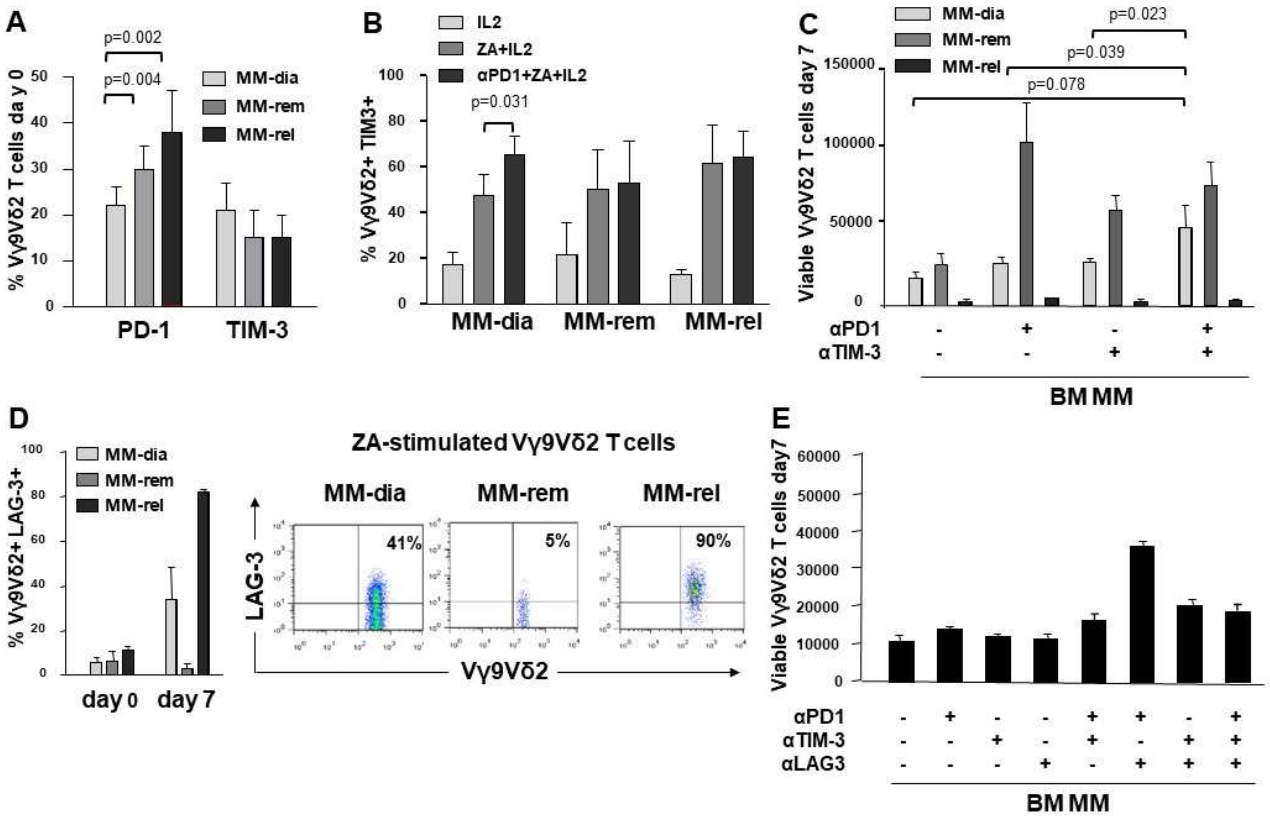

Figure 9 **The ICP/ICP-L network is dynamically shaped by the disease status** **A**) PD-1 and TIM-3 expression in resting BM Vγ9Vδ2 T cells from MM patients at different stages of disease (MM-dia, MM-rem and MM-rel). Bars represent the mean values ± from 7 (MM-rel) to 50 (MM-dia). **B**) TIM-3 expression in BM MM Vγ9Vδ2 T cells after 7-day ZA stimulation in the presence or absence of αPD1. Bars represent the mean values ± from 3 (MM-rem) to 6 (MM-dia). **C**) BM MM Vγ9Vδ2 T-cell proliferation in MM-dia, MM-rem and MM-rel after 7-day ZA stimulation in the presence of αPD1, αTIM-3, and the combination thereof. Bars represent the mean values ± from 4 (MM-rem) to 8 (MM-dia). **D**) *left:* LAG-3 expression in resting (day 0) or ZA-stimulated BM Vγ9Vδ2 T cells from MM patients at different stages of disease (MM-dia, MM-rem and MM-rel). Bars represent the mean ± SE from 4 (MM-rel) to 5 (MM-dia) experiments; *right:* cytofluorimetric analyses of LAG-3 expression in ZA-stimulated Vγ9Vδ2 T cells from one representative MM-dia, MM-rem, and MM-rel. **E**) BM MM Vγ9Vδ2 T-cell proliferation in MM-rel after 7-day ZA stimulation in the presence αPD1, αTIM-3, and αLAG-3 as single agents or in combination. Bars represent the mean ± SE of 3 experiments.

DISCUSSION

BM MM Vγ9Vδ2 T cells epitomize the paradigm of dysfunctional immune effector cells become anergic and senescent as a consequence of the multifaceted immune suppression operated by tumor cells and bystander cells in the TME. We have previously reported that BM MM Vγ9Vδ2 T cells become PD-1+ and anergic to ZA stimulation very early, when myeloma cells are less than 10% in the BM, and even at this stage they cannot be fully rescued by single anti-PD-1 blockade (9).

In this work, we have extended our investigation of dysfunctional BM MM Vγ9Vδ2 T cells to deepen our understanding of the multifaceted role played by the ICP/ICP-L network in the TME of MM patients. A significant fraction of resting BM MM Vγ9Vδ2 T cells showed PD-1 and TIM-3 co-expression, as previously reported in conventional T cells from patients with solid cancers (27–30), AML (31), and MM (32–34), and in Vγ9Vδ2 T cells chronically exposed to infectious agents (35) or cancer cells in solid (36,37) and blood tumors (38). PD-1 and TIM-3 co-expression is considered a phenotypic hallmark of functional exhaustion (31–34). However, ICP co-expression is not sufficient per se to identify functional exhausted cells. Immune competent effector T cells can also express ICP after activation, but in this case, ICP expression is transient and finalized to dampen the activation driven by TCR and co-stimulatory molecules to prevent uncontrolled immune reactions eventually leading to autoimmunity, especially if antigen challenges occur in inflammatory microenvironment. In contrast, ICP expression on chronically activated T cells reflects a dysfunctional state induced by the long-term exposure to antigens in the context of an inappropriate microenvironment. Thus, BM MM Vγ9Vδ2 T cells fulfil the operational criteria of functionally exhausted cells because: 1) PD-1/TIM-3 co-expression is associated with functional dysfunctions; 2) functional dysfunctions are observed after challenging the normal counterpart (i.e., BM Ctrl Vγ9Vδ2 T cells) with the same antigen (i.e., ZA) in the same microenvironment (i.e., BM) (61). After ZA stimulation, BM MM Vγ9Vδ2 T cells further up-regulated PD-1 and TIM-3 expression. In mice, functionally exhausted cells are hierarchically organized from progenitor to terminally differentiated exhausted T cells (61), the latter being more difficult to rescue compared with the former. Our data indicate that also in humans inadvertent or inappropriate engagement of immune effector cells can worsen their functional exhaustion in the TME.

PD-1+ TIM-3+ BM MM Vγ9Vδ2 T cells also express immune senescence markers (40,48,49). Vγ9Vδ2 T cells from normal individuals are particularly resistant to immune senescence due to their peculiar capacity to adapt to life-long stimulation (74). In MM, the immune suppressive TME hampers the capacity of Vγ9Vδ2 T cells to resist life-long stimulation. CD160 expression was mainly restricted to CM and TEMRA BM MM VγVδ2 T cells, which is the subset with the highest

ICP expression. Interestingly, the loss of CD27 and CD28 and the expression of TIM-3 and CD57 on T cells has been associated with resistance to ICP blockade (42).

Immune senescence of BM MM Vγ9Vδ2 T cells was confirmed by the expression of pγH2AX. A weak pγH2AX expression was already detectable in freshly isolated BM γδ T cells, but significantly increased after ZA stimulation, whereas no expression was detected in resting or ZA-stimulated BM Ctrl samples. γH2AX phosphorylation is used by mammalian cells to prevent genomic instability after DNA breakage induced by genotoxic stress or senescence (75). Our data indicate that pgH2AX quantification can be used to predict the functional outcome of immune effector cells after stimulation, and not only to screen the genotoxic profile of drugs and to identify senescent cells in aging and disease (76).

The functional plasticity of Vγ9Vδ2 T cells embedded in the immune suppressive TME can lead to the acquisition of regulatory or pro-tumoral functions (53–55). We have not found any phenotypic or functional evidence to support a regulatory/pro-tumoral shift of BM Vγ9Vδ2 T cells in MM , unlike colon, breast and other solid cancers in which senescent γδ T cells have been reported to suppress the proliferation of conventional T cells (57–59,77,78).

ICP expression reflects a dysfunctional state induced by the long-term exposure to antigens in the context of an inappropriate microenvironment. During tumor development, there is usually a long latency period after an initiating clonal oncogenic event during which tumor antigens are presented to the immune system in a noninflammatory, non- stimulatory context (79). In MM, BM MM Vγ9Vδ2 T cells are exposed to supra-physiological IPP concentrations released in large amounts by BMSC in the TME and to a lower extent by myeloma cells (26). Interestingly, BMSC from MGUS individuals released very high IPP amounts, significantly higher than those released by BMSC from MM patients with active disease. Early IPP chronic stimulation in conjunction with ICP-L expression (*i.e.* PD-L1 and Gal-9) and metabolic alterations that we observed poison the TME in favor of immune suppressor cells to the expense of immune effector cells, including Vγ9Vδ2 T cells. Data using MM BMSC and fully competent Vγ9Vδ2 T cells from Ctrl PB confirmed that both soluble factors and cell-to-cell contact were important to induce the refractoriness to ZA stimulation and ICP upregulation. MGUS individuals are healthy people with less than 10% myeloma cell infiltration and no organ damage, but BM Vγ9Vδ2 T cells in MGUS are already as dysfunctional as in MM with active disease at diagnosis or in relapse. The current wisdom is that the immune competence of MGUS individuals is preserved to explain why myeloma cells are hold in check for years even if they already harbour many genetic and epigenetic alterations. Our findings challenge this wisdom by showing that the TME is reprogrammed very early to induce dysfunctional immune effector cells and

establish a favourable groundwork to promote the growth and survival of myeloma cells (9). Similar results have been reported for tumor-specific CD8+ cells. *Schietinger et al.* showed in a tamoxifen-inducible liver cancer mouse model that tumor-specific CD8+ cells become dysfunctional early during the pre-malignant phase of tumorigenesis (80).

Exhaustion and immune senescence in BM MM Vγ9Vδ2 T cells were associated with alterations in the TCR signaling pathway. pAKT, pSTAT1, pJAK1, and ZAP-70 were down-regulated, while PTEN was up-regulated in MM BM Vγ9Vδ2 T cells. ZAP-70 was also down-regulated in BM CD3+ Vγ9Vδ2- T cells of MM patients. The significantly lower ZAP-70 expression in BM compared further confirms how powerful is the immune conditioning exerted by the prolonged exposure to tumor cells in the TME. In contrast, we have not observed CD3-ζ chain down-modulation in Vγ9Vδ2 T cells and CD3+ Vγ9Vδ2- T cells unlike previous reports (66). Increasing evidence suggests that ZAP-70 down-regulation in T cells and NK cells can contribute to impairment of anti -tumor immune responses and bias the efficacy of immunotherapy (81). We are currently investigating whether ZAP-70 expression is correlated with Vγ9Vδ2 T-cell dysfunctions in MM.

TIM-3 was significantly up-regulated after ZA stimulation in the presence of αPD1, whereas PD-1 was not up-regulated after ZA stimulation in the presence of αTIM3, indicating a one-way rather than two-way cross-talk between these molecules. TIM-3 up-regulation after PD-1 blockade in conventional T cells is considered a potential mechanism of adaptive resistance to αPD-1 *in vitro* (69,70,82) and *in vivo* (69,70,83).

Dual PD-1/TIM-3 blockade was more effective than single ICP blockade to partially recover proliferation, IFN-γ production, and CD107 expression in BM Vγ9Vδ2 T cells, and to mitigate the altered expression of TCR-associated molecules. Dual PD-1/TIM-3 blockade has also been reported to up-regulate IFN-γ and TNF-α production in PB Vγ9Vδ2 T cells of AML patients after pAg stimulation (38).

Dual ICP blockade is currently carried on in the clinical setting using mAb combinations willing to improve response rates and/or overcome acquired resistance to single ICP blockade (84). However, this strategy is burdened by clinical and financial toxicities (85). One alternative approach could be the identification of druggable intracellular intersections between these pathways. To this end, we have investigated the IL-27/pSTAT1/T-bet, and the PI3K/AKT pathways that have been reported to connect PD-1 and TIM-3 in tumor-bearing mice and patients with head and neck squamous cell carcinomas (HNSCC) (70,71). However, our data indicate that these pathways are not druggable in BM MM Vγ9Vδ2 T cells.

Interestingly, T-bet expression was low in resting BM MM Vγ9Vδ2 T cell,s as recently shown in the BM of patients with AML. In these patients, the emergence of severely exhausted (i.e., T-bet^{low}, PD-1+) T cells has been reported to predict disease relapse after allogeneic transplantation (72). By contrast, IL-27R expression was high in BM MM Vγ9Vδ2 T cells. After ZA stimulation in the presence of anti-PD-1, both T-bet and IL-27R expression remained unmodified, suggesting that T-bet up-regulation was not involved in TIM-3 up-regulation. To further elaborate on the possible role of IL-27 *via* the NFIL/STAT3/NFIL3 axis (71), we investigated IL27 in MM patients. Soluble IL-27 levels were low in the BM supernatants of BM MM patients and IL-27 concentrations did not increase in the supernatants of ZA-stimulated BM MM V9Vδ2 T cells with or without anti-PD-1. We speculate that BM MM Vγ9Vδ2 T cells are equipped with an high number of IL-27R to catch the very little amount of IL-27 available in the TME to eventually improve their antitumor activity, and not to up-regulate TIM-3.

This is the first report comparing the role of ICP/ICP-L and their blockade in the TME of MM-dia, MM-rem and MM-rel. PD-1 expression in BM MM Vγ9Vδ2 T cells was significantly higher in MM-rel than in MM-rem and MM-dia, whereas TIM-3 expression was not different. Interestingly, MM-rem showed significantly higher PD-1 expression than MM-dia, indicating that it not easy for BM MM Vγ9Vδ2 T cells to get rid of the immune suppressive imprinting operated by the TME. Single or dual blockade PD-1/TIM-3 showed different efficacy according to the disease status. MM-rem showed the best recovery in the presence of the anti-PD-1 or anti-TIM-3: the former was slightly better than the latter, whereas the combination did not show any additive or synergistic effect. Dual PD-1/TIM-3 blockade showed an additive effect in MM-dia, whereas MM-rel were totally refractory, no matter single or dual PD-1/TIM-3 blockade was applied. It remains to be determined in MM-rel whether the immune dysfunction anticipates the myeloma cell regrowth or vice-versa.

Our data confirm that the refractory/relapse setting remains the most difficult challenge for immune-based interventions. Paradoxically, this is also the clinical setting usually selected for first-in-man or phase I/II studies, as done in MM (86), with the risk to jeopardize future investigation since results will barely meet clinical expectations. Interestingly, BM Vγ9Vδ2 T cells from MM-rel significantly up-regulated LAG-3 after ZA stimulation in addition to PD-1 and TIM-3. In the MC38 mouse tumor model, dual PD-1/TIM-3 blockade increases the expression of LAG-3 in T cells, and LAG-3 expression confers resistance to anti-PD-1/TIM-3 treatment (87). Increased LAG-3 expression in T cells of patients with non-small cell lung cancer (NSCLC) has been associated with resistance to anti-PD-1 treatment and shorter progression-free survival(29). Likewise, co-expression of PD-1, TIM-3, and LAG-3 in TILs of patients clear cell renal cell carcinoma (CCRC) has been associated with high risk of early progression (30).

Dual PD-1/LAG-3 blockade was the most effective combination to improve the proliferative responses to ZA stimulation in MM-rel, but still insufficient to reach the range of BM Ctrl values, confirming the profound immune suppressive TME commitment in this setting. Triple PD-1/TIM-3/LAG-3 blockade has been proposed to overcome this barrier in syngeneic mouse tumor models (87), but in our hands triple blockade was less effective than dual PD-1/LAG-3 blockade. Alternative strategies can be dual ICP blockade after lymphodepletion by whole body radiation, as reported in the 5T33 murine MM model (88), or after the addition of TGF-β inhibitors as reported by Kwon et al.(32), but these strategies are not easy to apply to humans.

In conclusion, the immune suppressive TME contexture in MM is under dynamic evolution and ICP blockade should be individually tailored to gain the maximum efficacy. The remission phase remains the most favorable setting to deliver Vγ9Vδ2 T-cell-based immune interventions.

BIBLIOGRAPHY

1. Robert C. A decade of immune-checkpoint inhibitors in cancer therapy. *Nat Commun* (2020) 11:3801. doi: 10.1038/s41467-020-17670-y

2. Ansell SM, Lesokhin AM, Borrello I, Halwani A, Scott EC, Gutierrez M, Schuster SJ, Millenson MM, Cattry D, Freeman GJ, et al. PD-1 Blockade with Nivolumab in Relapsed or Refractory Hodgkin's Lymphoma. *New England Journal of Medicine* (2015) 372:311–319. doi: 10.1056/nejmoa1411087

3. Eroglu Z, Zaretsky JM, Hu-Lieskovan S, Kim DW, Algazi A, Johnson DB, Liniker E, Kong B, Munhoz R, Rapisuwon S, et al. High response rate to PD-1 blockade in desmoplastic melanomas. *Nature* (2018) 553:347–350. doi: 10.1038/nature25187

4. Finn RS, Ryoo BY, Merle P, Kudo M, Bouattour M, Lim HY, Breder V, Edeline J, Chao Y, Ogasawara S, et al. Pembrolizumab As Second-Line Therapy in Patients With Advanced Hepatocellular Carcinoma in KEYNOTE-240: A Randomized, Double-Blind, Phase III Trial. *J Clin Oncol* (2020) 38:193–202. doi: 10.1200/JCO.19.01307

5. Salik B, Smyth MJ, Nakamura K. Targeting immune checkpoints in hematological malignancies. *J Hematol Oncol* (2020) 13: doi: 10.1186/s13045-020-00947-6

6. García-Ortiz A, Rodríguez-García Y, Encinas J, Maroto-Martín E, Castellano E, Teixidó J, Martínez-López J. The role of tumor microenvironment in multiple myeloma development and progression. *Cancers (Basel)* (2021) 13:1–22. doi: 10.3390/cancers13020217

7. Lomas OC, Tahri S, Ghobrial IM. The microenvironment in myeloma. *Curr Opin Oncol* (2020) 32:170–175. doi: 10.1097/CCO.0000000000000615

8. Danziger SA, McConnell M, Gockley J, Young MH, Rosenthal A, Schmitz F, Reiss DJ, Farmer P, Alapat D V, Singh A, et al. Bone marrow microenvironments that contribute to patient outcomes in newly diagnosed multiple myeloma: A cohort study of patients in the Total Therapy clinical trials. *PLoS Med* (2020) 17: doi: 10.1371/journal.pmed.1003323

9. Castella B, Foglietta M, Sciancalepore P, Rigoni M, Coscia M, Griggio V, Vitale C, Ferracini R, Saraci E, Omedé P, et al. Anergic bone marrow Vγ9Vδ2 T cells as early and long-lasting markers of PD-1-targetable microenvironment-induced immune suppression in human myeloma. *Oncoimmunology* (2015) 4:e1047580. doi: 10.1080/2162402X.2015.1047580

10. Liu J, Hamrouni A, Wolowiec D, Coiteux V, Kuliczkowski K, Hetuin D, Saudemont A, Quesnel B. Plasma cells from multiple myeloma patients express B7-H1 (PD-L1) and increase expression after stimulation with IFN-γ and TLR ligands via a MyD88-, TRAF6-, and MEK-dependent pathway. *Blood* (2007) 110:296–304. doi: 10.1182/blood-2006-10-051482

11. An G, Acharya C, Feng X, Wen K, Zhong M, Zhang L, Munshi NC, Qiu L, Tai YT, Anderson KC. Osteoclasts promote immune suppressive microenvironment in multiple myeloma: Therapeutic implication. *Blood* (2016) 128:1590–1603. doi: 10.1182/blood-2016-03-707547

12. Sponaas AM, Waage A, Vandsemb EN, Misund K, Børset M, Sundan A, Slørdahl TS, Standal T. Bystander Memory T Cells and IMiD/Checkpoint Therapy in Multiple Myeloma: A Dangerous Tango? *Front Immunol* (2021) 12:636375. doi: 10.3389/fimmu.2021.636375

13. Castella B, Foglietta M, Riganti C, Massaia M. Vγ9Vδ2 T cells in the bone marrow of myeloma patients: A paradigm of microenvironment-induced immune suppression. *Front Immunol* (2018) 9:1492. doi: 10.3389/fimmu.2018.01492

14. Pont F, Familiades J, Déjean S, Fruchon S, Cendron D, Poupot M, Poupot R, L'Faqihi-Olive F, Prade N, Ycart B, et al. The gene expression profile of phosphoantigen-specific human γδ T lymphocytes is a blend of αβ T-cell and NK-cell signatures. *Eur J Immunol* (2012) 42:228–240. doi: 10.1002/eji.201141870

15. Designed Research; G J-JFP, Merville P, Milpied P. Single-cell RNA sequencing unveils the shared and the distinct cytotoxic hallmarks of human TCRVδ1 and TCRVδ2 γδ T lymphocytes contributed new reagents/ana-lytic tools; G. (2019) 116: doi: 10.1073/pnas.1818488116

16. Castella B, Vitale C, Coscia M, Massaia M. Vγ9Vδ2 T cell-based immunotherapy in hematological malignancies: From bench to bedside. *Cellular and Molecular Life Sciences* (2011) 68:2419–2432. doi: 10.1007/s00018-011-0704-8

17. Gruenbacher G, Thurnher M. Mevalonate metabolism in cancer. *Cancer Lett* (2015) 356:192–196. doi: 10.1016/j.canlet.2014.01.013

18. Harly C, Guillaume Y, Nedellec S, Peigné CM, Mönkkönen H, Mönkkönen J, Li J, Kuball J, Adams EJ, Netzer S, et al. Key implication of CD277/butyrophilin-3 (BTN3A) in cellular stress sensing by a major human γδ T-cell subset. *Blood* (2012) 120:2269–2279. doi: 10.1182/blood-2012-05-430470

19. Riganti C, Castella B, Massaia M. ABCA1, apoA-I, and BTN3A1: A Legitimate ménage à trois in dendritic cells. *Front Immunol* (2018) 9:1246. doi: 10.3389/fimmu.2018.01246

20. Rigau M, Ostrouska S, Fulford TS, Johnson DN, Woods K, Ruan Z, McWilliam HEG, Hudson C, Tutuka C, Wheatley AK, et al. Butyrophilin 2A1 is essential for phosphoantigen reactivity by γδ T cells. *Science* (2020) 5516:1–24. doi: 10.1126/science.aay5516

21. Karunakaran MM, Willcox CR, Salim M, Paletta D, Fichtner AS, Noll A, Starick L, Nöhren A, Begley CR, Berwick KA, et al. Butyrophilin-2A1 Directly Binds Germline-Encoded Regions of the Vγ9Vδ2 TCR and Is Essential for Phosphoantigen Sensing. *Immunity* (2020) 52:487-498.e6. doi: 10.1016/j.immuni.2020.02.014

22. Lo Presti E, Corsale AM, Dieli F, Meraviglia S. Γδ Cell-Based Immunotherapy for Cancer. *Expert Opin Biol Ther* (2019) 19:887–895. doi: 10.1080/14712598.2019.1634050

23. Silva-Santos B, Mensurado S, Coffelt SB. γδ T cells: pleiotropic immune effectors with therapeutic potential in cancer. *Nat Rev Cancer* (2019) 19:392–404. doi: 10.1038/s41568-019-0153-5

24. Chan KF, Duarte JDG, Ostrouska S, Behren A. γδ T Cells in the Tumor Microenvironment—Interactions With Other Immune Cells. *Front Immunol* (2022) 13:3598. doi: 10.3389/fimmu.2022.894315

25. Castella B, Melaccio A, Foglietta M, Riganti C, Massaia M. Vγ9Vδ2 T Cells as Strategic Weapons to Improve the Potency of Immune Checkpoint Blockade and Immune Interventions in Human Myeloma. *Front Oncol* (2018) 8:508. doi: 10.3389/fonc.2018.00508

26. Castella B, Kopecka J, Sciancalepore P, Mandili G, Foglietta M, Mitro N, Caruso D, Novelli F, Riganti C, Massaia M. The ATP-binding cassette transporter A1 regulates phosphoantigen release and Vγ39Vδ2 T cell activation by dendritic cells. *Nat Commun* (2017) 8:1–14. doi: 10.1038/ncomms15663

27. Granier C, Dariane C, Combe P, Verkarre V, Urien S, Badoual C, Roussel H, Mandavit M, Ravel P, Sibony M, et al. Tim-3 expression on tumor-infiltrating PD-1+CD8+ T cells correlates with poor clinical outcome in renal cell carcinoma. *Cancer Res* (2017) 77:1075–1082. doi: 10.1158/0008-5472.CAN-16-0274

28. Thommen DS, Schreiner J, Müller P, Herzig P, Roller A, Belousov A, Umana P, Pisa P, Klein C, Bacac M, et al. Progression of lung cancer is associated with increased dysfunction of T cells defined by coexpression of multiple inhibitory receptors. *Cancer Immunol Res* (2015) 3:1344–1354. doi: 10.1158/2326-6066.CIR-15-0097

29. Datar I, Sanmamed MF, Wang J, Henick BS, Choi J, Badri T, Dong W, Mani N, Toki M, Mejías LD, et al. Expression analysis and significance of PD-1, LAG-3, and TIM-3 in human non-small cell lung cancer using spatially resolved and multiparametric single-cell analysis. *Clinical Cancer Research* (2019) 25:4663–4673. doi: 10.1158/1078-0432.CCR-18-4142

30. Giraldo NA, Becht E, Vano Y, Petitprez F, Lacroix L, Validire P, Sanchez-Salas R, Ingels A, Oudard S, Moatti A, et al. Tumor-infiltrating and peripheral blood T-cell immunophenotypes predict early relapse in localized clear cell renal cell carcinoma. *Clinical Cancer Research* (2017) 23:4416–4428. doi: 10.1158/1078-0432.CCR-16-2848

31. Tan J, Chen S, Yao D, Zhang Y, Yang L, Lai J, Huang K, Chen J, Yu Z, Zhong J, et al. Higher Tim-3 expression concurrent with PD-1 in exhausted CD4+ and CD8+T cells in patients with acute myeloid leukemia. *Exp Hematol* (2017) 53:S84–S85. doi: 10.1016/j.exphem.2017.06.190

32. Kwon M, Kim CG, Lee H, Cho H, Kim Y, Lee EC, Choi SJ, Park J, Seo IH, Bogen B, et al. PD-1 blockade reinvigorates bone marrow CD8+ T cells from patients with multiple myeloma in the presence of TGFb inhibitors. *Clinical Cancer Research* (2020) 26:1644–1655. doi: 10.1158/1078-0432.CCR-19-0267

33. Batorov E v., Aristova TA, Sergeevicheva V v., Sizikova SA, Ushakova GY, Pronkina N v., Shishkova I v., Shevela EY, Ostanin AA, Chernykh ER. Quantitative and functional characteristics of circulating and bone marrow PD-1- and TIM-3-positive T cells in treated multiple myeloma patients. *Sci Rep* (2020) 10: doi: 10.1038/s41598-020-77941-y

34. Tan J, Chen S, Huang J, Chen Y, Yang L, Wang C, Zhong J, Lu Y, Wang L, Zhu K, et al. Increased exhausted CD8 + T cells with programmed death-1, T-cell immunoglobulin and mucin-domain-containing-3 phenotype in patients with multiple myeloma. *Asia Pac J Clin Oncol* (2018) 14:e266–e274. doi: 10.1111/ajco.13033

35. Gogoi D, Biswas D, Borkakoty B, Mahanta J. Exposure to Plasmodium vivax is associated with the increased expression of exhaustion markers on γδ T lymphocytes. *Parasite Immunol* (2018) 40:1–9. doi: 10.1111/pim.12594

36. Girard P, Charles J, Cluzel C, Degeorges E, Manches O, Plumas J, De Fraipont F, Leccia MT, Mouret S, Chaperot L, et al. The features of circulating and tumor-infiltrating γδ T cells in melanoma patients display critical perturbations with prognostic impact on clinical outcome. *Oncoimmunology* (2019) 8:1–16. doi: 10.1080/2162402X.2019.1601483

37. Li X, Lu H, Gu Y, Zhang X, Zhang G, Shi T, Chen W. Tim-3 suppresses the killing effect of Vγ9Vδ2 T cells on colon cancer cells by reducing perforin and granzyme B expression. *Exp Cell Res* (2019) 386:111719. doi: 10.1016/j.yexcr.2019.111719

38. Wu K, Feng J, Xiu Y, Li Z, Lin Z, Zhao H, Zeng H, Xia W, Yu L, Xu B. Vδ2 T cell subsets, defined by PD-1 and TIM-3 expression, present varied cytokine responses in acute myeloid leukemia patients. *Int Immunopharmacol* (2020) 80:106122. doi: 10.1016/j.intimp.2019.106122

39. Zhao Y, Shao Q, Peng G. Exhaustion and senescence: two crucial dysfunctional states of T cells in the tumor microenvironment. *Cell Mol Immunol* (2020) 17:27–35. doi: 10.1038/s41423-019-0344-8

40. Suen H, Brown R, Yang S, Weatherburn C, Ho PJ, Woodland N, Nassif N, Barbaro P, Bryant C, Hart D, et al. Multiple myeloma causes clonal T-cell immunosenescence: Identification of potential novel targets for promoting tumour immunity and implications for checkpoint blockade. *Leukemia* (2016) 30:1716–1724. doi: 10.1038/leu.2016.84

41. Zelle-Rieser C, Thangavadivel S, Biedermann R, Brunner A, Stoitzner P, Willenbacher E, Greil R, Jöhrer K. T cells in multiple myeloma display features of exhaustion and senescence at the tumor site. *J Hematol Oncol* (2016) 9:1–12. doi: 10.1186/s13045-016-0345-3

42. Moreira A, Gross S, Kirchberger MC, Erdmann M, Schuler G, Heinzerling L. Senescence markers: Predictive for response to checkpoint inhibitors. *Int J Cancer* (2019) 144:1147–1150. doi: 10.1002/ijc.31763

43. Mariani S, Muraro M, Pantaleoni F, Fiore F, Nuschak B, Peola S, Foglietta M, Palumbo A, Coscia M, Castella B, et al. Effector gammadelta T cells and tumor cells as immune targets of zoledronic acid in multiple myeloma. *Leukemia* (2005) 19:664–670. doi: 10.1038/SJ.LEU.2403693

44. Fichtner AS, Ravens S, Prinz I. Human γδ TCR Repertoires in Health and Disease. *Cells* (2020) 9: doi: 10.3390/cells9040800

45. Gober HJ, Kistowska M, Angman L, Jenö P, Mori L, De Libero G. Human T cell receptor gammadelta cells recognize endogenous mevalonate metabolites in tumor cells. *J Exp Med* (2003) 197:163–168. doi: 10.1084/JEM.20021500

46. Li Y, Li G, Zhang J, Wu X, Chen X. The Dual Roles of Human γδ T Cells: Anti-Tumor or Tumor-Promoting. *Front Immunol* (2021) 11: doi: 10.3389/fimmu.2020.619954

47. Roux C, Mucciolo G, Kopecka J, Novelli F, Riganti C, Cappello P. IL-17a depletion affects the metabolism of macrophages treated with gemcitabine. *Antioxidants* (2021) 10:1–24. doi: 10.3390/antiox10030422

48. Crespo J, Sun H, Welling TH, Tian Z, Zou W. T cell anergy, exhaustion, senescence, and stemness in the tumor microenvironment. *Curr Opin Immunol* (2013) 25:214–221. doi: 10.1016/j.coi.2012.12.003

49. Dey M, Huff WX, Kwon JH, Henriquez M, Fetcko K. The evolving role of CD8+CD28- immunosenescent T cells in cancer immunology. *Int J Mol Sci* (2019) 20: doi: 10.3390/ijms20112810

50. Noren Hooten N, Evans MK. Techniques to Induce and Quantify Cellular Senescence. *J Vis Exp* (2017)55533. doi: 10.3791/55533

51. Zhang Y, Pfannenstiel LW, Bolesta E, Montes CL, Zhang X, Chapoval AI, Gartenhaus RB, Strome SE, Gastman BR. Interleukin-7 inhibits tumor-induced CD27 -CD28 - suppressor T cells: Implications for cancer immunotherapy. *Clinical Cancer Research* (2011) 17:4975–4986. doi: 10.1158/1078-0432.CCR-10-3328

52. Aiello A, Farzaneh F, Candore G, Caruso C, Davinelli S, Gambino CM, Ligotti ME, Zareian N, Accardi G. Immunosenescence and its hallmarks: How to oppose aging strategically? A review of potential options for therapeutic intervention. *Front Immunol* (2019) 10:1–19. doi: 10.3389/fimmu.2019.02247

53. Zhao Y, Niu C, Cui J. Gamma-delta (γδ) T Cells: Friend or Foe in Cancer Development. *J Transl Med* (2018) 16:1–13. doi: 10.1186/s12967-017-1378-2

54. Lafont V, Sanchez F, Laprevotte E, Michaud HA, Gros L, Eliaou JF, Bonnefoy N. Plasticity of γδ T cells: Impact on the anti-tumor response. *Front Immunol* (2014) 5:622. doi: 10.3389/fimmu.2014.00622

55. Fleming C, Morrissey S, Cai Y, Yan J. γδ T Cells: Unexpected Regulators of Cancer Development and Progression. *Trends Cancer* (2017) 3:561–570. doi: 10.1016/j.trecan.2017.06.003

56. Horenstein AL, Quarona V, Toscani D, Costa F, Chillemi A, Pistoia V, Giuliani N, Malavasi F. Adenosine generated in the bone marrow niche through a CD38-mediated pathway correlates with progression of human myeloma. *Molecular Medicine* (2016) 22:694–704. doi: 10.2119/molmed.2016.00198

57. Daley D, Zambirinis CP, Seifert L, Akkad N, Mohan N, Werba G, Barilla R, Torres-Hernandez A, Hundeyin M, Mani VRK, et al. γδ T Cells Support Pancreatic Oncogenesis by Restraining αβ T Cell Activation. *Cell* (2016) 166:1485-1499.e15. doi: 10.1016/j.cell.2016.07.046

58. Wu P, Wu D, Ni C, Ye J, Chen W, Hu G, Wang Z, Wang C, Zhang Z, Xia W, et al. γδT17 cells promote the accumulation and expansion of myeloid-derived suppressor cells in human colorectal cancer. *Immunity* (2014) 40:785–800. doi: 10.1016/j.immuni.2014.03.013

59. Sureshbabu SK, Chaukar D, Chiplunkar SV. Hypoxia regulates the differentiation and anti-tumor effector functions of γδT cells in oral cancer. *Clin Exp Immunol* (2020)0–3. doi: 10.1111/cei.13436

60. Chen X, Shang W, Xu R, Wu M, Zhang X, Huang P, Wang F, Pan S. Distribution and functions of γδ T cells infiltrated in the ovarian cancer microenvironment. *J Transl Med* (2019) 17:144. doi: 10.1186/s12967-019-1897-0

61. Blank CU, Haining WN, Held W, Hogan PG, Kallies A, Lugli E, Lynn RC, Philip M, Rao A, Restifo NP, et al. Defining 'T cell exhaustion.' *Nat Rev Immunol* (2019) 19:665–674. doi: 10.1038/s41577-019-0221-9

62. Lugo-Villarino G, Maldonado-López R, Possemato R, Peñaranda C, Glimcher LH. T-bet is required for optimal production of IFN-γ and antigen-specific T cell activation by dendritic cells. *Proc Natl Acad Sci U S A* (2003) 100:7749–7754. doi: 10.1073/pnas.1332767100

63. Wu X, Wang Y, Xu J, Luo T, Deng J, Hu Y. MM-BMSCs induce naïve CD4+ T lymphocytes dysfunction through fibroblast activation protein a. *Oncotarget* (2017) 8:52614–52628. doi: 10.18632/oncotarget.17538

64. Zuazo M, Gato-Cañas M, Llorente N, Ibañez-Vea M, Arasanz H, Kochan G, Escors D. Molecular mechanisms of programmed cell death-1 dependent T cell suppression: Relevance for immunotherapy. *Ann Transl Med* (2017) 5:1–9. doi: 10.21037/atm.2017.06.11

65. Pereira BI, De Maeyer RPH, Covre LP, Nehar-Belaid D, Lanna A, Ward S, Marches R, Chambers ES, Gomes DCO, Riddell NE, et al. Sestrins induce natural killer function in senescent-like CD8+ T cells. *Nat Immunol* (2020) 21:684–694. doi: 10.1038/s41590-020-0643-3

66. Whiteside TL. Down-regulation of ζ-chain expression in T cells: A biomarker of prognosis in cancer? *Cancer Immunology, Immunotherapy*. Cancer Immunol Immunother (2004). p. 865–878 doi: 10.1007/s00262-004-0521-0

67. Nakagomi H, Petersson M, Magnusson I, Juhlin C, Matsuda M, Mellstedt H, Vivier JLT, Anderson P, Kiessling R. Decreased Expression of the Signal-transducing ζ Chains in Tumor-infiltrating T-Cells and NK Cells of Patients with Colorectal Carcinoma. *Cancer Res* (1993) 53:5610–5612.

68. Koneru M, Schaer D, Monu N, Ayala A, Frey AB. Defective Proximal TCR Signaling Inhibits CD8 + Tumor-Infiltrating Lymphocyte Lytic Function. *The Journal of Immunology* (2005) 174:1830–1840. doi: 10.4049/jimmunol.174.4.1830

69. Koyama S, Akbay EA, Li YY, Herter-Sprie GS, Buczkowski KA, Richards WG, Gandhi L, Redig AJ, Rodig SJ, Asahina H, et al. Adaptive resistance to therapeutic PD-1 blockade is associated with upregulation of alternative immune checkpoints. *Nat Commun* (2016) 7:1–9. doi: 10.1038/ncomms10501

70. Shayan G, Srivastava R, Li J, Schmitt N, Kane LP, Ferris RL. Adaptive resistance to anti-PD1 therapy by tim-3 upregulation is mediated by the PI3k-akt pathway in head and neck cancer. *Oncoimmunology* (2017) 6:1–11. doi: 10.1080/2162402X.2016.1261779

71. Zhu C, Sakuishi K, Xiao S, Sun Z, Zaghouani S, Gu G, Wang C, Tan DJ, Wu C, Rangachari M, et al. An IL-27/NFIL3 signalling axis drives Tim-3 and IL-10 expression and T-cell dysfunction. *Nat Commun* (2015) 6:1–11. doi: 10.1038/ncomms7072

72. Noviello M, Manfredi F, Ruggiero E, Perini T, Oliveira G, Cortesi F, de Simone P, Toffalori C, Gambacorta V, Greco R, et al. Bone marrow central memory and memory stem T-cell exhaustion in AML patients relapsing after HSCT. *Nat Commun* (2019) 10: doi: 10.1038/s41467-019-08871-1

73. Luo YL, Wang S, Fang ZX, Nie YC, Zhang LT, Huang CQ, Long L, Lai KF. STAT1 participates in the induction of substance P expression in airway epithelial cells by respiratory syncytial virus. *Exp Lung Res* (2021) 47:78–86. doi: 10.1080/01902148.2020.1850922

74. Xu W, Monaco G, Wong EH, Tan WLW, Kared H, Simoni Y, Tan SW, How WZY, Tan CTY, Lee BTK, et al. Mapping of γ/δ T cells reveals Vδ2+ T cells resistance to senescence. *EBioMedicine* (2019) 39:44–58. doi: 10.1016/j.ebiom.2018.11.053

75. Rahmanian N, Shokrzadeh M, Eskandani M. Recent advances in γH2AX biomarker-based genotoxicity assays: A marker of DNA damage and repair. *DNA Repair (Amst)* (2021) 108:103243. doi: 10.1016/j.dnarep.2021.103243

76. Biran A, Zada L, Abou Karam P, Vadai E, Roitman L, Ovadya Y, Porat Z, Krizhanovsky V. Quantitative identification of senescent cells in aging and disease. *Aging Cell* (2017) 16:661–671. doi: 10.1111/acel.12592

77. Liu X, Mo W, Ye J, Li L, Zhang Y, Hsueh EC, Hoft DF, Peng G. Regulatory T cells trigger effector T cell DNA damage and senescence caused by metabolic competition. *Nat Commun* (2018) 9: doi: 10.1038/s41467-017-02689-5

78. Schilbach K, Krickeberg N, Kaißer C, Mingram S, Kind J, Siegers GM, Hashimoto H. Suppressive activity of Vδ2+ γδ T cells on αβ T cells is licensed by TCR signaling and correlates with signal strength. *Cancer Immunology, Immunotherapy* (2020) 69:593–610. doi: 10.1007/s00262-019-02469-8

79. Willimsky G, Blankenstein T. Sporadic immunogenic tumours avoid destruction by inducing T-cell tolerance. *Nature* (2005) 437:141–146. doi: 10.1038/nature03954

80. Andrea Schietinger, Mary Philip, Varintra E. Krisnawan, Edison Y. Chiu, Jeffrey J. Delrow, Ryan S. Basom, Peter Lauer, Dirk G. Brockstedt, Sue E. Knoblaugh, Günter J. Hämmerling, Todd D. Schell, Natalio Garbi PDG. Tumor-Specific T Cell Dysfunction Is a Dynamic Antigen-Driven Differentiation Program Initiated Early during Tumorigenesis. *Physiol Behav* (2017) 176:139–148. doi: 10.1016/j.immuni.2016.07.011.Tumor-Specific

81. Chen J, Moore A, Ringshausen I. ZAP-70 Shapes the Immune Microenvironment in B Cell Malignancies. *Front Oncol* (2020) 10: doi: 10.3389/fonc.2020.595832

82. Saleh R, Toor SM, Khalaf S, Elkord E. Breast cancer cells and PD-1/PD-L1 blockade upregulate the expression of PD-1, CTLA-4, TIM-3 and LAG-3 immune checkpoints in CD4+ T cells. *Vaccines (Basel)* (2019) 7:1–13. doi: 10.3390/vaccines7040149

83. Kato R, Yamasaki M, Urakawa S, Nishida K, Makino T, Morimoto-Okazawa A, Kawashima A, Iwahori K, Suzuki S, Ueda R, et al. Increased Tim-3+ T cells in PBMCs during nivolumab therapy correlate with responses and prognosis of advanced esophageal squamous cell carcinoma patients. *Cancer Immunology, Immunotherapy* (2018) 67:1673–1683. doi: 10.1007/s00262-018-2225-x

84. Kalbasi A, Ribas A. Tumour-intrinsic resistance to immune checkpoint blockade. *Nat Rev Immunol* (2020) 20:25–39. doi: 10.1038/s41577-019-0218-4

85. Abdel-Wahab N, Shah M, Suarez-Almazor ME. Adverse events associated with immune checkpoint blockade in patients with cancer: A systematic review of case reports. *PLoS One* (2016) 11:1–16. doi: 10.1371/journal.pone.0160221

86. Ribrag V, Avigan DE, Green DJ, Wise-Draper T, Posada JG, Vij R, Zhu Y, Farooqui MZH, Marinello P, Siegel DS. Phase 1b trial of pembrolizumab monotherapy for relapsed/refractory multiple myeloma: KEYNOTE-013. *Br J Haematol* (2019) 186:e41–e44. doi: 10.1111/bjh.15888

87. Yang M, Du W, Yi L, Wu S, He C, Zhai W, Yue C, Sun R, Menk A V., Delgoffe GM, et al. Checkpoint molecules coordinately restrain hyperactivated effector T cells in the tumor microenvironment. *Oncoimmunology* (2020) 9:1–11. doi: 10.1080/2162402X.2019.1708064

88. Jing W, Gershan JA, Weber J, Tlomak D, McOlash L, Sabatos-Peyton C, Johnson BD. Combined immune checkpoint protein blockade and low dose whole body irradiation as immunotherapy for myeloma. *J Immunother Cancer* (2015) 3:1–15. doi: 10.1186/s40425-014-0043-z

SUPPLEMENTAL DATA

Immune dysfunctions affecting bone marrow Vγ9Vδ2 T cells in multiple myeloma: role of immune and metabolic checkpoints

Supplemental Table 1. *List of antibodies used for flow cytometry*

Antigen	Fluorochrome	Catalog #	Company	clone
TCR Vγ9	FITC	130-125-242	Miltenyi Biotech	REA470
TCR Vγ9	PE	130-107-434	Miltenyi Biotech	REA470
TCR Vγ9	APC	130-111-010	Miltenyi Biotech	REA470
CD3	PerCpC-Vio700	130-113-141	Milteny Biotech	REA613
Program death-1 (PD-1)	APC	130-120-383	Milteny Biotech	REA1165
T-cell immunoglobulin mucin 3 (TIM-3)	PE	130-117-364	Milteny Biotech	F38-2E2
Lymphocyte-activation gene 3 (LAG-3)	PE	369306	BioLegend	11C3C65
Cytotoxic T-Lymphocyte Antigen 4 (CTLA-4)	APC	130-124-016	Miltenyi Biotech	BNI3
CD27	FITC	130-113-639	Miltenyi Biotech	REA499
CD45RA	PerCP	304156	BioLegend	HI100
CD57	FITC	130-122-935	Miltenyi Biotech	TB03
CD28	PE	130-126-202	Miltenyi Biotech	1,50E+09
CD160	APC	341208	BioLegend	BY55
CD39	PE	130-110-650	Miltenyi Biotech	REA739
CD38	FITC	356610	Biolgend	HB-7
CD73	PE	130-112-060	Miltenyi Biotech	REA804
CD4	PerCP-Vio 700	130-113-228	Miltenyi Biotech	REA623
CD8	APC	130-113-154	Miltenyi Biotech	BW135/80
Programmed Death-Ligand 1 (PD-L1)	PE	329706	BioLegend	29E.2A3
Galectin-9 (Gal-9)	APC	130-106-474	Miltenyi Biotech	REA435
IL-17A	PE	12-7179-42	eBioscience	eBio64DEC17
ZAP-70	PE	313404	BioLegend	1E7.2
CD3-ζ chain	FITC	644103	Biolegend	6B10.2
IFNγ	APC	502512	BioLegend	4S.B3
CD107	PE	328608	BioLegend	H4A3
Tbet	APC	130-098-607	Miltenyi Biotech	REA102
IL27 Receptor (R-IL27)	APC	FAB14791A	R&D Systems	191106
CD105	FITC	130-112-327	Miltenyi Biotech	REA794
Herpesvirus entry mediator (HVEM)	PE	318805	BioLegend	122
B And T Lymphocyte Associated BTLA	APC	344510	BioLegend	MIH26

Supplemental Table 2. *List of antibodies used for Western Blot*

Antibody name	clone	Diluition	Catalog #	Company
anti-phopho(Ser139)γ-H2A.X	rabbit polyclonal	1:1000	ab11171	Abcam, Cambridge, MA
phospho(Ser473)Akt	rabbit polyclonal	1:1000	9271	Cell Signallling Technology, Danvers, MA
anti-Akt	rabbit polyclonal	1:1000	9272	Cell Signallling Technology,
anti-SHP2	rabbit polyclonal	1:500	131541	Abcam
anti-PTEN	rabbit polyclonal	1:500	137337	Abcam
anti-phospho(Tyr1022/1023) JAK1	rabbit clone 59H4L5	1:1000	700028	ThermoFisher Scientific, Waltham, MA
anti-JAK1	rabbit clone JM75-03	1:2000	MA5-32780	ThermoFisher Scientific, Waltham, MA
anti-phospho(Tyr701)-STAT1	rabbit clone 15H13H67	1:1000	700349	ThermoFisher Scientific, Waltham, MA
anti-STAT1	mouse clone STAT1-79	1:500	HAO0832	ThermoFisher Scientific
β-tubulin	mouse clone D10	1:500	sc5274	Santa Cruz Biotechnology, Santa Cruz, CA;

Supplemental Figure 1

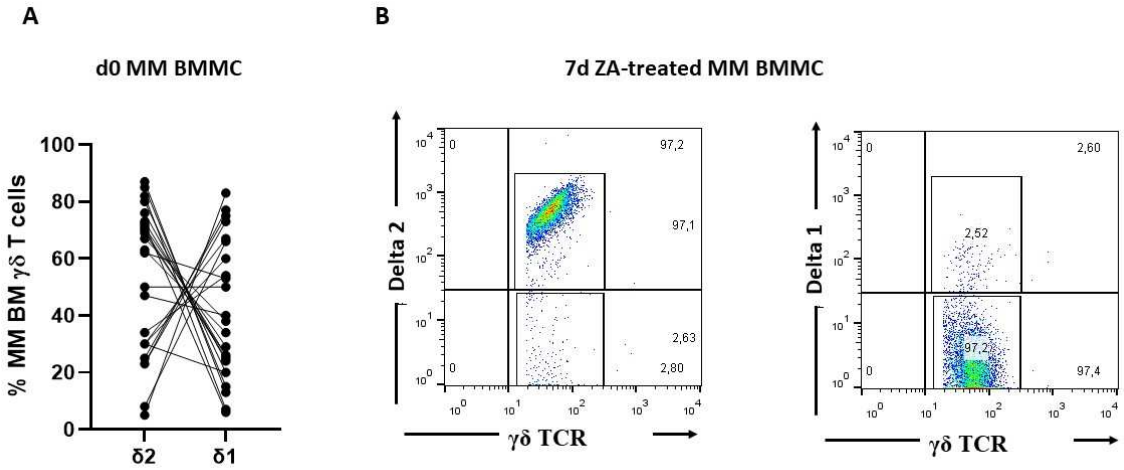

Vδ1 and Vδ2 T-cell subset distribution. A) Vδ1 and Vγ9Vδ2 T cells (Vδ2) distribution in freshly isolated (day 0) BMMC from 24 MM-dia; **B)** Representative cytofluorimetric analyses of Vδ1 and Vγ9Vδ2 T cell distribution after 7day stimulation of BMMC with ZA. Based on these data, we postulate that isolation of γδ T cells by immune magnetic separation using Anti-pan-γδ-conjugated magnetic microbeads (Miltenyi Biotec, Germany #130-050-701) will result in mixed Vδ1/Vδ2 subpopulations in freshly isolated BMMC (day 0) and almost only Vγ9Vδ2 T cells after ZA stimulation which is specific for these cells.

Supplemental Figure 2

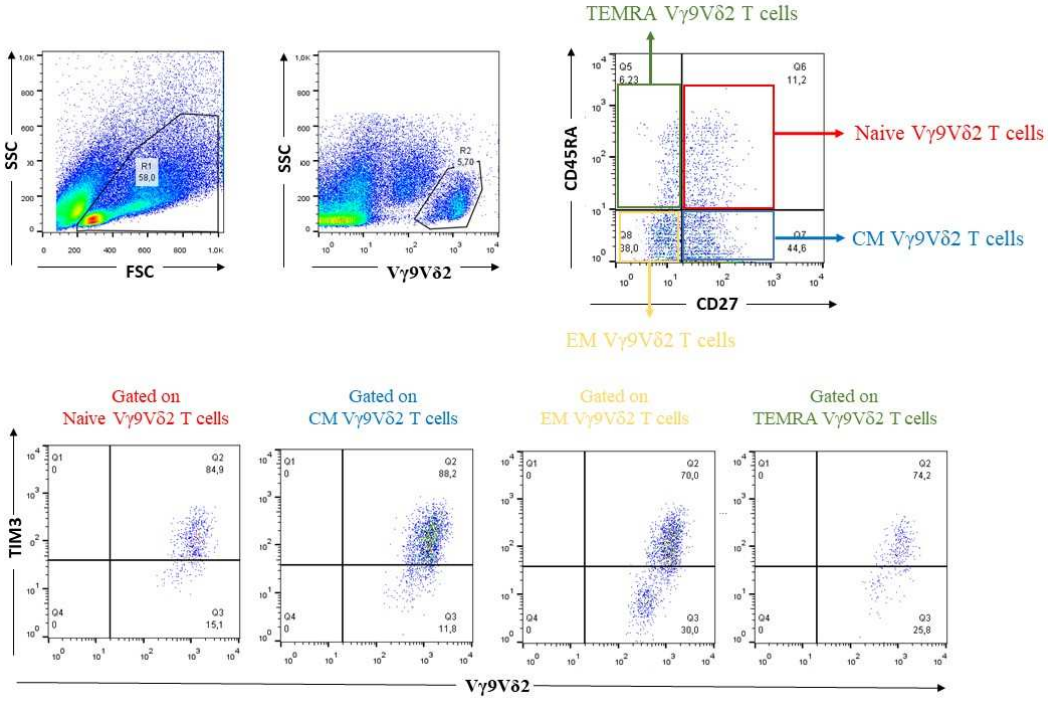

TIM-3 expression in Vγ9Vδ2 T-cell subsets . Gating strategy used to investigate TIM-3 expression Vγ9Vδ2 T-cell subsets..

Supplemental Figure 3

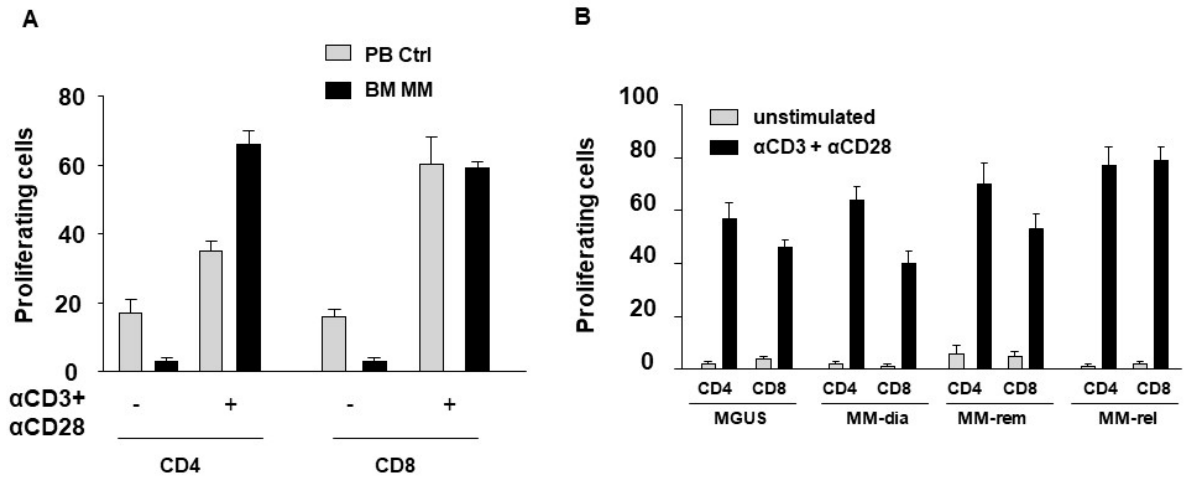

Preserved proliferation of BM MM CD4+ and CD8+ T cells to αCD3+αCD28 stimulation
A) CFSE-based proliferation of PB Ctrl and BM MM CD4+ and CD8+ T cells after 72 hours stimulation with αCD3+αCD28 stimulation. Proliferative responses are similar to those of PB Ctrl CD4+ and CD8+ cells. Bars represent mean values ± SE from 5 (PB Ctrl) to 10 (BM MM) experiments. Differences are not statistically significant **B)** CFSE-based proliferation of BM MM CD4+ and CD8+ T cells from MGUS and MM at different stages of the disease (MM-dia; MM-rem; MM-rel) after 72-hour stimulation with αCD3 + αCD28. BM MM CD4+ and CD8+ cell proliferation are not affected by the disease status. Bars represent mean values ± SE from 3 (MGUS, MM-rem, MM-rel) to 4 (MM-dia) experiments.

Supplemental Figure 4

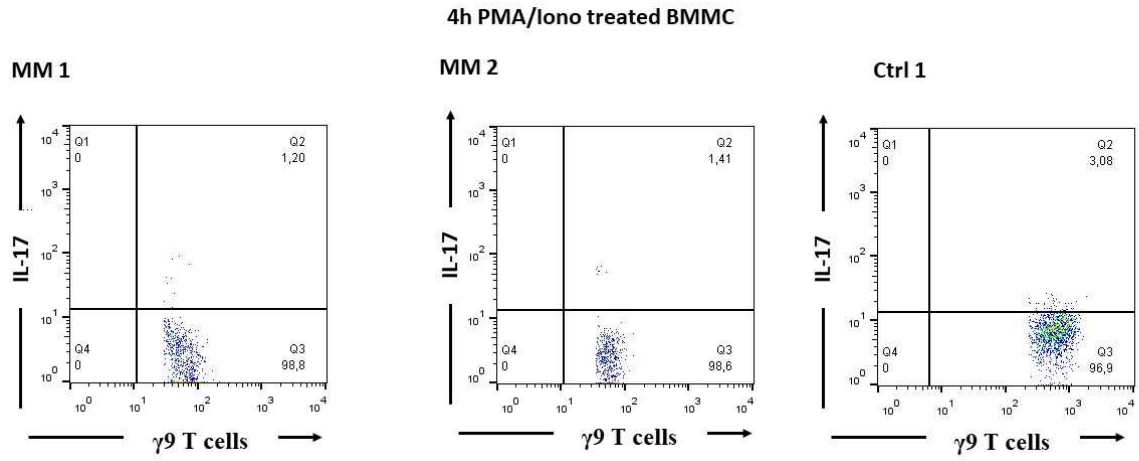

IL-17 expression in BM MM and Ctrl Vγ9Vδ2 T cells. IL-17 production was evaluated in freshly isolated BMMC after 4-hour incubation at 37°C with PMA (50 ng/ml)+ ionomycin (1 μg/ml) followed by 1-hour incubation with brefeldin (500 ng/ml).

Supplemental Figure 5

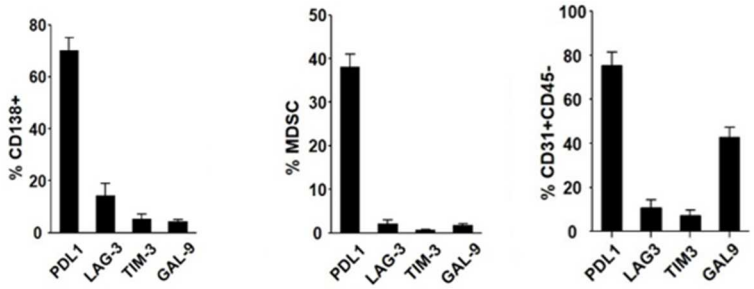

ICP expression on TME of MM patients. PD-L1, LAG-3, TIM3, and Gal-9 expression on myeloma cells (CD138+), MDSC (CD33+CD11b+), and EC (CD31+CD45-) from BM of MM patients.

Supplemental Figure 6

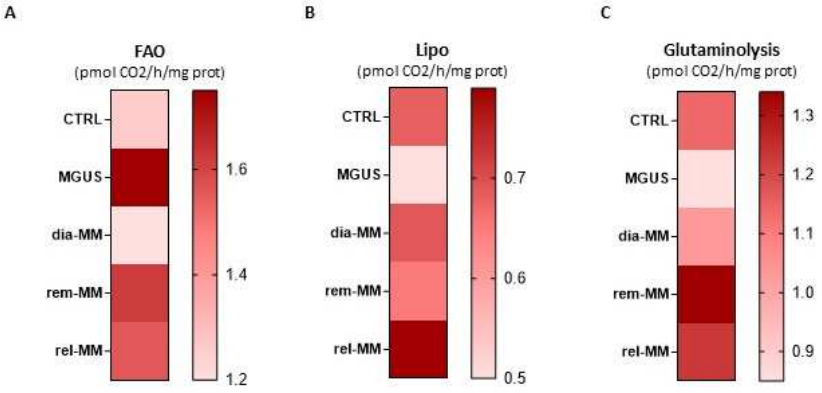

Metabolic analysis of BMSC. A) Analysis of fatty acid beta oxidation (FAO). **B**) Analysis of lipolysis. **C**) Analysis of Glutaminolysis.

Supplemental Figure 7

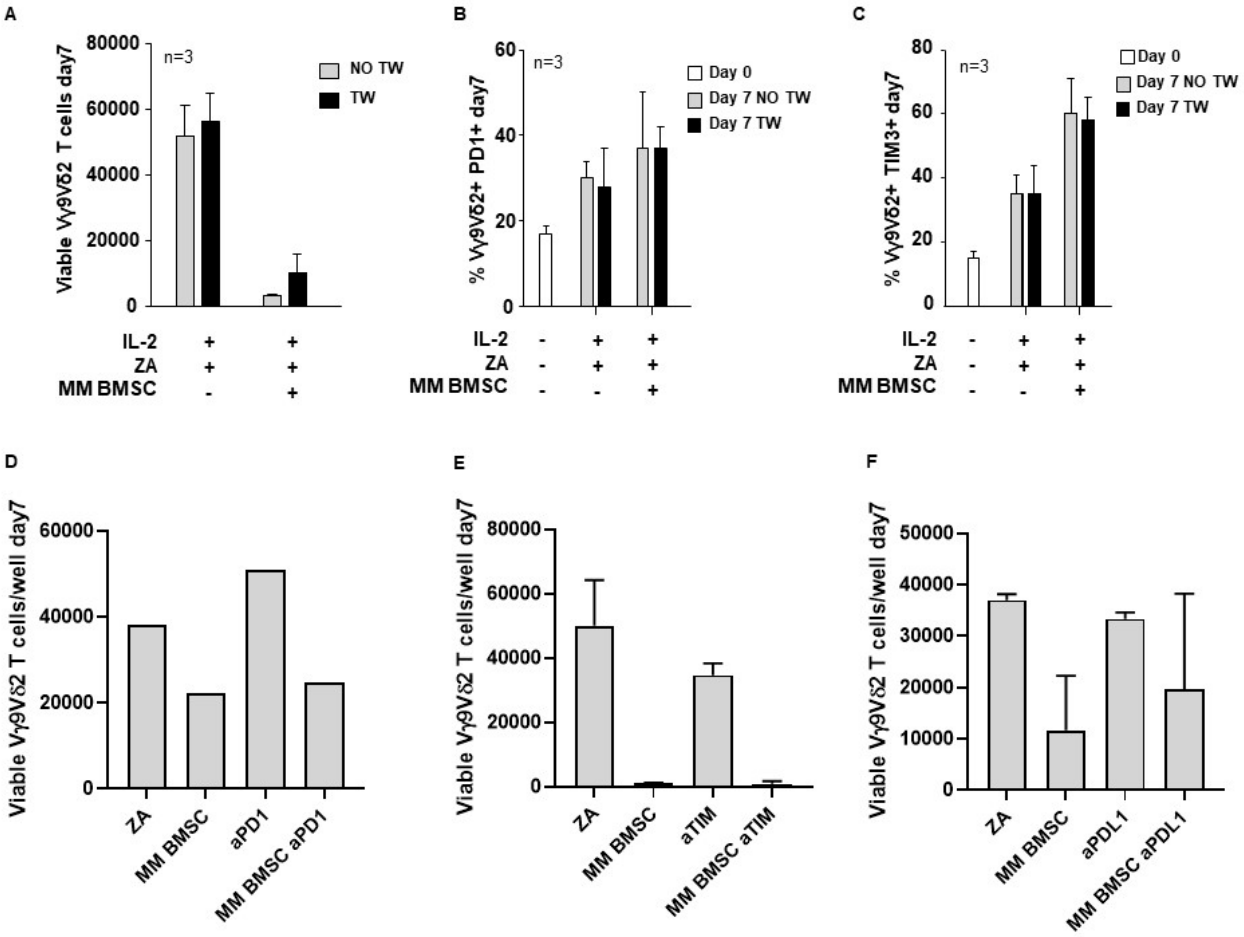

MM BMSC induce Vγ9Vδ2 T-cell dysfunction. A) Proliferative response, **B**) PD-1 and **C**) TIM-3 expression on Vγ9Vδ2 T cells after 7day co-colture with MM BMSC in presence or absence of TW. Bars represent mean values ± SE from 3 experiments. **D-F**) Proliferative response of Vγ9Vδ2 T cells after 7day co-colture with MM BMSC in presence or absence of **D**) anti-PD1, **E**) anti-TIM3, and **F**) anti-PDL1. Bars represent mean values ± SE from 1 (anti-PD1 treatment) to 2 experiments.

Supplemental Figure 8

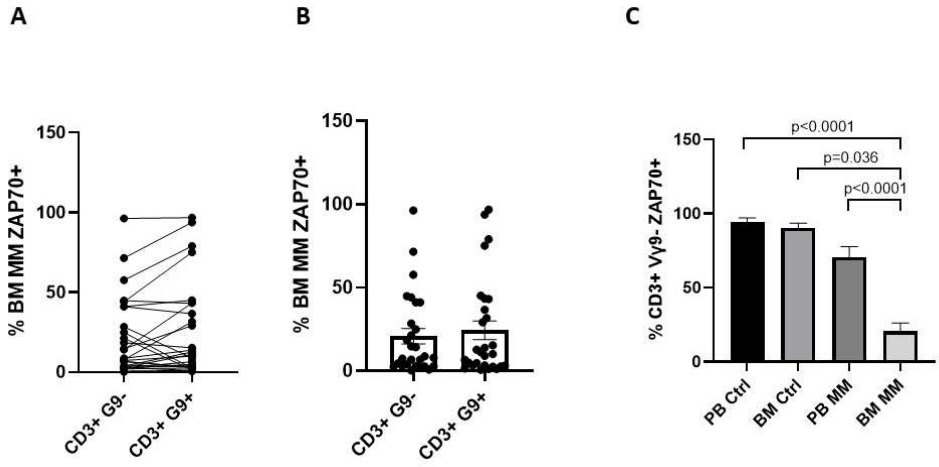

Analysis of ZAP-70 expression in Vγ9Vδ2 and CD3+ Vγ9Vδ2^{neg} cells. A) Paired analysis of ZAP-70 expression in Vγ9Vδ2 (CD3+ G9+) and CD3+ Vγ9Vδ2^{neg} (CD3+ G9-) cells from 28 BM MM-dia. **B**) Results are shown as bars representing mean values ± SE of 28 experiments. The differences is not statistically significant. **C**) ZAP-70 expression in freshly isolated PB and BM CD3+ Vγ9Vδ2^{neg} T cells from Ctrl and MM-dia. BM MM Vγ9Vδ2 T cells have the lowest mean ZAP-70 expression. Bars represent mean values ± SE from 3 (BM Ctrl) to 14 (PB MM) experiments.

Supplemental Figure 9

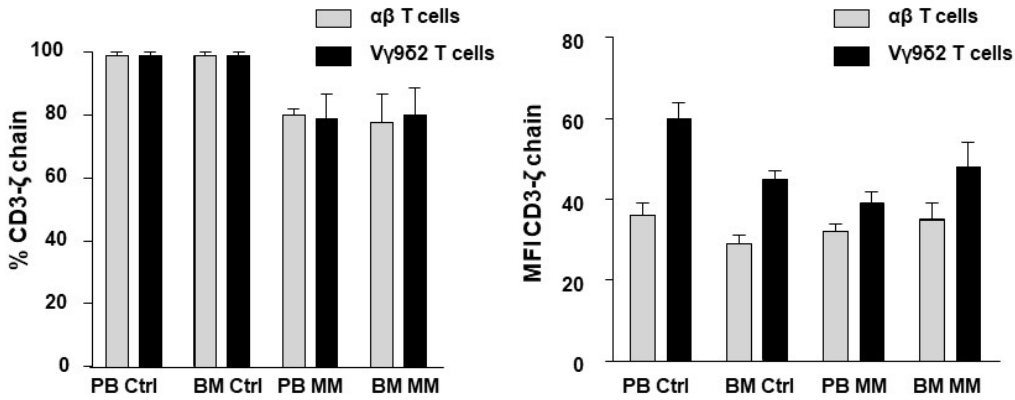

Preserved CD3-ζ chain expression in BM MM Vγ9Vδ2 T cells. Percentage (left) and MFI (right) of CD3-ζ chain expression are similar in PB and BM Ctrl and MM Vγ9Vδ2 T cells. Bars represent mean values ± SE from 3 (PB Ctrl, BM Ctrl and PB MM) to 14 (BM MM) experiments.

Supplemental Figure 10

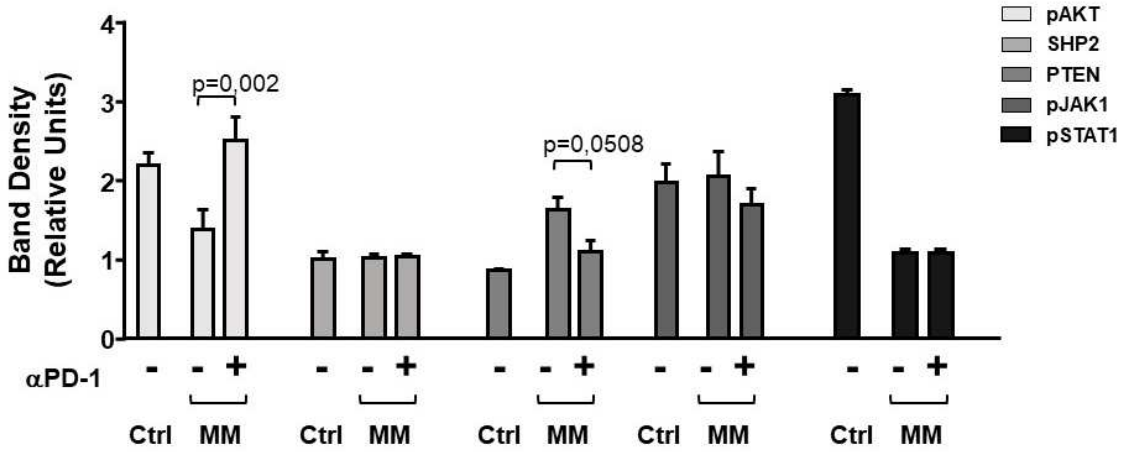

αPD-1 effect on TCR-associated molecules in ZA-stimulated BM MM Vγ9Vδ2 T cells.
Densitometric analysis of pAKT, AKT, SHP2, PTEN, pJAK-1, JAK-1, pSTAT-1, and STAT-1 expression in BM MM Vγ9Vδ2 T cells after ZA stimulation in the absence or in the presence of αPD1 Bars represent mean values ± SE from 3 (BM Ctrl) to 10 experiments (BM MM).

Supplemental Figure 11

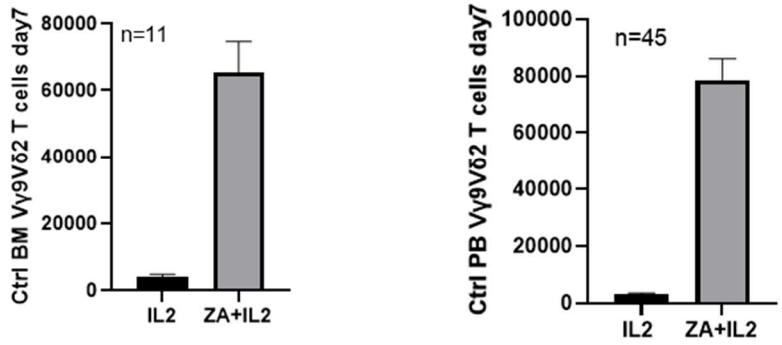

Proliferative response of Ctrl PB and BM Vγ9Vδ2 T cells after ZA stimulation. Bars represents mean values ± SE of 11 experiments in BM Ctrl (left) and 45 experiments in PB Ctrl (right). Viable Vγ9Vδ2 T cells were counted on day 7 with the trypan blue staining assay and flow cytometry after gating for CD3 in combination with αVg9 mAb. Numerical values are: BM Ctrl: 62,187±10,562; PB Ctrl: 78,676 ± 7,486

Vγ9Vδ2 T cells for immunotherapy in blood cancers: ready for prime time?

ABSTRACT

In the last years, the tumor microenvironment (TME) has emerged as a promising target for therapeutic interventions in cancer. Cancer cells are highly dependent on the TME to growth and evade the immune system. Three major cell subpopulations are facing each other in the TME: cancer cells, immune suppressor cells, and immune effector cells. These interactions are influenced by the tumor stroma which is composed of extracellular matrix, bystander cells, cytokines, and soluble factors. The TME can be very different depending on the tissue where cancer arises with very strong differences between solid tumors and hematological malignancies.

Several studies have shown correlations between the clinical outcome and specific patterns of TME immune cell infiltration. In the recent years, a growing body of evidence suggests that unconventional T cells like natural killer T cells (NKT), mucosal-associated invariant T (MAIT) cells, and γδ T cells are key players in the protumoral or antitumor TME commitment in solid tumors and hematological malignancies. In this review, we will focus on γδ T cells, especially Vγ9Vδ2 T cells, to discuss their peculiarities as potent immune effector cells in hematological malignancies and as potential platform for therapeutic interventions.

INTRODUCTION

γδ T cells are equipped with a T-cell Receptor (TCR) composed of a γ-chain (TRG) and a δ-chain (TRD). The genes encoding TRG and TRD undergo somatic DNA recombination of variable (V), diversity (D, only in TRD) and joining (J) elements during γδ T cell maturation in the thymus (1). γδ TCR and αβ TCR are structurally similar and associated with the same subunits of the CD3 complex that are arranged differently and characterized by unique glycosylation patterns and other minor peculiarities (2,3). One major difference are the antigens recognized by αβ and γδ T cells and the modality of antigen recognition which is not dependent on the major histocompatibility complex (MHC) in γδ T cells (2,4). This feature is particularly exciting from the perspective of using γδ T cells as a source for adoptive cell transfer (ACT) or chimeric antigen receptor (CAR)-T cells: MHC-independency reduces the risk of graft-versus-host disease (GvHD) and favors the development of "off-the shelf" cellular products (5).

In humans, γδ T cells represent 1-5% of blood circulating cells (6). Their development begins early during gestation (5-7 weeks), initially in the liver and then also in the thymus after 8 weeks of gestation (7). Later on, γδ T cells colonize the liver and predetermined mucosal and epithelial locations to contribute to tissues homeostasis and immune responses against pathogens (8).

Human γδ T cells can be divided in three main subsets: $V\delta1^+$ cells, $V\delta2^+$ cells, and $V\delta3^+$ cells (2). $V\delta2^+$ T cells are the predominant γδ T-cell population in the peripheral blood (PB) of adult humans (9,10) characterized by the expression of the semi-invariant Vγ9Vδ2 TCR made up of public germline CDR3γ sequence and a more diverse CDR3δ sequence (11). $V\delta1^+$ and $V\delta3^+$ cells are commonly found in mucosal, epithelial tissues, and in the liver, even if a small amount can be detected also in the PB (2).

The importance of γδ T cells in the clearance of pathogens during bacterial or viral infections (8,12,13) and cancer immunosurveillance (14–16) is very well recognized. However, there are also evidences that γδ T cells can negatively affect the outcome of immune reactions to pathogens and tumor cells depending on the tissue microenvironment that they have colonized, the cytokines and soluble factors they are exposed to, and the multifaceted interactions engaged with bystander cells and the extracellular matrix (17–19). γδ T cells can acquire regulatory functions leading to immune suppression activity and protumoral functions. For instance, accumulation of CD39-expressing γδ T cells has been reported in colorectal cancer (19), and interleukin (IL) -17 producing $V\delta1^+$ T cells have been identified as major promoters of tumor progression and metastasis in humans (20–22). Regulatory γδ T cells have also been reported in hematological malignancies and associated with poor overall survival (23,24). Fewer data are available about Vγ9Vδ2 T cells and other Vδ2- cells (25). Recently, we have reported that bone marrow (BM) Vγ9Vδ2 T cells in multiple myeloma (MM)

patients are dysfunctional, but they do not produce IL-17 (26), whereas Lo Presti et al. have reported the presence of IL-17 producing Vγ9Vδ2 T cells in the TME of patients with squamous cell carcinoma (27).

In this minireview, we will discuss the peculiarity of Vγ9Vδ2 T cells in hematological cancers and the pros and cons to build on these cells autologous or allogenic immune-based interventions.

Activation and functional characteristics of Vγ9Vδ2 T cells

Vγ9Vδ2 T cells can recognize supraphysiological concentrations of phosphoantigens (pAg) produced by pathogens or eukaryotic cells via the mevalonate pathway (Mev) or Mev-independent pathways of isoprenoid biosynthesis (28). The Mev-independent pathways (MEP/DOXP or Rohmer pathway) are restricted to eubacteria, cyanobacteria, plants, and apicomplexan protozoa (29). The prototype pAg generated in the Mev pathway is isopentenyl pyrophosphate (IPP) which is over-produced by stressed cells and cancer cells and promotes the selective activation of Vγ9Vδ2 T cells (30). The mechanism of pAg recognition by Vγ9Vδ2 T cells are very different from the canonical MHC-antigen complex recognition by αβ T cells and still under investigation. Three immunoglobulin superfamily members, butyrophilin 3A1 (BTN3A1), butyrophilin 3A2 (BTN3A2), and butyrophilin 2A1 (BTN2A1) are involved in pAg-induced Vγ9Vδ2 T-cell activation (8,31–34). The intracellular 30.2 domain of BTN3A1 senses pAg accumulation in antigen presenting cells (APCs) or target cells (8,32) and promotes an inside-out modification of extracellular BTN3A1. Once modified, BTN3A1 is stabilized by BTN3A2 and binds to the Vδ2 and γ-chain TCR regions of Vγ9Vδ2 T cells. At the same time, BTN2A1 provides a costimulatory signal via interactions with BTN3A1 and the germline-encoded regions of the Vγ9 chain on the opposite side of the TCR (33,34).

BTN3A1 and BTN2A1 are also expressed on the cell surface of Vγ9Vδ2 T cells implying that, in the presence of exogenous pAg eventually internalized by ATP-binding cassette transporter A1 ABCA1 (35), Vγ9Vδ2 T cells can self-activate each other without the intervention of APC or target cells (36). Self-activation is associated with CD107a upregulation and increased interferon-γ (IFNγ) production, potentially leading to Vγ9Vδ2 T-cell fratricide. This undesired side-effect can partially explain why pAg-based immune interventions have fallen short of expectations in the clinical setting (36).

Aminobisphosphonates (A-BP) like zoledronic acid (ZA), and alkylamines enhance the ability of APC and cancer cells to activate Vγ9Vδ2 T cells by increasing the intracellular production and extracellular release of IPP via inhibition of the farnesyl diphosphate synthase in the Mev pathway (37–40). Vγ9Vδ2 cells can also be activated by natural killer (NK) receptors like the natural killer 2D receptor (NKG2D) and the DNA X accessory molecule 1 (DNAM-1). The former interacts with

MICA, MICB, ULBP1-4, the latter with Nectin-2 and PVR. These interactions contribute to the induction of cytotoxic responses against target cells and cytokine production (21). Upon activation, Vγ9Vδ2 T cells can exert a wide range of functions halfway between adaptive and natural immunity, including cytolytic functions, chemokine and cytokine production, and behave as cellular adjuvants to support antigen-specific immune responses mediated by B cells and MHC-restricted αβ T cells (2,40–45).

Based on their maturation status, four distinct subsets of Vγ9Vδ2 T cells have been identified after pAg stimulation (38). Naïve $CD45RA^{+}CD27^{+}$ Vγ9Vδ2 T cells produce low amount of IFNγ, and they differentiate into $CD45RA^{-}CD27^{+}$ central memory (CM) Vγ9Vδ2 T cells with higher proliferation capacity. Later on, CM cells further differentiate into $CD45RA^{-}CD27^{-}$ effector memory (EM) Vγ9Vδ2 T cells that produce high levels of IFNγ and tumor necrosis factor-α (TNFα) (46). EM cells or, alternatively, CM cells in the presence of IL-15, can differentiate into late effector memory $CD45RA^{+}CD27^{-}$ T cells (TEMRA) characterized by high cytotoxic potential, low proliferation potential, and limited IFNγ production (38,46). It has also been reported that T_{EMRA} cells can be further divided in two subsets based on CD45RA expression levels: $CD27^{-}CD45RA^{hi}$ and $CD27^{-}CD45RA^{int}$ cells. The former are reminiscent of functionally exhausted cells, while the latter are the "classical" TEMRA mentioned above (47). The maturation status is highly influenced by the microenvironment in which Vγ9Vδ2 T cells are resident and the stimuli they are exposed to. In the presence of tumor cells, maturation can be pushed to immune senescence and/or functional exhaustion which are tumor permissive conditions (26).

Vγ9Vδ2 T cells in cancer: a delicate balance between antitumor and protumoral functions

The antitumor activity of Vγ9Vδ2 T cells encompasses: 1) direct killing of cancer cells through granzyme B (GzmB) and perforin (Prf) secretion; 2) antibody-dependent cellular cytotoxicity (ADCC) against malignant cells due to CD16 expression; 3) Fas/FasL-mediated cancer cell death; 4) production of cytokines like IFNγ and TNFα; 5) interactions with other TME-resident immune cells (21,41,48,49). Furthermore, Vγ9Vδ2 T cells can cross-present tumor antigens to αβ $CD8^{+}$ T cells to boost antigen-specific IFNγ production and increase antitumor T-cell response (50). We and others have also demonstrated that Vγ9Vδ2 T cells deliver co-stimulatory signals to dendritic cells (DC) after ZA stimulation in vitro that increase the frequency of antigen-specific $CD8^{+}$ αβ T cells and concurrently restrain the expansion of IL-2-dependent regulatory T cells (Tregs). Altogether, these data indicate that Vγ9Vδ2 T cells can behave as cellular adjuvants and orchestrate a wide rally of immune cells against cancer cells (45,51,52).

Unfortunately, it appears that Vγ9Vδ2 T cells are very early targeted and neutralized by cancer cells, especially in the TME. In MM, BM Vγ9Vδ2 T cells are PD-1$^+$ TIM-3$^+$, and anergic to pAg stimulation (26,53). These dysfunctions are long-lasting and already detectable in monoclonal gammopathy of undetermined significance (MGUS) (53). PD-1$^+$ BM MM Vγ9Vδ2$^+$ T cells combine phenotypic, functional, and TCR-associated alterations consistent with chronic exhaustion and immune senescence not easily reversible by single or even dual immune checkpoint (ICP) blockade (26). However, ICP$^+$ Vγ9Vδ2 T cells maintain the ability to produce IFNγ and to secrete GzmB and Prf in MM, acute myeloid leukemia (AML), and other cancers (26,54,55) raising the question whether these cells are still able of carrying out some immunological effect in the TME and whether it is still worth trying to fully recover their antitumor functions.

On the other hand, the functional plasticity gives Vγ9Vδ2 T cells a constant risk of switching from antitumor to protumoral function (21,41). Depending on the cytokines they are exposed after activation, Vγ9Vδ2 T cells can polarize into Th1-like, Th2-like, Th17-like, T_{FH}-like, T_{reg}-like, T_{APC}-like phenotypes (38,56–58). The input to undertake one way of differentiation rather than another also depends on the tissue environment and the local influence exerted by cancer cells. Similarly to what has been reported about total γδ T cells in breast, colon, and pancreatic cancer (17,22,48,59), Th17-like Vγ9Vδ2 T cells with protumoral functions have been identified in the TME and associated with negative outcome in squamous cell carcinoma (27). In the presence of IL-21, Vγ9Vδ2 T cells can become CD73+ and suppress the antitumor activity of conventional T cells via the adenosine suppressive circuitry (56). Anti-tumor and pro-tumor functions of Vγ9Vδ2 T cells are represented in Figure 1.

Interestingly, blood cancer cells are more susceptible to the antitumor activity of Vγ9Vδ2 T cells than solid tumors (30,48). Possible mechanisms are the enhanced Mev pathway activity and the increased expression of alternative ligands (30). Another very relevant player is the TME which is very different in solid and blood cancer. The emergence of protumoral Vγ9Vδ2 T cells has more frequently been reported in the former, whereas in the latter Vγ9Vδ2 T cells are mainly dysfunctional and chronically exhausted, but not fully differentiated into Vγ9Vδ2 T cells with protumoral functions (26,60–62).

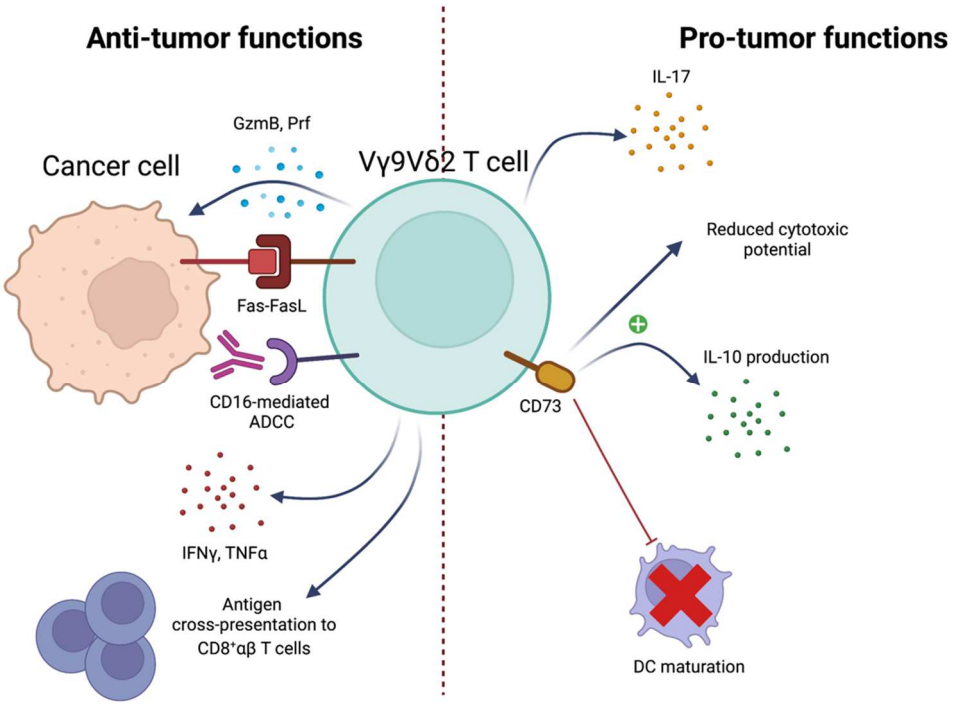

Figure **1: Schematic representation of antitumor and protumoral functions of Vγ9Vδ2 T cells**. Left panel: Antitumor functions. Vγ9Vδ2 T cells exert antitumor functions by: 1) direct killing of cancer cells producing GzmB and Prf; 2) cancer cell killing via Fas-FasL interactions; 3) CD16-mediated ADCC against malignant cells; 4) production of antitumor cytokines like IFNγ and TNFα; 5) Interaction with immune cells, for instance cross-presenting antigens to CD8+ αβ T cells. Right panel: Protumoral functions. Vγ9Vδ2 T cells can: 1) produce the protumoral cytokine IL-17; 2) acquire regulatory phenotypes expressing CD73. CD73 promotes IL-10 production, reduces the cytotoxic potential of Vγ9Vδ2 T cells and impairs DC maturation. Abbreviations: Granzyme B (GzmB), Perforin (Prf), Antibody-dependent cell cytotoxicity (ADCC), Interferon γ (IFNγ), Tumor Necrosis Factor α (TNFα), Interleukin-17 (IL-17), Interleukin-10 (IL-10), Dendritic cells (DC). Created by BioRender.com

Vγ9Vδ2 T cells as candidates for immunotherapy: a failed promise or insufficient knowledge?

The unique properties of Vγ9Vδ2 T cells have raised a great interest as potential candidates for immune-based interventions in solid tumors and hematological malignancies. First, Vγ9Vδ2 T-cell activation can be induced by a wide array of ligands making possible to target cancer cells devoid of specific tumor-associated antigens (TAA) or tumors with a limited mutational burden. Moreover, a broad antitumor reactivity could prevent the emergence of tumor variants leading to immune escape and tumor relapse (63).

MHC independency is another major feature making Vγ9Vδ2 T cells safer effector cells than αβ T cells in the context of allogenic hematopoietic stem-cell transplantation (allo-HCT) or other mismatched adoptive immunotherapy approaches. Vγ9Vδ2 T cells can exert effective graft-*versus*-tumor (GvT) activity with minimal GvHD activity which remains a major cause of early and late

morbidity and mortality after allo-HCT (64). MHC-independent recognition of TAA should also limit the ability of cancer cells to evade immune recognition via MHC down-regulation (65).

The frequency of Vγ9Vδ2 T cells in the PB is low, but still significantly higher than any other frequency of MHC-restricted TAA-specific αβ T cells, and stimulation with pAg can be considered a polyclonal stimulation recruiting all Vγ9Vδ2 T cells and not only selected clonal or subclonal populations. MHC-independency allows the possibility to eventually mix and expand Vγ9Vδ2 T cells from different donors to skip the time-consuming and expensive manufacturing of personalized cell products and dilute any individual variability in the reactivity to pAg-induced activation (66).

Lastly, pAg-activated Vγ9Vδ2 T cells have been shown in vitro to behave as cellular adjuvants with the ability to engage immune effector cells of adaptive immunity and boost their antitumor immune responses (45,49,50,52,67).

Despite these excellent premises, Vγ9Vδ2 T-cell based immune interventions have not hit the target. In this minireview, we will focus mainly on progresses and pitfalls in hematological malignancies.

Early approaches have used A-BP like pamidronate and ZA to induce Vγ9Vδ2 T-cell activation in vivo followed by IL-2 to support proliferation and expansion. Synthetic pAg like bromohydrin pyrophosphate (BrHPP) and 2-methyl-3-butenyl-1-pyrophosphate (2M3B1PP) have been produced to increase the affinity for Vγ9Vδ2 T cells and extend half-life after in vivo injection. Synthetic pAg have been associated in vivo with monoclonal antibodies (mAbs) like rituximab, alemtuzumab, and obinutuzumab to boost ADCC in B-cell malignancies based on the in vitro findings that pAg-activated Vγ9Vδ2 T cells upregulate FcγR expression (68–70).

Early approaches of adoptive immunotherapy have also relied on the combination of pAg and IL-2 to induce the ex-vivo activation of autologous Vγ9Vδ2 T cells. This approach has been tested in MM showing minimal toxicity, but unsatisfactory clinical results (71). The adjuvant properties of Vγ9Vδ2 T cells and their capacity to promote the activation of tumor-specific MHC-restricted αβ T cells has been investigated in a very small series of elderly AML patients. These patients were treated with DC co-pulsed with WT1 peptide and ZA with some evidences of clinical benefit (72–74).

In conclusion, Vγ9Vδ2 T-cell based immunotherapy has proven to be safe and well tolerated in hematological malignancies, but unable to achieve deep and long-lasting responses (28,75,76). Failing clinical expectations has stimulated further research to understand the mechanisms exploited by tumor cells to escape Vγ9Vδ2 T-cell recognition and killing, especially in the TME (77,78), and which strategies are worth investigating to empower their antitumor activity.

A critical point is that the immune fitness of Vγ9Vδ2 T cells from cancer patients is very different from that of healthy individuals. We and others have shown that about 50% of PB Vγ9Vδ2

T cells from Chronic Lymphocytic Leukemia (CLL), MM, and other blood cancer patients are unable to respond to pAg stimulation (79,80). Naïve/CM/EM/TEMRA subset redistribution, ICP upregulation, immune senescence, and functional exhaustion due to chronic stimulation are some of the mechanisms responsible for Vγ9Vδ2 T-cell dysfunction (26,53). Unique to Vγ9Vδ2 T cells is the chronic stimulation operated by the supraphysiological IPP concentrations that are released in the TME by bone marrow stromal cells (BMSC) and to a lower extent by myeloma cells (35).

Interestingly, we have shown that Vγ9Vδ2 T-cell dysfunction in the TME of MM patients is highly persistent and not reverted even in the remission phase when myeloma cells have disappeared (53). One reason is that the TME remains strongly committed to keep unmodified its immune suppressive contexture as shown by the persistence of high numbers of PD-L1$^+$ myeloid-derived suppressor cells (MDSC), PD-L1$^+$ BMSC, and PD-L1$^+$ endothelial cells (EC). Moreover, we have shown that the disease status strongly influences the reactivity of BM MM Vγ9Vδ2 T cells to pAg stimulation and the response to ICP blockade. At diagnosis, the combination of PD-1 and TIM-3 blockade allows a partial recovery of Vγ9Vδ2 T-cell immune effector functions; in the remission phase, single PD-1 blockade is moderately effective, whereas PD-1 and LAG-3 blockade is the only combination to be minimally effective in relapsed MM (26).

These data indicate that TME-resident Vγ9Vδ2 T cells are probably not the preferred targets for cell-based immune interventions in the absence of appropriate ex-vivo or in vivo manipulation, unlike tumor-infiltrating lymphocytes (TIL) which have been deemed to be very well-suitable for cellular immunotherapy. The assumption is that, at least in solid tumors, tumor-reactive clones have already been primed in the TME and can be recruited more effectively against cancer cells (81). Moreover, the rates of γδ TIL are very low compared to TIL and comprise mainly Vδ1 T cells (82).

A possible alternative to TME-resident Vγ9Vδ2 T cells is the in vivo or ex-vivo recruitment of circulating Vγ9Vδ2 T cells. Side-by-side comparison of PB and BM Vγ9Vδ2 T cells in MM patients has shown that the former are functionally preserved slightly better than the latter. We and others have shown that approximately 50% of MM and CLL patients retain PB Vγ9Vδ2 T cells that can be stimulated by pAg (79,80). Interestingly, in the others the anergy can be reverted with ZA-stimulated DC that provide huge quantities of IPP and costimulatory signals (40,79,83). In CLL, pretreatment of PB Vγ9Vδ2 T cells with ibrutinib promotes a Th-1 differentiation with enhanced antitumor activity, probably mediated by ITK inhibition as previously reported in conventional αβ T cells (83).

However, the use of PB Vγ9Vδ2 T cells also presents a number of critical aspects. One is the progressive decline in the capacity to respond to reiterated ZA stimulations as shown in MM patients after autologous stem cell transplantation (84) and in pediatric acute leukemia patients receiving

haploidentical αβ T-cell depleted stem cell transplantation (85). Another critical aspect could be the inadvertent expansion of $CD4^+$ T cells with a regulatory phenotype which has been reported in neuroblastoma patients treated with ZA+IL-2 to intentionally activate Vγ9Vδ2 T cells in vivo (86).

Vγ9Vδ2 T-cell MHC independency gives the possibility to use allogeneic cells from the PB of healthy individuals (reviewed in Jhita et al. 2022) (87). Haploidentical γδ T cells have been infused in 4 patients with refractory hematologic malignancies followed by in vivo stimulation with ZA and IL-2. None of the patients showed any signs of acute or chronic GvHD proving that allogeneic Vγ9Vδ2 T cells can safely be transferred and stimulated in vivo without inducing any undesired alloreactivity (88). This proof-in-principle has unequivocally been validated in a large series of patients with advanced stage liver and in lung cancer patients who received allogeneic Vγ9Vδ2 T cells without any significant adverse effects (e.g., immune rejection, cytokine storm, or GvHD effects) (89).

Although very exciting, the use of Vγ9Vδ2 T cells from healthy individuals is not exempt from disadvantages and pitfalls. One is the unexpected induction of immune suppressive activity on conventional αβ T cells after repeated pAg stimulation (90). Other possible pitfalls are the unpredictable consequences of transferring Vγ9Vδ2 T cells that have been forced to respond to pAg. For example, IL-21 has been reported to promote the expansion of Vγ9Vδ2 T cells from non-responder donors after ZA stimulation (66). Unfortunately, IL-21 can also induce Vγ9Vδ2 T cells with immune suppressive and protumoral functions exerted via the CD73/adenosine-dependent circuit (56).

Altogether, these data indicate that both TME-resident and PB Vγ9Vδ2 T cells are very sensitive to stimuli delivered by TME, cytokines, and pAg. Their functional plasticity is a great plus, but at the same time a great risk to inadvertently induce undesirable protumoral properties by inappropriate engagement (26,91).

Strategies to bring Vγ9Vδ2 T-cell immune interventions to prime time

Over the last few years, we have seen an enormous acceleration in the knowledge of immune escape mechanisms, concurrently with great advances in the design of therapeutic mAbs and the development of genetically engineered immune effector cells. These very exciting progresses are revolutionizing cancer immunotherapy including Vδ1 and Vγ9Vδ2 T-cell based approaches (76,92).

Several approaches are under preclinical or clinical investigation to rescue the immune fitness of Vγ9Vδ2 T cells in cancer patients. Anti-ICP/ICP-ligands mAbs have been used in vitro to improve the pAg reactivity and immune effector functions of TME-resident Vγ9Vδ2 T cells in MM (26,53), AML (54) and follicular lymphoma (FL) (93). The agonistic humanized anti-BTN3A mAb ICT01 is

under investigation in a phase 1/2a clinical study in advanced-stage solid tumors and hematologic malignancies (94). Bispecific T-cell engagers antibodies (BiTe) are also under investigation to redirect cytotoxic Vγ9Vδ2 T-cell activity against cancer cells. The bispecific Vγ9/CD123 antibody has been shown to recruit and redirect Vγ9Vδ2 T cells against autologous AML blasts in vitro and in a xenograft mouse model (95). Similar results have been replicated in vitro and in a xenograft mouse model with the bispecific Vγ9Vδ2/CD40 antibody in CLL and MM patients (96). CD1d is another tumor-associated antigen which can be targeted in CLL with a CD1d-specific Vγ9Vδ2-T cell engager made by single-domain antibodies (VHH). Interestingly, this bispecific VHH does not affect pAg reactivity giving the possibility to boost the antitumor activity of Vγ9Vδ2 T cells with ZA (97). Van Diest et al. have developed a bispecific molecule which exploits the natural predisposition of Vγ9Vδ2 T cells to recognize cancer cells by linking the extracellular domains of tumor reactive Vγ9Vδ2 TCR to a CD3-binding moiety. This bispecific molecule confers to conventional αβ T cells the capacity to recognize cancer cells via pAg without the limitations imposed by MHC restriction and/or MHC downregulation (98).

A great effort is also ongoing to optimize the use of Vγ9Vδ2 T cells from healthy individuals. In this case, strategies are dedicated to improve the efficacy of in vitro expansion protocols and to reinforce their capacity to survive and exert a prolonged antitumor activity after infusion. One area of research is dedicated to the discovery of novel A-BP and synergistic interactions with other compounds. Tetrakis-pivaloyloxymethyl 2- (thiazole-2-ylamino) ethylidene-1,1-bisphosphonate (PTA) is a novel bisphosphonate prodrug which activates Vγ9Vδ2 T cells more efficiently than ZA (99), while vitamin C and its derivatives can enhance the activation and differentiation of human Vγ9Vδ2 T cells (100). A wise and careful selection of cytokines is also critical to promote the expansion of antitumor Vγ9Vδ2 T cells, and not the undesired expansion of Vγ9Vδ2 T cells with protumoral or immune suppressor functions (66,101).

The use of feeder cells is another workable tool to improve the efficacy of *in vitro* Vγ9Vδ2 T-cell expansion protocols (102–105). Side-by-side comparison of ZA + IL-2 *versus* K562-based artificial antigen-presenting cells (aAPC) has shown in mouse models that the latter induces Vγ9Vδ2 T cells with stronger antitumor activity and enhanced capacity to survive *in vivo* (103). However, the superiority of aAPC is threatened by the increased risk to induce an excessive IL-17A release leading to the differentiation of protumoral Vγ9Vδ2 T cells (103,106). Costimulation with ZA + IL-2 in addition to aAPC can overcome this undesired bias and support the expansion of large numbers of Vγ9Vδ2 T cells with low ICP expression and predominant memory phenotype which are important prerequisites for prolonged persistence in vivo after infusion (104). This approach has further been improved by introducing an intermediate step to remove αβ T cells between the first stimulation with

ZA + IL-2 and the second one with aAPC and ZA + IL-2. This strategy allows the manufacture of highly pure Vγ9Vδ2 T cells with an average fold expansion of >229,000-fold from healthy individuals (102). The cytotoxic activity of adoptively transferred Vγ9Vδ2 T cells can be reinforced by the combination with mAbs and/or BiTe to relieve ICP/ICP-ligand-dependent immune suppression (107,108) or to boost antitumor immune effector functions with agonistic anti-BTN3A 20.1 mAb (109).

Alternative strategies to potentiate antitumor effector functions of Vγ9Vδ2 T cells take advantage of their ability to recognize stress-induced self-ligands expressed by cancer cells via killer activating receptors (KAR) like NKG2D. This ability is counterbalanced by the expression of killer inhibitory receptors (KIR) (30), indicating that it is important to develop strategies that upregulate KAR and/or downregulate KIR to improve the cytotoxic activity of Vγ9Vδ2 T cells. Attempts to tilt the balance in favor of KAR range from nanobiomaterial-based strategy to conventional drugs. Lin et al. have shown in vitro that chitosan nanoparticles enhance Vγ9Vδ2 T-cell antitumor functions by upregulating NKG2D, CD56, FasL, and Prf secretion (110). Upregulation of NKG2D-ligands (NKG2D-L) on cancer cells can be a complementary strategy to tilt the balance in favor of Vγ9Vδ2 T-cell activation. Conventional drugs like temozolomide, doxorubicin, and 5-fluorouracyl have been reported to sensitize cancer cells from solid tumors to Vγ9Vδ2 T cells by inducing the upregulation of Fas, TRAIL-R1, and TRAL-R2 that are recognized by Vγ9Vδ2 T cells via NKG2D and TRAIL (111,112). These results have been replicated in patients with AML and acute T-cell lymphoblastic leukemia with bortezomib. Story et al. have shown that bortezomib enhances the recognition and killing of leukemia cells by ex-vivo activated Vγ9Vδ2 T cells from healthy individuals by increasing NKG2D/NKG2D-L interactions (113). Unfortunately, some of these drugs can also be toxic to Vγ9Vδ2 T cells. The easiest way to skip this drawback is to give chemotherapy before Vγ9Vδ2 T-cell activation in vivo or before ACT of ex-vivo activated Vγ9Vδ2 T cells (112). A more cumbersome approach is to genetically engineer Vγ9Vδ2 T cells to confer resistance to cytotoxic drug (111). The extracellular release of NKG2D-L is another mechanism exploited by cancer cells to elude NKG2D-dependent immune surveillance, especially after exposure to cytotoxic drugs. Thus, prevention of NKG2D-L shedding is another strategy that can be put in place to strengthen the antitumor activity of Vγ9Vδ2 T cells and synergistically improve the efficacy of combinations with cytotoxic drugs (114).

The immune adjuvant properties of Vγ9Vδ2 T cells are also of renewed interest. Early studies have focused on their ability to boost MHC-restricted antitumor immune responses mediated by conventional CD8+ T cells (74). More recently, it is under investigation the possibility to develop tumor cell/ Vγ9Vδ2 T-cell fusions as previously done with tumor cell/DC fusions in MM and AML

(115–117). In this approach, DC are replaced by pAg-activated Vγ9Vδ2 T cells to combine their abilities to support adaptive immune responses and to exploit at the same time their innate antitumor activity, a plus compared with DC which lack any direct antitumor activity. This approach has been validated in vitro by Wang et al. who have generated osteosarcoma/ Vγ9Vδ2 T-cell fusion vaccines able to induce multiple cytokine production and antitumor immune responses mediated by conventional αβ T cells (118).

Sharing innate-like and adaptive-like immune functions renders Vγ9Vδ2 T cells very attractive candidates for genetic engineering (119). Vγ9Vδ2 T cells have successfully been armed with CAR to target the B-cell Maturation Antigen (BCMA) in MM and CD123 in AML (120,121). Interestingly, in vitro data and in vivo mouse models have shown that, unlike conventional anti-CD19 CAR-T cells, ZA-stimulated anti-CD19 Vγ9Vδ2 CAR-T cells from healthy individuals can target both $CD19^+$ and CD19- allogeneic leukemia cells via the non-specific MHC-independent cytotoxic activity elicited by pAg stimulation (122). It is worth investigating whether the retained ability to target $CD19^-$ leukemic cells can be exploited to prevent the disease relapse observed in patients treated with conventional anti-CD19 CAR-T cells. In addition, CAR-transduced Vδ2 T cells maintained characteristics of professional APCs being able to cross-present the processed peptides to αβ T cells (123) although low persistence was observed (122,124).

Vγ9Vδ2 T cells can be transduced with αβ TCR, avoiding the risk of expression of mixed TCR dimers that limits TCR gene transfer in αβ T cells and results in autoreactivity (125). A side-by-side comparison of conventional αβ T cells and Vγ9Vδ2 T cells transduced with TCRs or CARs to target melanoma cells has shown comparable antigen-specific cytotoxic activity, but the latter retain also their intrinsic ability to lyse MHC-deficient cells. Moreover, the cytokines pattern released by transduced Vγ9Vδ2 T cells predicts a lower risk of cytokine release syndrome and autoimmunity compared with transduced αβ T cells (126).

Vγ9Vδ2 T cells can be transfected also with NKT cell-derived TCR to create a bi-potential innate lymphocytes combining NKT and Vγ9Vδ2 T-cell functionality and exerting cytotoxicity against glycolipid-expressing target cells and K562 cells (127).

Finally, another therapeutic approach exploits the high-affinity Vγ9Vδ2-TCR transduced in αβ T cells to generate “T cells engineered with defined gamma delta TCRs” (TEGs) (128), that are expected to develop durable, memory-based responses (28) and showed the ability to recognize and kill myeloma cells in a 3D model (129). TEGs safety and tolerability are under investigation (https://www. trialregister.nl/trial/6357).

Clinical trials testing the tumor killing function of engineered Vγ9Vδ2 T cells are ongoing and reviewed in Saura-Esteller et al. 2022 (76).

Strategies to optimize Vγ9Vδ2 T cell-based immunotherapy are summarized in Figure 2.

In conclusion, Vγ9Vδ2 T cells are very attractive platforms for immunotherapy but it is mandatory to decode the mechanisms underlying the immune dysfunctions induced by TME or by in vitro manipulation in order to translate their antitumor potential in successful clinical applications.

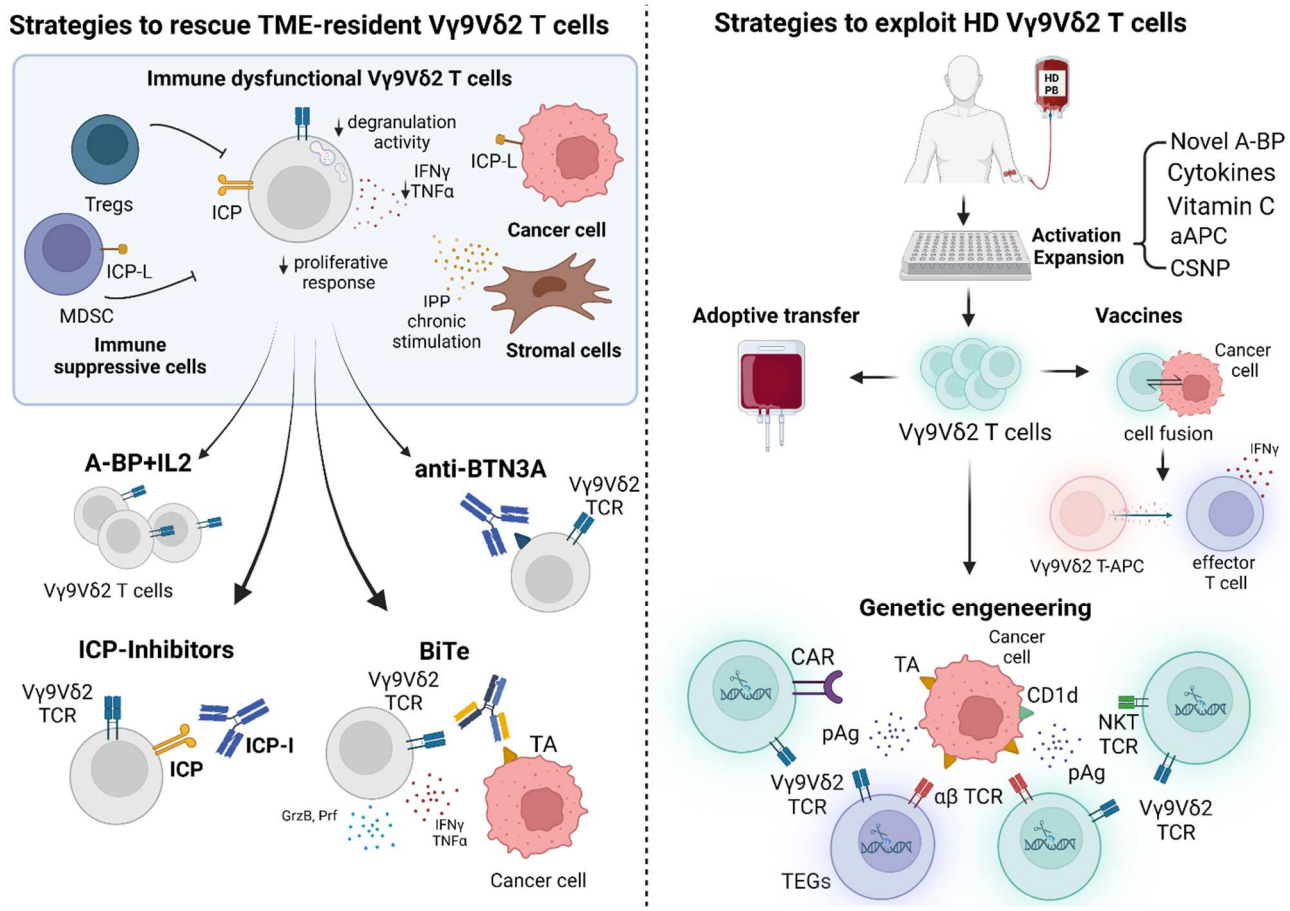

Figure **2** Current strategies to manipulate Vγ9Vδ2 T cells and optimize their therapeutic use. *Left panel*: Tumor microenvironment (TME) impairs anti-tumor functions of Vγ9Vδ2 T cells resulting in immune checkpoint (ICP) expression, low proliferative response, decreased cytokine production (IFNγ and TNFα), and degranulation activity. Traditional strategies aimed at rescuing immune fitness of Vγ9Vδ2 T cells, such as A-BP+IL2 administration, are now implemented by ICP-inhibitors (ICP-I), bispecific antibodies (BiTe), and monoclonal antibodies (i.e. anti-BTN3A). *Right panel*: Vγ9Vδ2 T cells from peripheral blood of healthy donors (HD PB) can be manipulated in vitro for allogenic use. Novel aminobisphosphonate (A-BP), selected cytokines, Vitamin C, artificial antigen presenting cells (aAPC) or chitosan nanoparticles (CSNP) improve the efficacy of Vγ9Vδ2 T-cell expansion and activation. Large-scale expanded Vγ9Vδ2 T cells can be used for Vγ9Vδ2 T-cell based vaccines or genetic engineering. Created by BioRender.com

Bibliography

1. Chien YH, Konigshofer Y. Antigen recognition by gammadelta T cells. *Immunol Rev* (2007) 215:46–58. doi: 10.1111/J.1600-065X.2006.00470.X

2. Chen D, Guo Y, Jiang J, Wu P, Zhang T, Wei Q, et al. γδ T cell exhaustion: Opportunities for intervention. *J Leukoc Biol* (2022)1–8. doi: 10.1002/JLB.5MR0722-777R

3. Morath A, Schamel WW. αβ and γδ T cell receptors: Similar but different. *J Leukoc Biol* (2020) 107:1045–1055. doi: 10.1002/JLB.2MR1219-233R

4. Silva-Santos B, Mensurado S, Coffelt SB. γδ T cells: pleiotropic immune effectors with therapeutic potential in cancer. *Nature Reviews Cancer 2019 19:7* (2019) 19:392–404. doi: 10.1038/s41568-019-0153-5

5. Deng J, Yin H. Gamma delta (γδ) T cells in cancer immunotherapy; where it comes from, where it will go? *Eur J Pharmacol* (2022) 919:174803. doi: 10.1016/j.ejphar.2022.174803

6. Godfrey DI, Le Nours J, Andrews DM, Uldrich AP, Rossjohn J. Unconventional T Cell Targets for Cancer Immunotherapy. Immunity. 2018 Mar 20;48(3):453-473. doi: 10.1016/j.immuni.2018.03.009

7. Pellicci DG, Koay HF, Berzins SP. Thymic development of unconventional T cells: how NKT cells, MAIT cells and γδ T cells emerge. *Nat Rev Immunol* (2020) 20:756–770. doi: 10.1038/S41577-020-0345-Y

8. Ribot JC, Lopes N, Silva-Santos B. γδ T cells in tissue physiology and surveillance. *Nature Reviews Immunology 2020 21:4* (2020) 21:221–232. doi: 10.1038/s41577-020-00452-4

9. de Libero G, Casorati G, Giachino C, Carbonara C, Migone N, Matzinger P, et al. Selection by two powerful antigens may account for the presence of the major population of human peripheral gamma/delta T cells. *J Exp Med* (1991) 173:1311–1322. doi: 10.1084/JEM.173.6.1311

10. Parker CM, Groh V, Band H, Porcelli SA, Morita C, Fabbi M, et al. Evidence for extrathymic changes in the T cell receptor gamma/delta repertoire. *J Exp Med* (1990) 171:1597–1612. doi: 10.1084/JEM.171.5.1597

11. Dimova T, Brouwer M, Gosselin F, Tassignon J, Leo O, Donner C, et al. Effector Vγ9Vδ2 T cells dominate the human fetal γδ T-cell repertoire. *Proc Natl Acad Sci U S A* (2015) 112:E556–E565. doi: 10.1073/PNAS.1412058112

12. Liu J, Qu H, Li Q, Ye L, Ma G, Wan H. The responses of γδ T-cells against acute Pseudomonas aeruginosa pulmonary infection in mice via interleukin-17. *Pathog Dis* (2013) 68:44–51. doi: 10.1111/2049-632X.12043

13. Sabbaghi A, Miri SM, Keshavarz M, Mahooti M, Zebardast A, Ghaemi A. Role of γδ T cells in controlling viral infections with a focus on influenza virus: implications for designing novel therapeutic approaches. *Virol J* (2020) 17: doi: 10.1186/S12985-020-01449-0

14. Saitoh A, Narita M, Watanabe N, Tochiki N, Satoh N, Takizawa J, et al. Anti-tumor cytotoxicity of gammadelta T cells expanded from peripheral blood cells of patients with myeloma and lymphoma. *Med Oncol* (2008) 25:137–147. doi: 10.1007/S12032-007-9004-4

15. Park JH, Kim HJ, Kim CW, Kim HC, Jung Y, Lee HS, et al. Tumor hypoxia represses γδ T cell-mediated antitumor immunity against brain tumors. *Nat Immunol* (2021) 22:336–346. doi: 10.1038/S41590-020-00860-7

16. Cazzetta V, Bruni E, Terzoli S, Carenza C, Franzese S, Piazza R, et al. NKG2A expression identifies a subset of human Vδ2 T cells exerting the highest antitumor effector functions. *Cell Rep* (2021) 37: doi: 10.1016/J.CELREP.2021.109871

17. Coffelt SB, Kersten K, Doornebal CW, Weiden J, Vrijland K, Hau CS, et al. IL-17-producing γδ T cells and neutrophils conspire to promote breast cancer metastasis. *Nature* (2015) 522:345–348. doi: 10.1038/NATURE14282

18. Ma S, Cheng Q, Cai Y, Gong H, Wu Y, Yu X, et al. IL-17A produced by γδ T cells promotes tumor growth in hepatocellular carcinoma. *Cancer Res* (2014) 74:1969–1982. doi: 10.1158/0008-5472.CAN-13-2534

19. Zhan Y, Zheng L, Liu J, Hu D, Wang J, Liu K, et al. PLA2G4A promotes right-sided colorectal cancer progression by inducing CD39+γδ Treg polarization. *JCI Insight* (2021) 6: doi: 10.1172/JCI.INSIGHT.148028

20. Fleming C, Morrissey S, Cai Y, Yan J. γδ T Cells: Unexpected Regulators of Cancer Development and Progression. *Trends Cancer* (2017) 3:561–570. doi: 10.1016/J.TRECAN.2017.06.003

21. Li Y, Li G, Zhang J, Wu X, Chen X. The Dual Roles of Human γδ T Cells: Anti-Tumor or Tumor-Promoting. *Front Immunol* (2021) 11: doi: 10.3389/fimmu.2020.619954

22. Wu P, Wu D, Ni C, Ye J, Chen W, Hu G, et al. γδT17 cells promote the accumulation and expansion of myeloid-derived suppressor cells in human colorectal cancer. *Immunity* (2014) 40:785–800. doi: 10.1016/J.IMMUNI.2014.03.013

23. Ma Y, Lei H, Tan J, Xuan L, Wu X, Liu Q. Characterization of γδ regulatory T cells from peripheral blood in patients with multiple myeloma. *Biochem Biophys Res Commun* (2016) 480:594–601. doi: 10.1016/j.bbrc.2016.10.098

24. Jin Z, Ye W, Lan T, Zhao Y, Liu X, Chen J, et al. Characteristic of TIGIT and DNAM-1 Expression on Foxp3+ γδ T Cells in AML Patients. (2020) doi: 10.1155/2020/4612952

25. Khairallah C, Chu TH, Sheridan BS. Tissue Adaptations of Memory and Tissue-Resident Gamma Delta T Cells. *Front Immunol* (2018) 9: doi: 10.3389/FIMMU.2018.02636

26. Giannotta C, Castella B, Tripoli E, Grimaldi D, Avonto I, D'Agostino M, et al. Immune dysfunctions affecting bone marrow Vγ9Vδ2 T cells in multiple myeloma: Role of immune checkpoints and disease status. *Front Immunol* (2022) 13:7591. doi: 10.3389/FIMMU.2022.1073227

27. lo Presti E, Toia F, Oieni S, Buccheri S, Turdo A, Mangiapane LR, et al. Squamous Cell Tumors Recruit γδ T Cells Producing either IL17 or IFNγ Depending on the Tumor Stage. *Cancer Immunol Res* (2017) 5:397–407. doi: 10.1158/2326-6066.CIR-16-0348

28. Kabelitz D, Serrano R, Kouakanou L, Peters C, Kalyan S. Cancer immunotherapy with γδ T cells: many paths ahead of us. *Cell Mol Immunol* (2020) 17:925–939. doi: 10.1038/s41423-020-0504-x

29. Gräwert T, Groll M, Rohdich F, Bacher A, Eisenreich W. *Biochemistry of the non-mevalonate isoprenoid pathway. Cell Mol Life Sci.* (2011) Dec;68(23):3797-814. doi: 10.1007/s00018-011-0753-z

30. Castella B, Vitale C, Coscia M, Massaia M. Vγ9Vδ2 T cell-based immunotherapy in hematological malignancies: from bench to bedside. *Cell Mol Life Sci* (2011) 68:2419–2432. doi: 10.1007/S00018-011-0704-8

31. Vantourout P, Laing A, Woodward MJ, Zlatareva I, Apolonia L, Jones AW, et al. Heteromeric interactions regulate butyrophilin (BTN) and BTN-like molecules governing γδ T cell biology. *Proc Natl Acad Sci U S A* (2018) 115:1039–1044. doi: 10.1073/pnas.1701237115

32. Gu S, Borowska MT, Boughter CT, Adams EJ. Butyrophilin3A proteins and Vγ9Vδ2 T cell activation. *Semin Cell Dev Biol* (2018) 84:65. doi: 10.1016/J.SEMCDB.2018.02.007

33. Karunakaran MM, Willcox CR, Salim M, Paletta D, Fichtner AS, Noll A, et al. Butyrophilin-2A1 Directly Binds Germline-Encoded Regions of the Vγ9Vδ2 TCR and Is Essential for Phosphoantigen Sensing. *Immunity* (2020) 52:487-498.e6. doi: 10.1016/J.IMMUNI.2020.02.014

34. Rigau M, Ostrouska S, Fulford TS, Johnson DN, Woods K, Ruan Z, et al. Butyrophilin 2A1 is essential for phosphoantigen reactivity by γδ T cells. *Science* (2020) 367: doi: 10.1126/SCIENCE.AAY5516

35. Castella B, Kopecka J, Sciancalepore P, Mandili G, Foglietta M, Mitro N, et al. The ATP-binding cassette transporter A1 regulates phosphoantigen release and Vγ39Vδ2 T cell activation by dendritic cells. *Nat Commun* (2017) 8:1–14. doi: 10.1038/ncomms15663

36. Laplagne C, Ligat L, Foote J, Lopez F, Fournié JJ, Laurent C, et al. Self-activation of Vγ9Vδ2 T cells by exogenous phosphoantigens involves TCR and butyrophilins. *Cell Mol Immunol* (2021) 18:1861–1870. doi: 10.1038/S41423-021-00720-W

37. Castella B, Foglietta M, Riganti C, Massaia M. Vγ9Vδ2 T Cells in the Bone Marrow of Myeloma Patients: A Paradigm of Microenvironment-Induced Immune Suppression. *Front Immunol* (2018) 9: doi: 10.3389/FIMMU.2018.01492

38. Pang DJ, Neves JF, Sumaria N, Pennington DJ. Understanding the complexity of γδ T-cell subsets in mouse and human. *Immunology* (2012) 136:283–290. doi: 10.1111/J.1365-2567.2012.03582.X

39. Thompson K, Rojas-Navea J, Rogers MJ. Alkylamines cause Vgamma9Vdelta2 T-cell activation and proliferation by inhibiting the mevalonate pathway. *Blood* (2006) 107:651–654. doi: 10.1182/BLOOD-2005-03-1025

40. Fiore F, Castella B, Nuschak B, Bertieri R, Mariani S, Bruno B, et al. Enhanced ability of dendritic cells to stimulate innate and adaptive immunity on short-term incubation with zoledronic acid. *Blood* (2007) 110:921–927. doi: 10.1182/BLOOD-2006-09-044321

41. Xiang Z, Tu W. Dual Face of Vγ9Vδ2-T Cells in Tumor Immunology: Anti- versus Pro-Tumoral Activities. *Front Immunol* (2017) 8: doi: 10.3389/FIMMU.2017.01041

42. Brandes M, Willimann K, Moser B. Professional antigen-presentation function by human gammadelta T Cells. *Science* (2005) 309:264–268. doi: 10.1126/SCIENCE.1110267

43. Beetz S, Wesch D, Marischen L, Welte S, Oberg HH, Kabelitz D. Innate immune functions of human gammadelta T cells. *Immunobiology* (2008) 213:173–182. doi: 10.1016/J.IMBIO.2007.10.006

44. Bonneville M, Scotet E. Human Vgamma9Vdelta2 T cells: promising new leads for immunotherapy of infections and tumors. *Curr Opin Immunol* (2006) 18:539–546. doi: 10.1016/J.COI.2006.07.002

45. Castella B, Riganti C, Fiore F, Pantaleoni F, Canepari ME, Peola S, et al. Immune modulation by zoledronic acid in human myeloma: an advantageous cross-talk between Vγ9Vδ2 T cells, αβ CD8+ T cells, regulatory T cells, and dendritic cells. *J Immunol* (2011) 187:1578–1590. doi: 10.4049/JIMMUNOL.1002514

46. Dieli F, Poccia F, Lipp M, Sireci G, Caccamo N, di Sano C, et al. Differentiation of effector/memory Vdelta2 T cells and migratory routes in lymph nodes or inflammatory sites. *J Exp Med* (2003) 198:391–397. doi: 10.1084/JEM.20030235

47. Odaira K, Kimura SN, Fujieda N, Kobayashi Y, Kambara K, Takahashi T, et al. CD27(-)CD45(+) γδ T cells can be divided into two populations, CD27(-)CD45(int) and CD27(-)CD45(hi) with little proliferation potential. *Biochem Biophys Res Commun* (2016) 478:1298–1303. doi: 10.1016/J.BBRC.2016.08.115

48. Schönefeldt S, Wais T, Herling M, Mustjoki S, Bekiaris V, Moriggl R, et al. The Diverse Roles of γδ T Cells in Cancer: From Rapid Immunity to Aggressive Lymphoma. *Cancers (Basel)* (2021) 13:6212. doi: 10.3390/CANCERS13246212

49. Chan KF, Duarte JDG, Ostrouska S, Behren A. γδ T Cells in the Tumor Microenvironment—Interactions With Other Immune Cells. *Front Immunol* (2022) 13: doi: 10.3389/fimmu.2022.894315

50. Holmen Olofsson G, Idorn M, Carnaz Simões AM, Aehnlich P, Skadborg SK, Noessner E, et al. Vγ9Vδ2 T Cells Concurrently Kill Cancer Cells and Cross-Present Tumor Antigens. *Front Immunol* (2021) 12: doi: 10.3389/FIMMU.2021.645131

51. Takahara M, Miyai M, Tomiyama M, Mutou M, Nicol AJ, Nieda M. Copulsing tumor antigen-pulsed dendritic cells with zoledronate efficiently enhance the expansion of tumor antigen-specific CD8+ T cells via Vgamma9gammadelta T cell activation. *J Leukoc Biol* (2008) 83:742–754. doi: 10.1189/JLB.0307185

52. Altvater B, Pscherer S, Landmeier S, Kailayangiri S, Savoldo B, Juergens H, et al. Activated human γδ T cells induce peptide-specific CD8+ T-cell responses to tumor-associated self-antigens. *Cancer Immunol Immunother* (2012) 61:385–396. doi: 10.1007/S00262-011-1111-6

53. Castella B, Foglietta M, Sciancalepore P, Rigoni M, Coscia M, Griggio V, et al. Anergic bone marrow Vγ9Vδ2 T cells as early and long-lasting markers of PD-1-targetable microenvironment-induced immune suppression in human myeloma. *Oncoimmunology* (2015) 4:e1047580. doi: 10.1080/2162402X.2015.1047580

54. Wu K, Feng J, Xiu Y, Li Z, Lin Z, Zhao H, et al. Vδ2 T cell subsets, defined by PD-1 and TIM-3 expression, present varied cytokine responses in acute myeloid leukemia patients. *Int Immunopharmacol* (2020) 80: doi: 10.1016/J.INTIMP.2019.106122

55. He W, Hu Y, Chen D, Li Y, Ye D, Zhao Q, et al. Hepatocellular carcinoma-infiltrating γδ T cells are functionally defected and allogenic Vδ2 + γδ T cell can be a promising complement. *Clin Transl Med* (2022) 12: doi: 10.1002/ctm2.800

56. Barjon C, Michaud HA, Fages A, Dejou C, Zampieri A, They L, et al. IL-21 promotes the development of a CD73-positive Vγ9Vδ2 T cell regulatory population. *Oncoimmunology* (2017) 7: doi: 10.1080/2162402X.2017.1379642

57. Doherty DG, Dunne MR, Mangan BA, Madrigal-Estebas L. Preferential Th1 cytokine profile of phosphoantigen-stimulated human Vγ9Vδ2 T cells. *Mediators Inflamm* (2010) 2010: doi: 10.1155/2010/704941

58. Caccamo N, la Mendola C, Orlando V, Meraviglia S, Todaro M, Stassi G, et al. Differentiation, phenotype, and function of interleukin-17-producing human Vγ9Vδ2 T cells. *Blood* (2011) 118:129–138. doi: 10.1182/BLOOD-2011-01-331298

59. McAllister F, Bailey JM, Alsina J, Nirschl CJ, Sharma R, Fan H, et al. Oncogenic Kras activates a hematopoietic-to-epithelial IL-17 signaling axis in preinvasive pancreatic neoplasia. *Cancer Cell* (2014) 25:621. doi: 10.1016/J.CCR.2014.03.014

60. Wu K, Zhao H, Xiu Y, Li Z, Zhao J, Xie S, et al. IL-21-mediated expansion of Vγ9Vδ2 T cells is limited by the Tim-3 pathway. *Int Immunopharmacol* (2019) 69:136–142. doi: 10.1016/J.INTIMP.2019.01.027

61. Tirier SM, Mallm JP, Steiger S, Poos AM, Awwad MHS, Giesen N, et al. Subclone-specific microenvironmental impact and drug response in refractory multiple myeloma revealed by single-cell transcriptomics. *Nat Commun* (2021) 12: doi: 10.1038/S41467-021-26951-Z

62. Noviello M, Manfredi F, Ruggiero E, Perini T, Oliveira G, Cortesi F, et al. Bone marrow central memory and memory stem T-cell exhaustion in AML patients relapsing after HSCT. *Nat Commun* (2019) 10: doi: 10.1038/s41467-019-08871-1

63. Liu Y, Yan X, Zhang F, Zhang X, Tang F, Han Z, et al. TCR-T Immunotherapy: The Challenges and Solutions. *Front Oncol* (2022) 11: doi: 10.3389/fonc.2021.794183

64. Jiang H, Fu D, Bidgoli A, Paczesny S. T Cell Subsets in Graft Versus Host Disease and Graft Versus Tumor. *Front Immunol* (2021) 12: doi: 10.3389/fimmu.2021.761448

65. Cornel AM, Mimpen IL, Nierkens S. MHC class I downregulation in cancer: Underlying mechanisms and potential targets for cancer immunotherapy. *Cancers (Basel)* (2020) 12:1–33. doi: 10.3390/cancers12071760

66. Burnham RE, Zoine JT, Story JY, Garimalla SN, Gibson G, Rae A, et al. Characterization of Donor Variability for γδ T Cell ex vivo Expansion and Development of an Allogeneic γδ T Cell Immunotherapy. *Front Med (Lausanne)* (2020) 7:588453. doi: 10.3389/fmed.2020.588453

67. Wajid M, Khan A, Eberl M, Moser B. Potential use of γδ T cell-based vaccines in cancer immunotherapy. (2014) doi: 10.3389/fimmu.2014.00512

68. Braza MS, Klein B, Fiol G, Rossi JF. γδ T-cell killing of primary follicular lymphoma cells is dramatically potentiated by GA101, a type II glycoengineered anti-CD20 monoclonal antibody. *Haematologica* (2011) 96:400–407. doi: 10.3324/HAEMATOL.2010.029520

69. Tokuyama H, Hagi T, Mattarollo SR, Morley J, Wang Q, Fai-So H, et al. V gamma 9 V delta 2 T cell cytotoxicity against tumor cells is enhanced by monoclonal antibody drugs--rituximab and trastuzumab. *Int J Cancer* (2008) 122:2526–2534. doi: 10.1002/IJC.23365

70. Gertner-Dardenne J, Bonnafous C, Bezombes C, Capietto AH, Scaglione V, Ingoure S, et al. Bromohydrin pyrophosphate enhances antibody-dependent cell-mediated cytotoxicity induced by therapeutic antibodies. *Blood* (2009) 113:4875–4884. doi: 10.1182/BLOOD-2008-08-172296

71. Abe Y, Muto M, Nieda M, Nakagawa Y, Nicol A, Kaneko T, et al. Clinical and immunological evaluation of zoledronate-activated Vgamma9gammadelta T-cell-based immunotherapy for patients with multiple myeloma. *Exp Hematol* (2009) 37:956–968. doi: 10.1016/J.EXPHEM.2009.04.008

72. Rezvani K, Yong ASM, Mielke S, Jafarpour B, Savani BN, Le RQ, et al. Repeated PR1 and WT1 peptide vaccination in Montanide-adjuvant fails to induce sustained high-avidity, epitope-specific CD8+ T cells in myeloid malignancies. *Haematologica* (2011) 96:432–440. doi: 10.3324/HAEMATOL.2010.031674

73. Kitawaki T, Kadowaki N, Fukunaga K, Kasai Y, Maekawa T, Ohmori K, et al. A phase I/IIa clinical trial of immunotherapy for elderly patients with acute myeloid leukaemia using dendritic cells co-pulsed with WT1 peptide and zoledronate. *Br J Haematol* (2011) 153:796–799. doi: 10.1111/J.1365-2141.2010.08490.X

74. Khan MWA, Eberl M, Moser B. Potential Use of γδ T Cell-Based Vaccines in Cancer Immunotherapy. *Front Immunol* (2014) 5: doi: 10.3389/FIMMU.2014.00512

75. Kunzmann V, Smetak M, Kimmel B, Weigang-Koehler K, Goebeler M, Birkmann J, et al. Tumor-promoting versus tumor-antagonizing roles of γδ T cells in cancer immunotherapy: Results from a prospective phase I/II trial. *Journal of Immunotherapy* (2012) 35:205–213. doi: 10.1097/CJI.0b013e318245bb1e

76. Saura-Esteller J, de Jong M, King LA, Ensing E, Winograd B, de Gruijl TD, et al. Gamma Delta T-Cell Based Cancer Immunotherapy: Past-Present-Future. *Front Immunol* (2022) 13: doi: 10.3389/fimmu.2022.915837

77. Presti E lo, Pizzolato G, Corsale AM, Caccamo N, Sireci G, Dieli F, et al. γδ T Cells and Tumor Microenvironment: From Immunosurveillance to Tumor Evasion. *Front Immunol* (2018) 9: doi: 10.3389/FIMMU.2018.01395

78. Capietto AH, Martinet L, Fournie JJ. How tumors might withstand γδ T-cell attack. *Cell Mol Life Sci* (2011) 68:2433–2442. doi: 10.1007/S00018-011-0705-7

79. Mariani S, Muraro M, Pantaleoni F, Fiore F, Nuschak B, Peola S, et al. Effector γδ T cells and tumor cells as immune targets of zoledronic acid in multiple myeloma. *Leukemia 2005 19:4* (2005) 19:664–670. doi: 10.1038/sj.leu.2403693

80. Coscia M, Vitale C, Peola S, Foglietta M, Rigoni M, Griggio V, et al. Dysfunctional Vγ9Vδ2 T cells are negative prognosticators and markers of dysregulated mevalonate pathway activity in chronic lymphocytic leukemia cells. *Blood* (2012) 120:3271–3279. doi: 10.1182/blood-2012-03-417519

81. Tas L, Jedema I, Haanen JBAG. Novel strategies to improve efficacy of treatment with tumor-infiltrating lymphocytes (TILs) for patients with solid cancers. (2023) doi: 10.1097/CCO.0000000000000925

82. Pizzolato G, Kaminski H, Tosolini M, Franchini D-M, Pont F, Martins F, et al. Single-cell RNA sequencing unveils the shared and the distinct cytotoxic hallmarks of human TCRVδ1 and TCRVδ2 γδ T lymphocytes. *PNAS* (2019) 116:11906–11915. doi: 10.1073/pnas.1818488116

83. de Weerdt I, Hofland T, Lameris R, Endstra S, Jongejan A, Moerland PD, et al. Improving CLL Vγ9Vδ2-T-cell fitness for cellular therapy by ex vivo activation and ibrutinib. *Blood* (2018) 132:2260–2272. doi: 10.1182/blood-2017-12-822569

84. Fazzi R, Petrini I, Giuliani N, Morganti R, Carulli G, Dalla Palma B, et al. Phase II Trial of Maintenance Treatment With IL2 and Zoledronate in Multiple Myeloma After Bone Marrow Transplantation: Biological and Clinical Results. *Front Immunol* (2021) 11:573156. doi: 10.3389/fimmu.2020.573156

85. Merli P, Algeri M, Galaverna F, Milano GM, Bertaina V, Biagini S, et al. Immune Modulation Properties of Zoledronic Acid on TcRγδ T-Lymphocytes After TcRαβ/CD19-Depleted Haploidentical Stem Cell Transplantation: An analysis on 46 Pediatric Patients Affected by Acute Leukemia. *Front Immunol* (2020) 11: doi: 10.3389/fimmu.2020.00699

86. Pressey JG, Adams J, Harkins L, Kelly D, You Z, Lamb LS. In vivo expansion and activation of gd T cells as immunotherapy for refractory neuroblastoma A phase 1 study. *Medicine (United States)* (2016) 95: doi: 10.1097/MD.0000000000004909

87. Jhita N, Raikar SS. Allogeneic gamma delta T cells as adoptive cellular therapy for hematologic malignancies. *Exploration of immunology* (2022) 2:334–350. doi: 10.37349/EI.2022.00054

88. Wilhelm M, Smetak M, Schaefer-Eckart K, Kimmel B, Birkmann J, Einsele H, et al. Successful adoptive transfer and in vivo expansion of haploidentical γδ T cells. *J Transl Med* (2014) 12: doi: 10.1186/1479-5876-12-45

89. Xu Y, Xiang Z, Alnaggar M, Kouakanou L, Li J, He J, et al. Allogeneic Vγ9Vδ2 T-cell immunotherapy exhibits promising clinical safety and prolongs the survival of patients with late-stage lung or liver cancer. *Cell Mol Immunol* (2021) 18:427–439. doi: 10.1038/S41423-020-0515-7

90. Schilbach K, Krickeberg N, Kaißer C, Mingram S, Kind J, Siegers GM, et al. Suppressive activity of Vδ2+ γδ T cells on αβ T cells is licensed by TCR signaling and correlates with signal strength. *Cancer Immunology, Immunotherapy* (2020) 69:593–610. doi: 10.1007/s00262-019-02469-8

91. Chabab G, Barjon C, Bonnefoy N, Lafont V. *Pro-tumor γδ T Cells in Human Cancer: Polarization, Mechanisms of Action, and Implications for Therapy*. Front Immunol. (2020) Sep 16;11:2186. doi: 10.3389/fimmu.2020.02186

92. Miyashita M, Shimizu T, Ashihara E, Ukimura O. Strategies to improve the antitumor effect of γδ T cell immunotherapy for clinical application. *Int J Mol Sci* (2021) 22: doi: 10.3390/ijms22168910

93. Rossi C, Gravelle P, Decaup E, Bordenave J, Poupot M, Tosolini M, et al. Boosting γδ T cell-mediated antibody-dependent cellular cytotoxicity by PD-1 blockade in follicular lymphoma. *Oncoimmunology* (2019) 8:1554175. doi: 10.1080/2162402X.2018.1554175

94. De Gassart A, Le KS, Brune P, Agaugué S, Sims J, Goubard A, et al. Development of ICT01, a first-in-class, anti-BTN3A antibody for activating Vγ9Vδ2 T cell-mediated antitumor immune response. *Sci Transl Med* (2021) 13:835. doi: 10.1126/SCITRANSLMED.ABJ0835

95. Ganesan R, Chennupati V, Ramachandran B, Hansen MR, Singh S, Grewal IS. Selective recruitment of γδ T cells by a bispecific antibody for the treatment of acute myeloid leukemia. *Leukemia* (2021) 35:2274–2284. doi: 10.1038/s41375-021-01122-7

96. de Weerdt I, Lameris R, Scheffer GL, Vree J, de Boer R, Stam AG, et al. A bispecific antibody antagonizes prosurvival CD40 signaling and promotes Vγ9Vδ2 T cell-mediated antitumor responses in human B-cell malignancies. *Cancer Immunol Res* (2021) 9:50–61. doi: 10.1158/2326-6066.CIR-20-0138

97. de Weerdt I, Lameris R, Ruben JM, de Boer R, Kloosterman J, King LA, et al. A Bispecific Single-Domain Antibody Boosts Autologous Vγ9Vδ2-T Cell Responses Toward CD1d in Chronic Lymphocytic Leukemia. *Clin Cancer Res* (2021) 27:1744–1755. doi: 10.1158/1078-0432.CCR-20-4576

98. van Diest E, Hernández López P, Meringa AD, Vyborova A, Karaiskaki F, Heijhuurs S, et al. Gamma delta TCR anti-CD3 bispecific molecules (GABs) as novel immunotherapeutic compounds. *J Immunother Cancer* (2021) 9:3850. doi: 10.1136/jitc-2021-003850

99. Okuno D, Sugiura Y, Sakamoto N, Tagod MSO, Iwasaki M, Noda S, et al. Comparison of a Novel Bisphosphonate Prodrug and Zoledronic Acid in the Induction of Cytotoxicity in Human Vγ2Vδ2 T Cells. *Front Immunol* (2020) 11:1405. doi: 10.3389/fimmu.2020.01405

100. Kouakanou L, Xu Y, Peters C, He J, Wu Y, Yin Z, et al. Vitamin C promotes the proliferation and effector functions of human γδ T cells. *Cell Mol Immunol* (2020) 17:462–473. doi: 10.1038/s41423-019-0247-8

101. van Acker HH, Anguille S, Willemen Y, van den Bergh JM, Berneman ZN, Lion E, et al. Interleukin-15 enhances the proliferation, stimulatory phenotype, and antitumor effector functions of human gamma delta T cells. *J Hematol Oncol* (2016) 9:1–13. doi: 10.1186/s13045-016-0329-3

102. Landin AM, Cox C, Yu B, Bejanyan N, Davila M, Kelley L. Expansion and enrichment of gamma-delta (γδ) t cells from apheresed human product. *Journal of Visualized Experiments* (2021) 2021: doi: 10.3791/62622

103. Choi H, Lee Y, Hur G, Lee SE, Cho H Il, Sohn HJ, et al. γδ T cells cultured with artificial antigen-presenting cells and IL-2 show long-term proliferation and enhanced effector functions compared with γδ T cells cultured with only IL-2 after stimulation with zoledronic acid. *Cytotherapy* (2021) 23:908–917. doi: 10.1016/j.jcyt.2021.06.002

104. Boucher JC, Yu B, Li G, Shrestha B, Sallman D, Landin AM, et al. Large Scale Ex Vivo Expansion of γδ T cells Using Artificial Antigen-presenting Cells. *Journal of Immunotherapy* (2023) 46:5–13. doi: 10.1097/CJI.0000000000000445

105. Hernandez Tejada FN, Jawed J, Olivares S, Mahadeo KM, Singh H. Gamma Delta T Cells for Acute Myeloid Leukemia. *Blood* (2022) 140:12696–12696. doi: 10.1182/BLOOD-2022-162635

106. Lawrence M, Wiesheu R, Coffelt SB. The duplexity of unconventional T cells in cancer. *International Journal of Biochemistry and Cell Biology* (2022) 146: doi: 10.1016/j.biocel.2022.106213

107. Yang R, He Q, Zhou H, Gong C, Wang X, Song X, et al. Vg2 x PD-L1, a Bispecific Antibody Targeting Both the Vg2 TCR and PD-L1, Improves the Anti-Tumor Response of Vg2Vd2 T Cell. *Front Immunol* (2022) 13: doi: 10.3389/fimmu.2022.923969

108. Nada MH, Wang H, Hussein AJ, Tanaka Y, Morita CT. PD-1 checkpoint blockade enhances adoptive immunotherapy by human Vγ2Vδ2 T cells against human prostate cancer. *Oncoimmunology* (2021) 10: doi: 10.1080/2162402X.2021.1989789

109. Benyamine A, Le Roy A, Mamessier E, Gertner-Dardenne J, Castanier C, Orlanducci F, et al. BTN3A molecules considerably improve Vγ9Vδ2T cells-based immunotherapy in acute myeloid leukemia. *Oncoimmunology* (2016) 5: doi: 10.1080/2162402X.2016.1146843

110. Lin L, He J, Li J, Xu Y, Li J, Wu Y. Chitosan nanoparticles strengthen Vγ9Vδ2 T-cell cytotoxicity through upregulation of killing molecules and cytoskeleton polarization. *Int J Nanomedicine* (2019) 14:9325–9336. doi: 10.2147/IJN.S212898

111. Lamb LS, Bowersock J, Dasgupta A, Gillespie GY, Su Y, Johnson A, et al. Engineered drug resistant γδ T cells kill glioblastoma cell lines during a chemotherapy challenge: a strategy for combining chemo- and immunotherapy. *PLoS One* (2013) 8: doi: 10.1371/JOURNAL.PONE.0051805

112. Todaro M, Orlando V, Cicero G, Caccamo N, Meraviglia S, Stassi G, et al. Chemotherapy Sensitizes Colon Cancer Initiating Cells to Vc9Vd2 T Cell-Mediated Cytotoxicity. (2013) doi: 10.1371/journal.pone.0065145

113. Story JY, Zoine JT, Burnham RE, Hamilton JAG, Spencer HT, Doering CB, et al. Bortezomib enhances cytotoxicity of ex vivo-expanded gamma delta T cells against acute myeloid leukemia and T-cell acute lymphoblastic leukemia. *Cytotherapy* (2021) 23:12–24. doi: 10.1016/J.JCYT.2020.09.010

114. Alves da Silva PH, Xing S, Kotini AG, Papapetrou EP, Song X, Wucherpfennig KW, et al. MICA/B antibody induces macrophage-mediated immunity against acute myeloid leukemia. *Blood* (2022) 139:205. doi: 10.1182/BLOOD.2021011619

115. Raje N, Hideshima T, Davies FE, Chauhan D, Treon SP, Young G, et al. Tumour cell/dendritic cell fusions as a vaccination strategy for multiple myeloma. *Br J Haematol* (2004) 125:343–352. doi: 10.1111/J.1365-2141.2004.04929.X

116. Rosenblatt J, Avivi I, Vasir B, Uhl L, Munshi NC, Katz T, et al. Vaccination with dendritic cell/tumor fusions following autologous stem cell transplant induces immunologic and clinical responses in multiple myeloma patients. *Clin Cancer Res* (2013) 19:3640–3648. doi: 10.1158/1078-0432.CCR-13-0282

117. Gong J, Koido S, Kato Y, Tanaka Y, Chen D, Jonas A, et al. Induction of anti-leukemic cytotoxic T lymphocytes by fusion of patient-derived dendritic cells with autologous myeloblasts. *Leuk Res* (2004) 28:1303–1312. doi: 10.1016/j.leukres.2004.03.018

118. Wang Y, Zhu J, Yu W, Wang J, Xia K, Liang C, et al. Allogenic γδ T cell and tumor cell fused vaccine for enhanced immunotherapeutic efficacy of osteosarcoma. *J Bone Oncol* (2020) 21: doi: 10.1016/J.JBO.2018.100214

119. Willcox CR, Mohammed F, Willcox BE. The distinct MHC-unrestricted immunobiology of innate-like and adaptive-like human γδ T cell subsets—Nature's CAR-T cells. *Immunol Rev* (2020) 298:25–46. doi: 10.1111/imr.12928

120. Zhang X, Ng YY, Du Z, Li Z, Chen C, Xiao L, et al. Vγ9Vδ2 T cells expressing a BCMA—Specific chimeric antigen receptor inhibit multiple myeloma xenograft growth. *PLoS One* (2022) 17: doi: 10.1371/journal.pone.0267475

121. Zhang X, Ang WX, Du Z, Ng YY, Zha S, Chen C, et al. A CD123-specific chimeric antigen receptor augments anti-acute myeloid leukemia activity of Vγ9Vδ2 T cells. *Immunotherapy* (2022) 14:321–336. doi: 10.2217/imt-2021-0143

122. Rozenbaum M, Meir A, Aharony Y, Itzhaki O, Schachter J, Bank I, et al. Gamma-Delta CAR-T Cells Show CAR-Directed and Independent Activity Against Leukemia. *Front Immunol* (2020) 11:1347. doi: 10.3389/fimmu.2020.01347

123. Capsomidis A, Benthall G, Van Acker HH, Fisher J, Kramer AM, Abeln Z, et al. Chimeric Antigen Receptor-Engineered Human Gamma Delta T Cells: Enhanced Cytotoxicity with Retention of Cross Presentation. *Molecular Therapy* (2018) 26:354–365. doi: 10.1016/j.ymthe.2017.12.001

124. Zhai X, You F, Xiang S, Jiang L, Chen D, Li Y, et al. MUC1-Tn-targeting chimeric antigen receptor-modified Vγ9Vδ2 T cells with enhanced antigen-specific anti-tumor activity. *Am J Cancer Res* (2021) 11:79–91.

125. van der Veken LT, Coccoris M, Swart E, Falkenburg JHF, Schumacher TN, Heemskerk MHM. αβ T Cell Receptor Transfer to γδ T Cells Generates Functional Effector Cells without Mixed TCR Dimers In Vivo. *The Journal of Immunology* (2009) 182:164–170. doi: 10.4049/jimmunol.182.1.164

126. Harrer DC, Simon B, Fujii S ichiro, Shimizu K, Uslu U, Schuler G, et al. RNA-transfection of γ/δ T cells with a chimeric antigen receptor or an α/β T-cell receptor: A safer alternative to genetically engineered α/β T cells for the immunotherapy of melanoma. *BMC Cancer* (2017) 17: doi: 10.1186/s12885-017-3539-3

127. Shimizu K, Shinga J, Yamasaki S, Kawamura M, Dörrie J, Schaft N, et al. Transfer of mRNA encoding invariant NKT cell receptors imparts glycolipid specific responses to T cells and γδT cells. *PLoS One* (2015) 10: doi: 10.1371/journal.pone.0131477

128. Straetemans T, Kierkels GJJ, Doorn R, Jansen K, Heijhuurs S, dos Santos JM, et al. GMP-grade manufacturing of T cells engineered to express a defined γδTCR. *Front Immunol* (2018) 9:1062. doi: 10.3389/fimmu.2018.01062

129. Braham MVJ, Minnema MC, Aarts T, Sebestyen Z, Straetemans T, Vyborova A, et al. Cellular immunotherapy on primary multiple myeloma expanded in a 3D bone marrow niche model. *Oncoimmunology* (2018) 7: doi: 10.1080/2162402X.2018.1434465

Daratumumab-induced *in vivo* immune modulation in relapsed and/refractory multiple myeloma patients enrolled in the NCT03848676 clinical study [Daratumumab, Lenalidomide, Dexamethasone (D-Rd)]

ABSTRACT

Daratumumab (Dara) has become a mainstay in the treatment of naïve and relapsed/refractory Multiple Myeloma (RRMM) patients. In the clinical practice, Dara is delivered continuously until relapse or toxicity. Dara binds to CD38, a cell surface antigen that is expressed not only by myeloma cells, but also by other cells populating the tumor microenvironment (TME). At diagnosis, Dara is expected to target mainly myeloma cells since this is the predominant CD38+ cell subpopulation; later on, Dara is expected to redirect its activity against other TME-resident CD38+ cells including immune suppressor and immune effector cells. The clinical consequence of this redirected CD38-targeted activity is unclear and worth of investigation to understand the mechanisms of relapse and maximize the efficacy and duration of Dara-based treatments.

In this study, we have investigated the immune modulation induced by Dara in 32 relapsed/refractory (RRMM) patients enrolled in the NCT03848676 clinical study [Daratumumab, Lenalidomide, Dexamethasone (D-Rd)]. CD38 expression was down-regulated in NK cells, classical and intermediate monocytes, T cells, Vγ9Vδ2 T cells, monocytic-myeloid derived suppressor cells (Mo-MDSC), regulatory T cells (Tregs), and regulatory B cells (Bregs). CD38 down-regulation in NK cells was associated with CD16 (FcγRIII) down-modulation and NK-cell subset re-distribution.

Dara also induced changes in total counts of immune cells mainly consisting in the decrease of CD38+Tregs and CD38+Bregs and the increase of functionally exhausted CD8+ T cells.

A comparison between responder (R) (n=19) and non-responder (NR) patients (n= 12) indicates that the clinical outcome is associated with specific patterns of CD38 expression in BM NK cells, PB T-cell subpopulations redistribution, and expression of functional exhaustion T-cell markers.

In conclusion, long-term Dara treatment induces a significant modulation of selected CD38+ immune effector and suppressor cells potentially involved in the disease control.

GRAPHICAL ABSTRACT

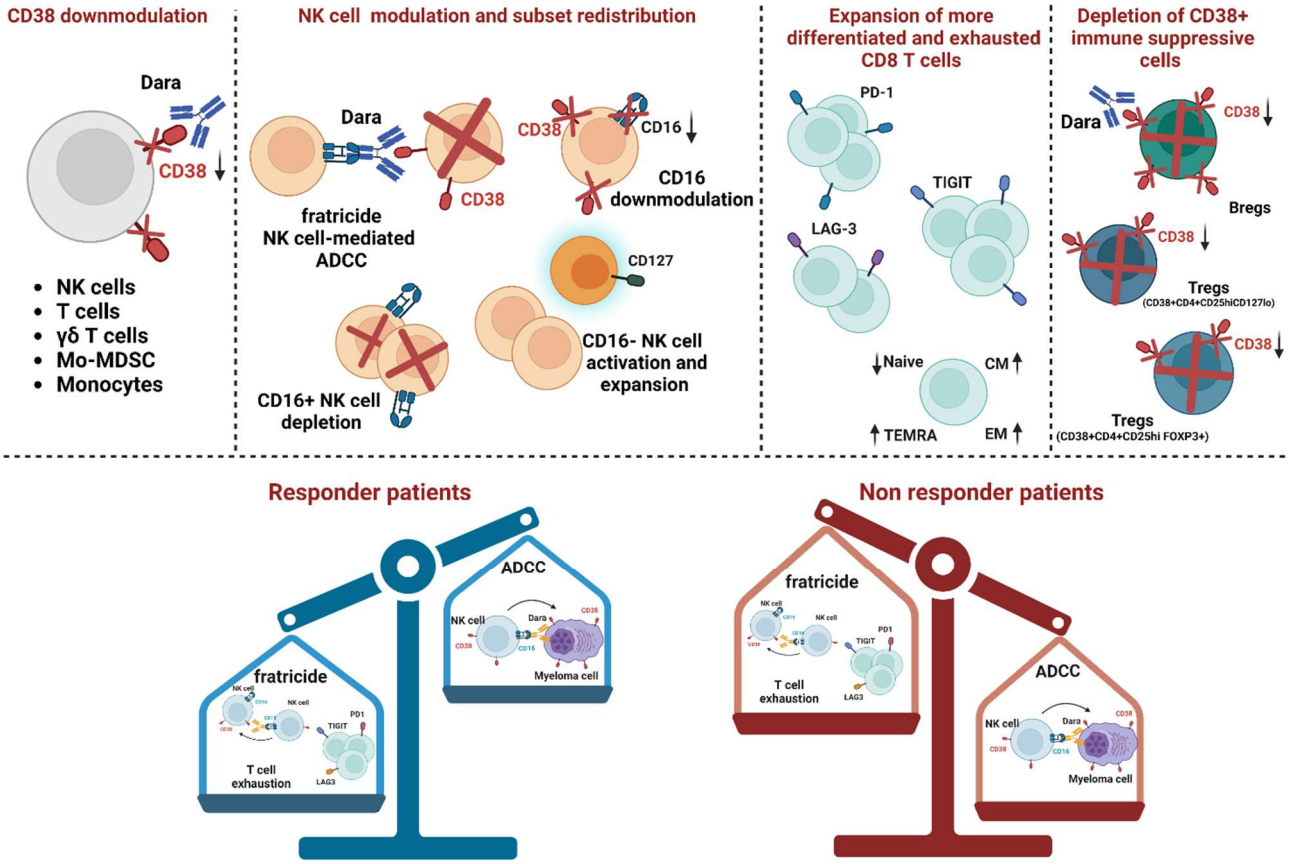

Long-term Daratumumab-induced immune modulation in relapsed and/refractory MM patients enrolled in the NCT03848676 clinical study. Immune changes induced by Daratumumab include CD38 downmodulation on targeted immune cells, NK cell modulation and subset redistribution, expansion of more differentiated and exhausted CD8 T cells, and depletion of CD38+ immune suppressive cells. Immune profile of relapsed/refractory MM patients before treatment affects Daratumumab response.

INTRODUCTION

Daratumumab (Dara) is a fully human IgG1-kappa monoclonal antibody (mAb) that has become a mainstay in the treatment of MM patients in combination with immunomodulatory agents (IMiDs) or proteasome inhibitors (PI) in newly diagnosed (NDMM) and relapsed/refractory patients (RRMM) (1).

CD38 is expressed by myeloma cells, but also by immune effector and suppressor cells in the tumor microenvironment (TME) (2). CD38 is a pleiotropic molecule with receptor and ecto-enzymatic functions. CD38 cyclase and hydrolase activity enables myeloma and BM-resident cells to generate adenosine (Ado) in cooperation with other ecto-enzymes like CD73 and CD39. Ado is an immune suppressive nucleoside involved in metabolic reprogramming of BM niche (3).

Dara acts through a broad-spectrum of killing activities. Direct antitumor activity is mediated by Fc-dependent immune effector mechanisms. Dara-opsonized myeloma cells can elicit Fc-induced cytotoxicity of monocytes/macrophages through antibody-dependent cellular phagocytosis (ADCP) or NK cells through antibody-dependent cellular cytotoxicity (ADCC). Moreover, C1q can be fixed to Dara-Fc and trigger complement-dependent cytotoxicity (CDC) resulting in complement proteolytic cascade activation and myeloma cell lysis. Induction of programmed cell death after cross-linking also contribute to Dara antitumor activity (1). Indirect antitumor activity is mainly dependent on CD38+ immune cell targeting and lies in the ability to improve immune surveillance by inhibiting immune suppressor cells like regulatory T cells (Tregs), regulatory B cells (Bregs) and myeloid-derived suppressor cells (MDSC) (4).

Although Dara and anti-CD38 mAbs have significantly improved the outcome in all clinical setting, refractoriness (primary resistance) and late relapse (acquired resistance) remain a major issue (5). Determinants of treatment failure should be sought in both myeloma cells and the TME. Tumor-related resistance mechanisms include: 1) low pre-treatment CD38 expression levels in myeloma cells; 2) CD38 shedding vehiculated by microvescicles with immunomodulatory properties (6); 3) up-regulation of complement inhibitory proteins CD55 and CD59 on myeloma cells (6).

Other mechanisms involved in Dara resistance are related to its immune modulatory activity. Interestingly, in the clinical practice Dara is administered undefinitely until progression or unacceptable toxicity. Even if the clinical outcome of Dara-treated patients is significantly improved, PFS curves do not reach a plateau in both MAIA and Pollux studies indicating that even patients with undetectable minimal residual disease (uMRD) suffer from relapse (7). These clinical observations raise the question about the long-term effects of Dara treatment on CD38+ cells apart from myeloma cells.

In this work, we have monitored the effect of Dara treatment on peripheral blood (PB) and bone marrow (BM) CD38+ cells potentially involved in direct and indirect anti-myeloma activity. Moreover, we have evaluated some immune features that can be important in the disease control. Our data provide information about the long-lasting immune modulation induced by D-Rd in in RRMM and unveil for the first time an association between CD38+ expression in selected immune cell subsets at baseline, Dara treatment, and response to treatment.

METHODS

Clinical study design

RRMM patients receiving Dara-based treatments included in a prospective observational study (NCT03848676) supported by AIRC IG 2017- 20541 were analyzed. 40 patients have been enrolled in the project from AOU Città della Salute e della Scienza (Torino) and Fondazione IRCCS Istituto Nazionale dei Tumori (Milano). Dara treatment was administered once per week (16 mg/ kg) for 8 weeks, then once every two weeks for 8 weeks, and then once per month. Patients were grouped into responders (R) (i.e., patients who did not relapse during the observation time and maintained the response) and non responders (NR) (i.e., patients with a progressive disease [PD]). Data obtained from 32 RRMM patients are included in this analysis. Clinical characteristics are shown in Table 1.

Blood cell collection

PB and BM samples were collected in heparinized tubes at baseline and at specified time points during treatment [baseline, at follow up every 3 months during therapy (PB only), response to therapy and progression disease (PD)]. White Blood Cells (WBC) obtained after red blood cell lysis were evaluated using real-time flow cytometry or frozen in a solution of FBS containing 10% DMSO.

Immune cell subsets phenotyping and quantification

Immune phenotyping and quantification of T cells, B cells, monocytes, Vγ9Vδ2 T cells, NK cells, MDSC, Tregs, and Bregs were performed serially on BM and PB samples.
Cells were washed once with a solution containing PBS and 1% FBS before staining. For membrane immunofluorescence, the cells were incubated with their respective anti-human monoclonal antibodies (mAbs) at 4 ° C in the dark for 30 minutes. Afterward, the cells were washed twice and fixed with para-formaldehyde-PBS 1% before the cytofluorimetric acquisition. Cell surface proteins were targeted with fluorescinated isocyanine (FITC), r-phycoerythrin (PE), chlorophyll protein peridine (Per-CP) or allophycocyanin (APC), conjugated with mAb, according to the list in Supplemental Table 2.

For FOXP-3 intracellular staining, cells were fixed and permeabilized using the FoxP3 Staining Buffer Set according manufacturer instructions (Miltenyi #130-093-142).

The mAbs used in the study are listed in Supplemental Table 2. The gating strategies are shown in Supplemental Figure 1. Data were acquired with FACS Calibur cytometers and analyzed using FlowJo software as previously reported (8).

Statistical analysis

The results are expressed as mean ± SEM. Data normality was evaluated with the Shapiro-Wilk test. Comparisons between normally distributed variables were performed using two-tailed Student's t-test. When data were not normally distributed, differences between the groups have been evaluated with a one-way analysis of variance, a Wilcoxon–Mann–Whitney non-parametric test for paired or unpaired samples as appropriate and considered to be statistically significant for P values <0.05. The GraphPad software has been used for the statistical analyses; GraphPad symbology has been adopted to report statistical significance (*P<0.05; **P<0.01; ***P<0.001; ****P<0.0001).

RESULTS

Baseline CD38 expression profiles in PB and BM RRMM patients

Analysis of CD38 expression pattern at baseline is shown in Figure 1. Comparison of total counts of CD38+ immune cells highlights that MDSC, monocytes, and NK cells are the most abundant CD38+ subpopulation in both BM (Figure 1A left panel) and PB (Figure 1B left panel) of RRMM patients before D-Rd treatment. Percentage of CD38+ in each subpopulation is shown in Supplemental Figure 2.

Although monocytic-MDSC (Mo-MDSC) express more CD38+ than granulocytic-MDSC (Gn-MDSC) at baseline, they are less frequent than Gn-MDSC in the PB and BM of RRMM (Supplemental Figure 3 A-B). Classical monocytes are the most abundant monocyte subset in PB and BM of RRMM patients and showed the highest proportion of CD38+ cells; however, CD38 expression levels, evaluated as Mean Fluorescence Intensity (MFI), are higher in intermediate monocytes (Int Mono) of both PB and BM (Supplemental Figure 3 C-D). CD38 expression is also high in NK cells, mainly in cytotoxic NK cells in comparison to proliferative NK cells (Supplemental Figure 3E).

Significantly lower total counts and proportion of CD38+ cells was observed in conventional CD4+ and CD8+ T cells, Vγ9Vδ2 T cells, Bregs, and Tregs (Figure 1 A-B and Supplemental Figure 2).

The comparison of the CD38 MFI shows that, although CD38+ Bregs represent a small population in PB and BM, they expressed high intensity of CD38 (Figure 1 A-B right panel).

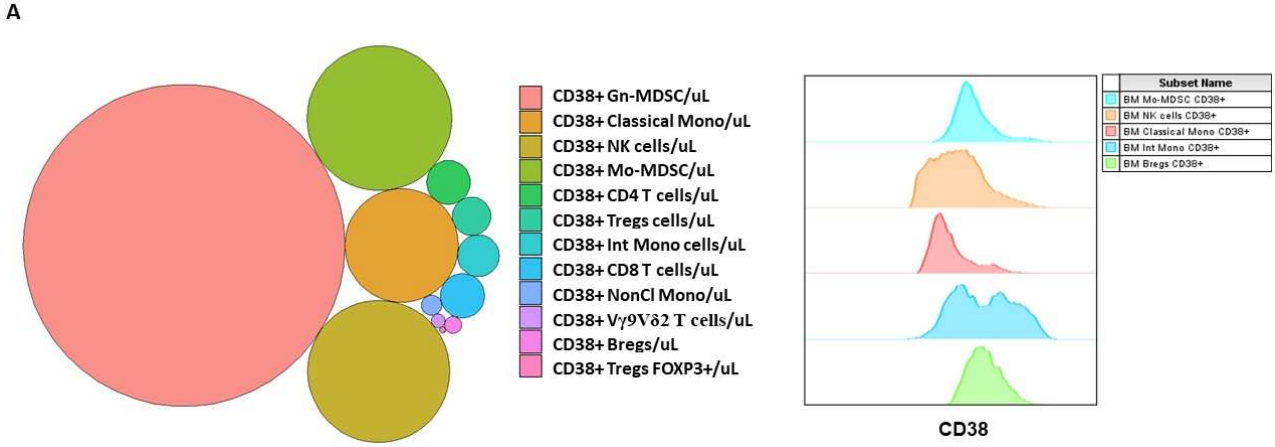

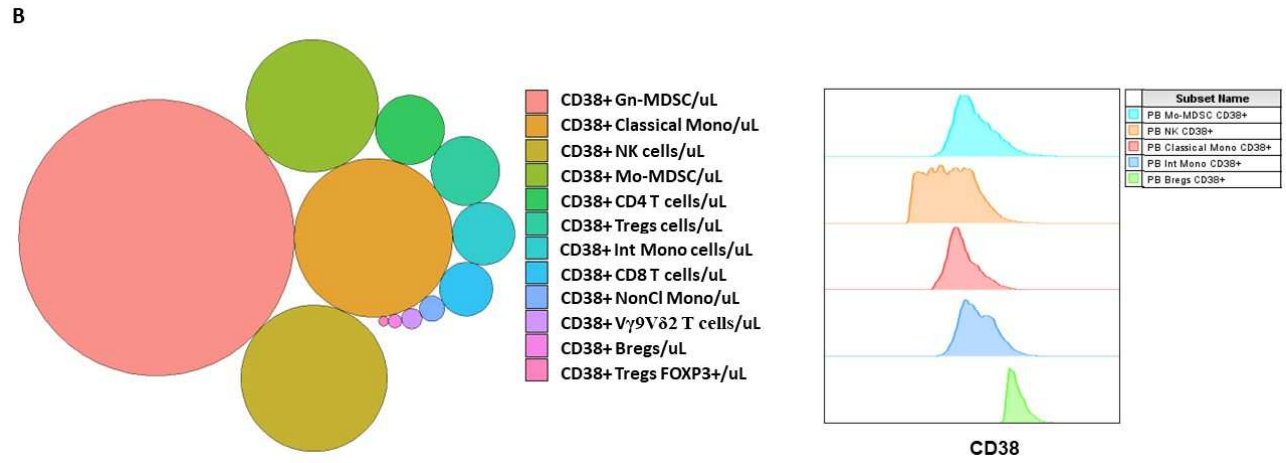

Figure 1 ***CD38 expression pattern is highly heterogenous in PB and BM of RRMM patients. A****) Left panel: Bubble chart of BM CD38+ immune cell total counts at baseline in MM patients before D-Rd treatment; Right: Comparison of the mean fluorescent intensity (MFI) of CD38+ across immune populations in BM of RRMM patients.* ***B****) Left panel: Bubble chart of PB CD38+ immune cell total counts at baseline in MM patients before D-Rd treatment; Right: Comparison of the mean fluorescent intensity (MFI) of CD38+ across immune populations in PB of RRMM patients. Circles represent mean values from 9 to 35 experiments.*

Immune modulation induced by D-Rd treatment

Phenotypic and quantitative changes were evaluated in PB during D-Rd treatment, by performing a comprehensive immune cell phenotyping on PB samples collected every three months. We assessed frequency, absolute number, subset distribution, and phenotypic changes of NK cells, classical, intermediate and non classical monocytes, B cells, CD4+ T cells, CD8+ T cells, Vγ9Vδ2 T cells, MDSC, Bregs, and Tregs. In these analyses, CD38 evaluation was performed with an anti-human CD38 multi-epitope reagent containing a mixture of antibodies specifically developed to identify CD38 expression in patients receiving CD38-targeted therapy.

D-Rd treatment induced a significant decrease of NK-cell total counts by month 3 (Figure 2A). Afterwards, a trend of increase of NK cell total counts was observed (Figure 2A). By contrast, CD38 down-regulation was persistent (Figure 2B) and associated with NK-cell subsets redistribution characterized by the increase of CD16- NK cells and the decrease of CD16+ NK cells (Figure 2 C-D). Cytofluorimetric analysis of NK-cell subset distribution at baseline and after D-Rd treatment from one representative patient is shown in Figure 2E. Residual NK cells showed a tendency to acquire an activated phenotype during the first 12 months as shown by the increased CD127 expression and the decreased CD45RA expression during this period. These changes were associated with a persistent decrease of CD25 expression (Figure 2 F-H).

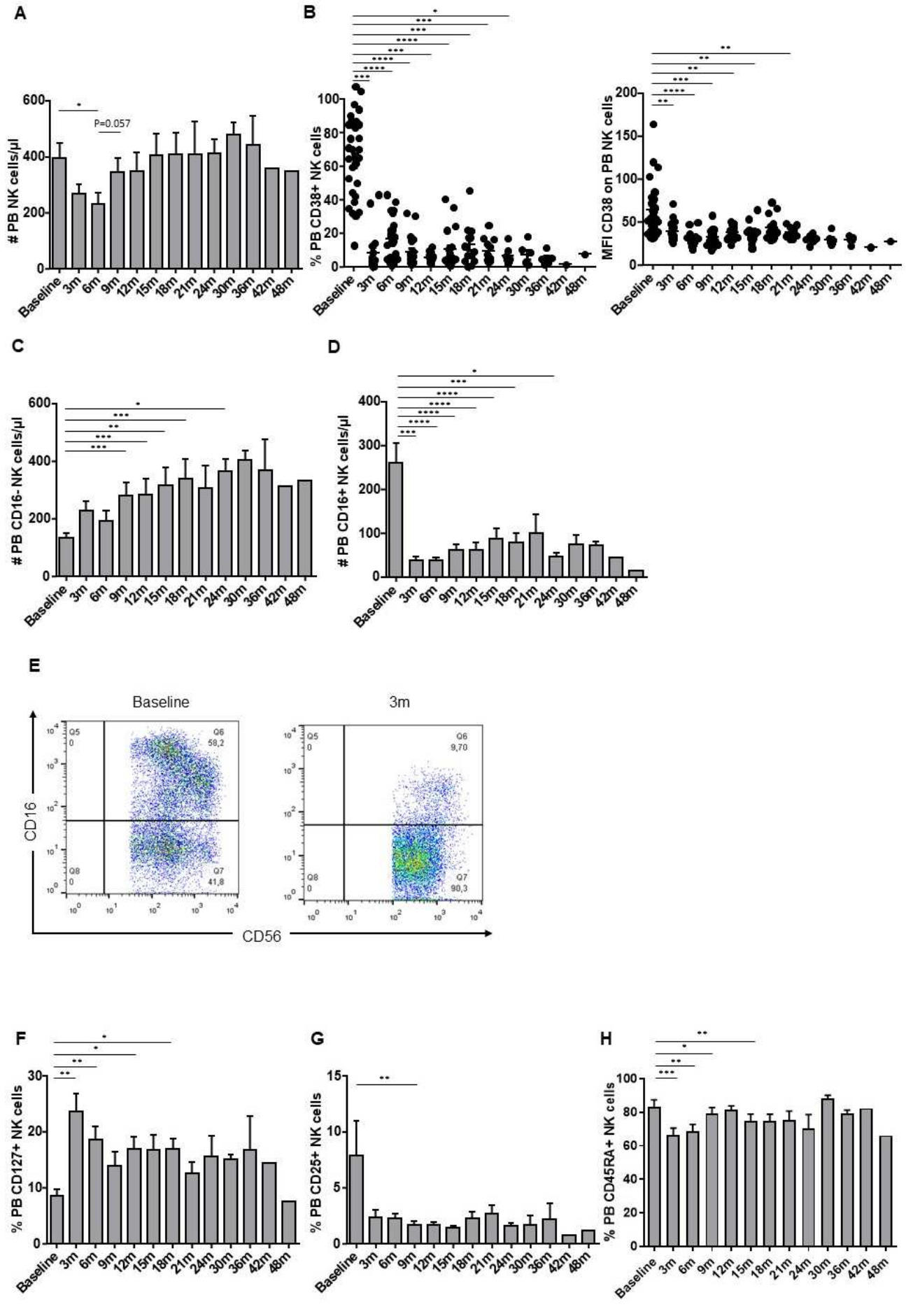
A
# PB NK cells/µl
P=0.057
B
% PB CD38+ NK cells
MFI CD38 on PB NK cells
C
PB CD16- NK cells/µl
D
PB CD16+ NK cells/µl
E
Baseline
3m
CD16
CD56
Q6 58,2
Q7 41,8
Q6 9,70
Q7 90,3
F
% PB CD127+ NK cells
G
% PB CD25+ NK cells
H
% PB CD45RA+ NK cells
Baseline 3m 6m 9m 12m 15m 18m 21m 24m 30m 36m 42m 48m

*Figure **2 D-Rd affected NK cells. A**) Absolute counts of NK cells during D-Rd treatment. Bars represent mean values ±SE from 1 (42m and 48m) to 28 (Baseline) patients. **B**) Percentage of CD38+ NK cells (left panel) and MFI (right panel) of CD38 expression on NK cells from PB of RRMM patients treated with D-Rd. **C**) Absolute counts of NK cells CD16- and **D**) NK cells CD16+ from PB of RRMM patients treated with D-Rd. Bars represent mean values ±SE from 1 (42m and 48m) to 28 (Baseline) patients. **E**) Cytofluorimetric analyses of NK cell subset distribution before (upper panel) and after (lower panel) D-Rd treatment from one representative RRMM patient. (**F**) CD127, (**G**) CD25, and (**H**) CD45RA expression in NK cells from PB of RRMM patients during D-Rd treatment. Bars represent mean values ±SE from 1 (42m and 48m) to 23 (Baseline) patients.*

The frequency and total counts of PB monocyte subsets were not significantly affected by Dara treatment (Supplemental Figure 4), whereas the proportion of CD38+ cells and MFI were significantly decreased in classical (Figure 3A) and intermediate (Figure 3B) monocytes.

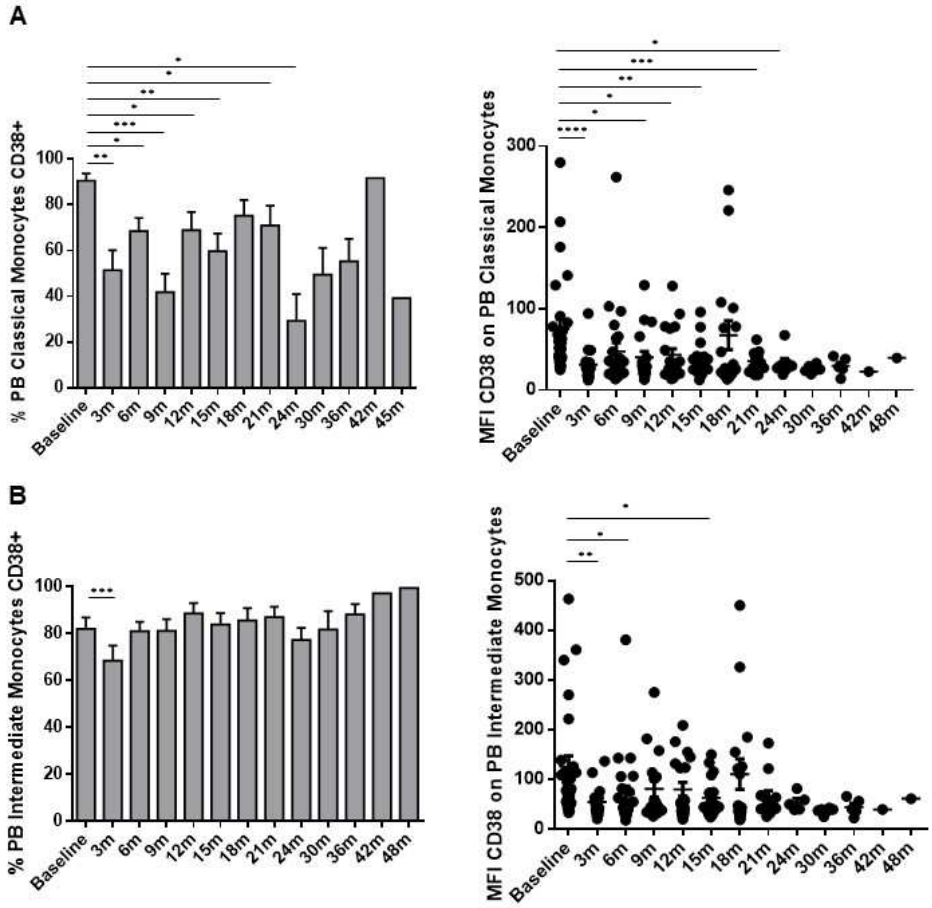

*Figure **3 CD38 expression is down-modulated in monocytes after D-Rd treatment**. **A**)Percentage of CD38+ (left panel) and MFI of CD38 (right panel) in classical monocytes from PB of RRMM patients during D-Rd treatment. Bars represent mean values ±SE from 1 (42m and 48m) to 28 (Baseline) patients. **B**) Percentage of CD38+ (left panel) and MFI of CD38 (right panel) in intermediate monocytes from PB of RRMM patients during D-Rd treatment. Bars represent mean values ±SE from 1 (42m and 48m) to 28 (Baseline) patients.*

Total B-cell counts (CD19+ cells) showed a progressive and persistent decrease in PB during D-Rd treatment (Figure 4A).

D-Rd treatment also induced significant changes in PB CD4+ and CD8+ T-cell distribution: the former decreased (Supplemental Figure 5A), whereas the latter increased as total counts (Figure 4B) and percentages (Supplemental Figure 5B). D-Rd induced a decreased CD38 expression in both CD4+ and CD8+ T cells (Figure 4 C-D).

The distribution of maturation subsets in CD8+ T cells was also modulated by D-Rd which induced a sharp decrease of total naïve (CD62L+CD45RA+) CD8+ T-cell counts in PB in the first 3-6 months coupled with a significant increase of CM (CD62L+CD45RA-), EM (CD62L-CD45RA-) and TEMRA cells (CD62L-CD45RA+) (Figure 4 E-H).

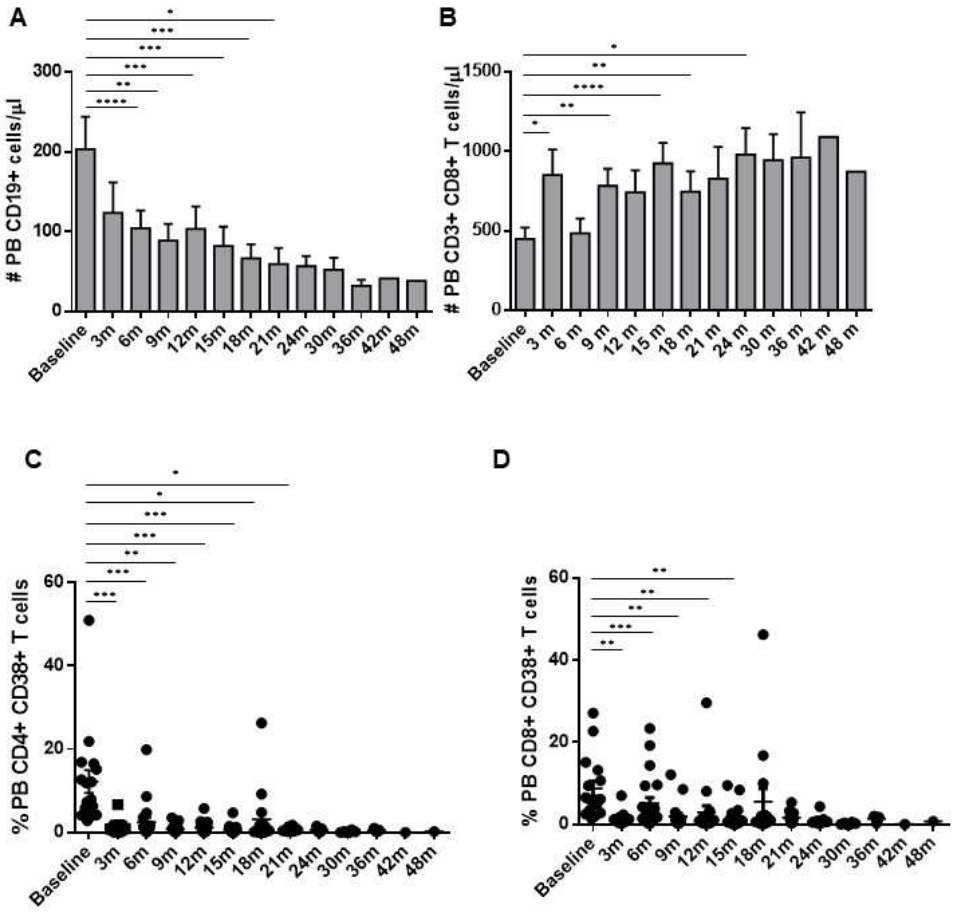

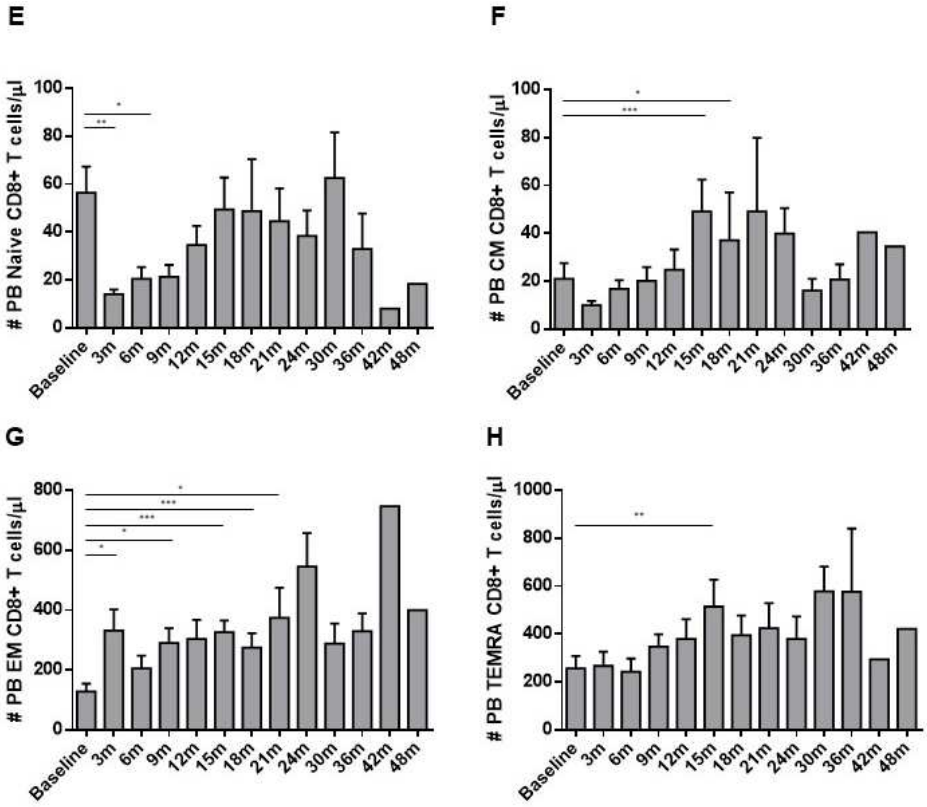

*Figure **4 Effects of D-Rd treatment on B and T cells**. **A**) Absolute counts of PB B cells during D-Rd treatment. Bars represent mean values ±SE from 1 (42m and 48m) to 29 (Baseline) patients. **B**) Absolute counts of PB CD8 T cells during D-Rd treatment. Bars represent mean values ±SE from 1 (42m and 48m) to 30 (Baseline) patients. **C**) Percentage of CD38+ CD4 T cells and **D**) CD8 T cells from PB of RRMM patients during D-Rd treatment. **E**) Absolute counts of PB CD8 T cells with Naïve, **F**) Central Memory, **G**) Effector Memory, and* **H***) TEMRA phenotype during D-Rd treatment. Bars represent mean values ±SE from 1 (42m and 48m) to 27 (Baseline) patients.*

At baseline, PD-1 and TIGIT were highly expressed by PB and BM CD4+ and CD8+ T cells as expected based on their functionally exhausted and immune senescence status (Figure 5 A-B). Paired analyses of PB and BM samples in individual patients showed that PD-1 and TIM-3 expression was higher in BM compared with PB (Figure 5 C-E), confirming that the BM represents the privileged site where the immune suppressive circuits are operated by myeloma cells and bystander cells.

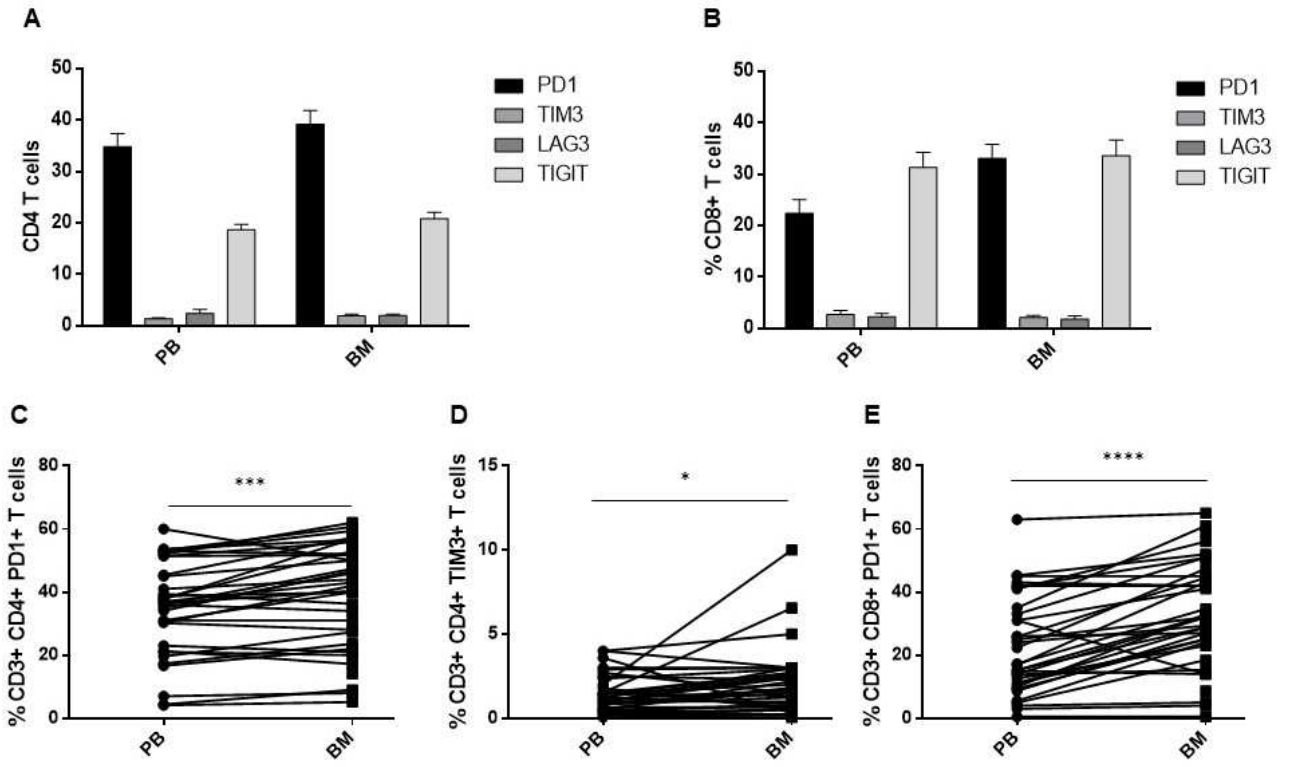

*Figure **5 Multiple ICP expression in CD4 and CD8 T cells is strengthened by tumor site**. PD-1, TIM-3, LAG-3 and TIGIT expression in **A**) CD4 T cells and **B**) CD8 T cells from RRMM patients before D-Rd treatment. Bars represent mean values ±SE from 32 patients. Analysis of **C**) CD4 PD1+, **D**) CD4 TIM3+ and **E**) CD8 PD1+ percentage on paired BM and PB of RRMM patients before D-Rd treatment.*

D-Rd treatment increased total counts of PD1+, TIGIT+ and LAG3+ CD8+ T cells (Fig 6 A-C) and LAG3+ CD4+ T cells in PB (Figure 6D). By contrast, TIM3+ expression was downmodulated in both CD4 and CD8 T cells (Figure 6 E-F).

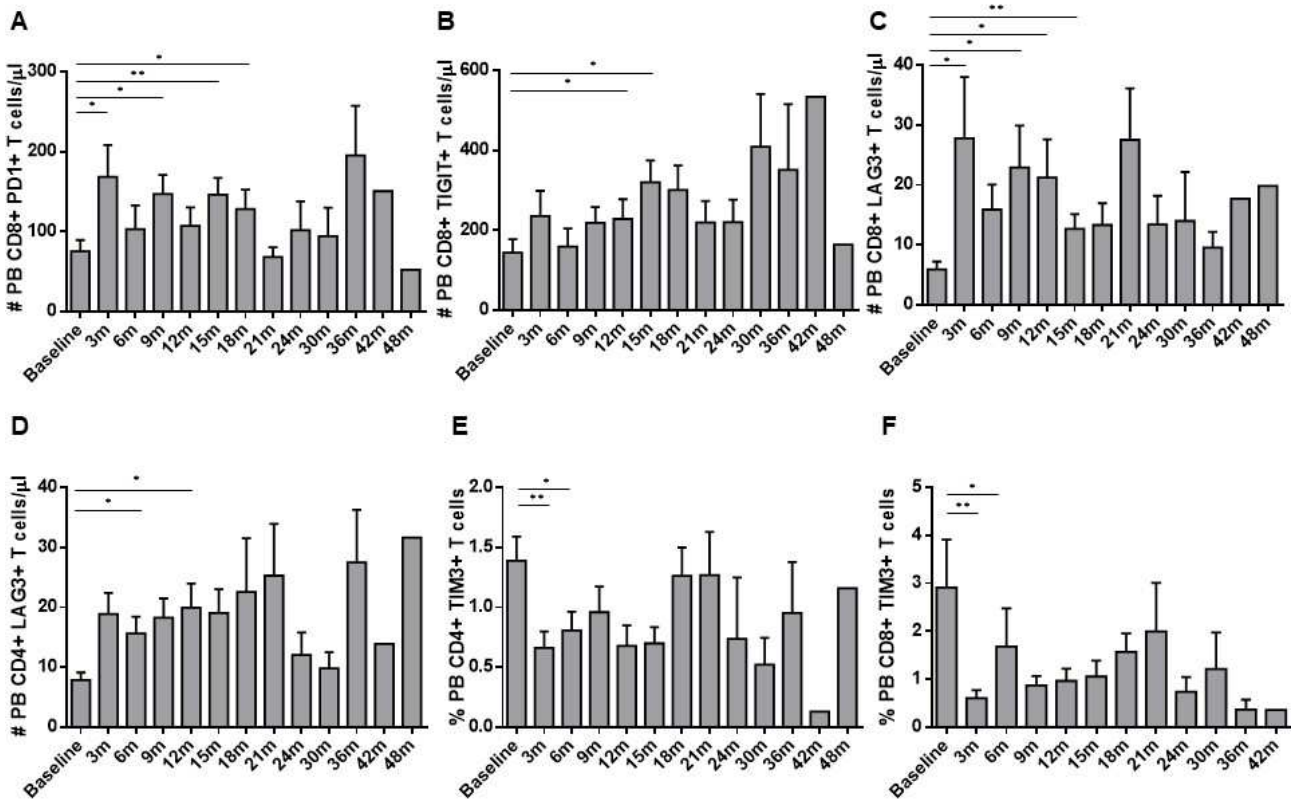

Figure 6 D-Rd treatment boosted exhaustion features of CD4 and CD8 T cells*. Total counts of PB CD8 T cells expressing* ***A****) PD-1,* ***B****) TIGIT, and* ***C****) LAG-3 at baseline and during D-Rd treatment. Bars represent mean values ±SE from 1 (42m and 48m) to 32 (Baseline) patients.* ***D****) Total counts of PB CD4 T cells expressing LAG-3. Bars represent mean values ±SE from 1 (42m and 48m) to 32 (Baseline) patients. Percentage of* ***E****) PB CD4 T cells LAG-3+ and* ***F****) CD8 T cells TIM-3+ at baseline and during D-Rd treatment. Bars represent mean values ±SE from 1 (42m and 48m) to 33 (Baseline) patients.*

We analyzed Vγ9Vδ2 T cell counts and CD38+ proportion in PB and BM samples at baseline and during D-Rd treatment. Although Vγ9Vδ2 T cell frequency and total counts were not affected (Supplemental Figure 6), we observed marked reduction of percentage and total counts of CD38+ Vγ9Vδ2 T cells after D-Rd treatment (Figure 7 A-B).

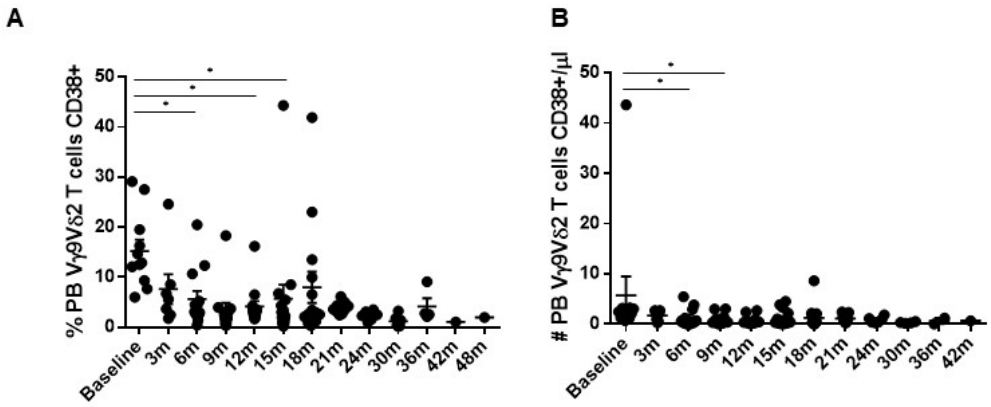

*Figure **7 CD38 was downmodulated in Vγ9Vδ2 T cells during D-Rd treatment**. **A**) Percentage and **B**) total counts of CD38+ Vγ9Vδ2 T cells from PB of RRMM patients during D-Rd treatment.*

Percentages and total counts of Tregs were increased in the PB of MM treated with D-Rd. Tregs were identified as CD4+CD25^{hi} Foxp3+ cells (Fig 8 A-B). This increase was counterbalanced by the decreased percentages of CD38+ Tregs (Figure 8C). Likewise, the percentages of Tregs characterized

by the CD4+CD25+CD127^{lo} CD38+ phenotype, recently identified by *Krejcik et al.* (9), progressively declined during D-Rd treatment (Fig 8D).

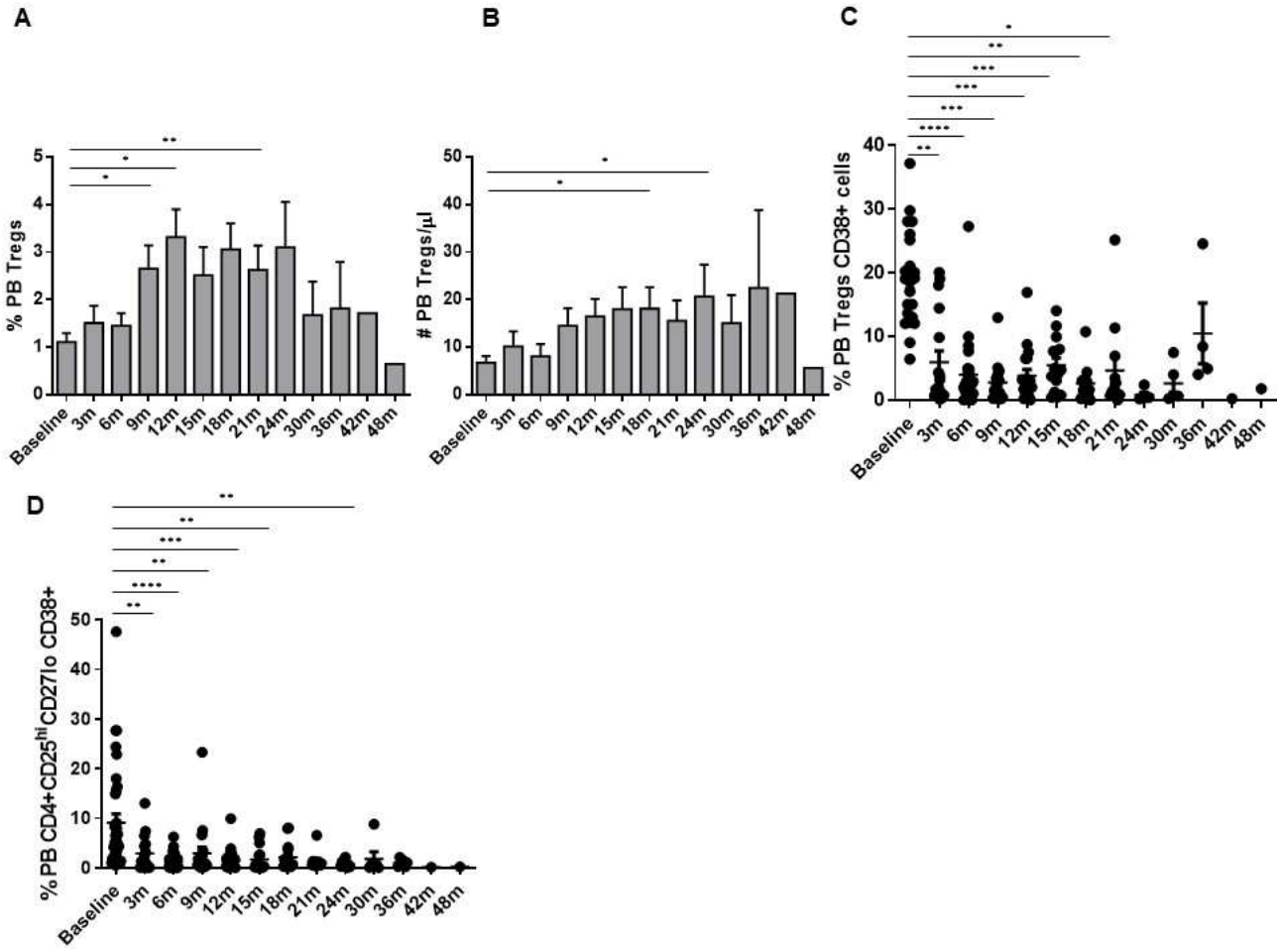

Figure 8 Dara induced sharp depletion of CD38+ Tregs. A) *Percentage and* ***B****) total counts of PB Tregs from RRMM patients during D-Rd treatment. D-Rd induced a slight increase of Tregs total counts in PB. Bars represent mean values ± SEM from 1 (42m and 48m) to 23 (Baseline) patients.* ***C****) Percentage of CD38+ Tregs in PB of RRMM patients during D-Rd treatment.* ***D****) Percentage of CD38+Tregs (CD4+CD25hiCD127lo) in PB of RRMM patients during D-Rd treatment.*

Percentages and total counts of PB CD38+ Bregs were also downregulated during D-Rd treatment (Figure 9A-B).

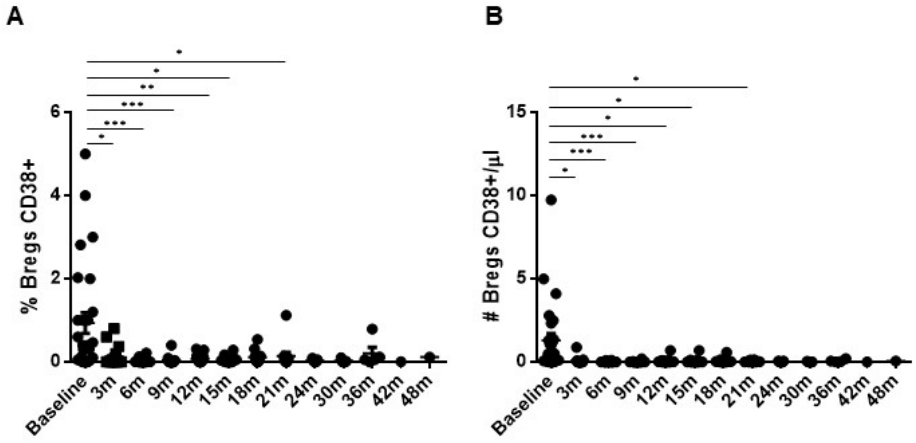

Figure 9 Dara impacts on Bregs. A) *Frequency and* ***B****) absolute counts of PB CD38+Bregs from RRMM patients during D-Rd treatment. Bregs expressing CD38 were sharply decreased after D-Rd.*

MDSC are another major immune suppressor subpopulation contributing to myeloma cell survival. Percentages and total counts of MDSC in the PB were not significantly modified by D-Rd treatment (Supplemental Figure 7 A-B), but a slight decrease in the proportion and the intensity of CD38 expression was observed in Mo-MDSC after the first 3 months of treatment (Figure 12A). A significant decrease of CD38 was also observed in Gn-MDSC (Figure 12B) with a tendency to become more evident after the 24 months of treatment.

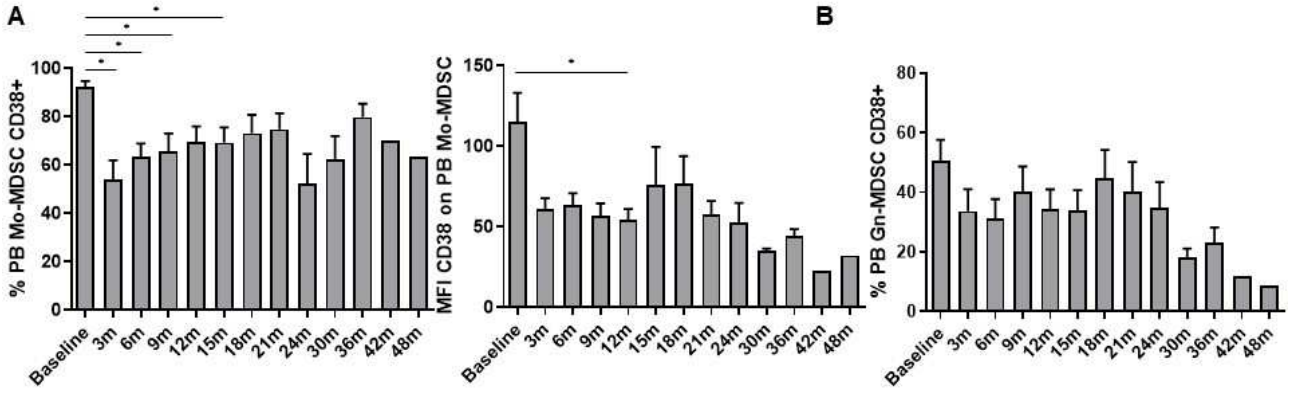

Figure ***12 Dara induced CD38 downmodulation in Mo-MDSC****.* ***A****) Left panel: percentage of CD38+ Mo-MDSC from PB of RRMM patients during D-Rd treatment. Bars represent mean values ±SEM from 1 (42m and 48m) to 22 (Baseline) patients; right panel: MFI of CD38 on Mo-MDSC from PB of RRMM patients during D-Rd treatment. Bars represent mean values ±SEM from 1 (42m and 48m) to 22 (Baseline) patients.* ***B****) Percentage of CD38+ Gn-MDSC from PB of RRMM patients during D-Rd treatment. Bars represent mean values ±SEM from 1 (42m and 48m) to 22 (Baseline) patients.*

At baseline, PDL-1 expression was higher in Mo-MDSC than Gn-MDSC in both PB and BM (Supplemental Figure 6 C). After Dara-Rd, the frequency of PB PDL-1+ MDSC exhibited a trend of increase after the first doses of D-Rd (data not shown).

Correlations between immune baseline patterns and clinical outcome

Based on the clinical outcome and the criteria reported in the Materials and Methods section, 19 patients were defined as responders (R) and 12 patients as non-responders (NR). Figure 13A shows CD38 expression in NK cells from R and NR patients in PB and BM at baseline. The latter showed significantly higher proportion of CD38+ NK cells in BM and significantly higher MFI than BM NK cells from R patients (Figure 13 A-B). The analysis of NK-cell subsets in the BM of NR patients showed a preferential accumulation of CD38+ CD16- NK cells in BM of NR patients (Figure 13C).

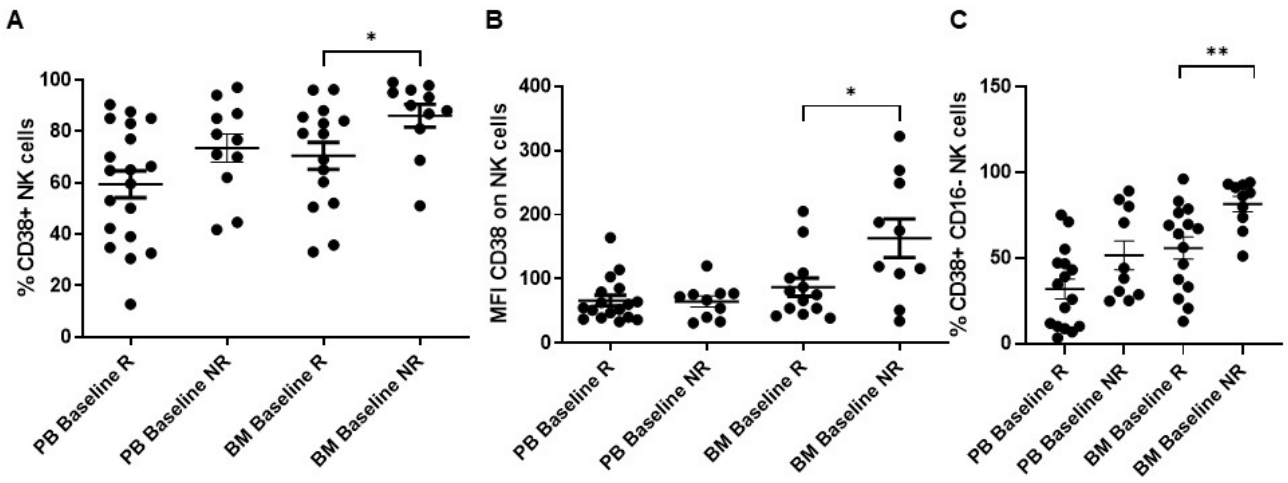

*Figure **13 High CD38 NK cells before D-Rd treatment can hamper Dara efficacy**. **A**) CD38 percentage of NK cells from PB and BM of R and NR patients at baseline. **B**) CD38 MFI on NK cells from PB and BM of R and NR patients at baseline. **C**) CD38 percentage of CD16- NK cells from PB and BM of R and NR patients at baseline.*

CD4/CD8 T-cell subset distribution was also different in the BM of R and NR patients at baseline (Fig 14) as a consequence of a lower percentage of CD4+ and higher percentage of CD8+ cells in NR compared with R (Figure 14 B-C). Interestingly, both CD4 and CD8 T cells from NR patients showed higher TIM-3 expression than R patients which was significantly different in PB but not in BM (Figure 15 D-E).

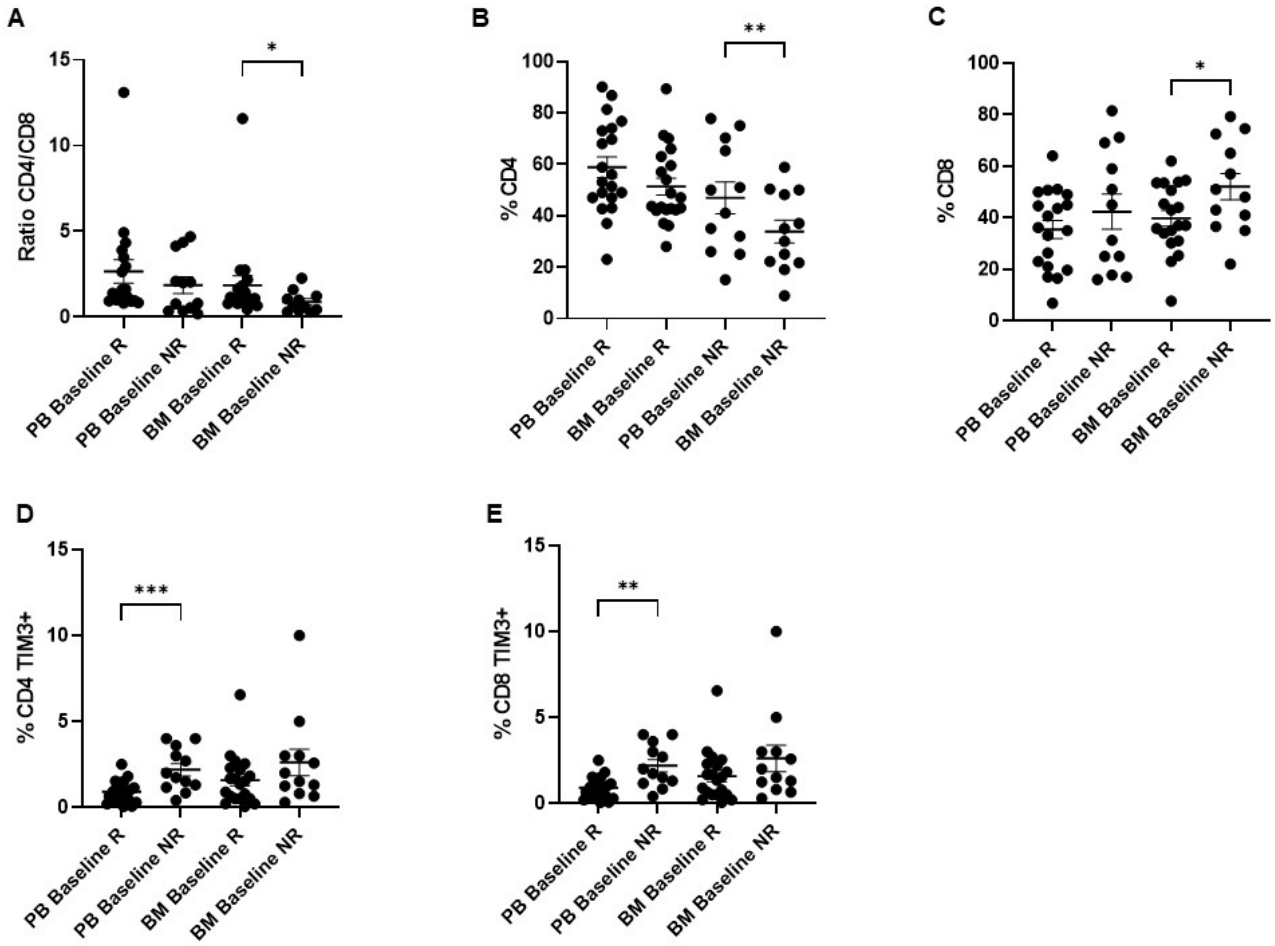

*Figure **14 Different T cell distribution affects to D-Rd response**. **A**) CD4 and CD8 T cell ratio in PB and BM of R and NR patients at baseline. **B**) Frequency of CD4 T cells and **C**) CD8 T cells from PB and BM of R and NR patients at baseline. **D**) Percentage of TIM3+ CD4 T cells and **E**) CD8 T cells from PB and BM of R and NR patients at baseline.*

DISCUSSION

In this work, we have investigated CD38 expression in selected immune cell subsets from the PB and BM of RRMM patients enrolled in the NCT03848676 study and monitored the immune modulation operated in these subsets from the initiation of D-Rd treatment up to 4 years of follow-up.

Under physiological conditions, CD38 expression is considered an activation marker since CD38 interactions with TCR, BCR and CD16 potentially contribute to cell signaling. In addition, by interacting with CD31, CD38 is involved in adhesion to endothelial cells (10). CD38 ecto-enzymatic activity could also involve CD38+ immune suppressive cells in Ado production through a discontinuous multicellular pathway that has been postulated to contribute to immune suppression in BM niche (3).

In MM, the very strong CD38 expression in myeloma cells has inspired the development of several anti-CD38 mAbs, including Dara. However, the frequent CD38 expression in many other cells in the BM and PB implies that Dara will target not only myeloma cells, but also many other immune cells potentially involved in the control of myeloma cells. This on target/off tumor activity can become very relevant especially when most of myeloma cells have been removed from the TME after the first months of D-Rd treatment. At baseline, the main target of Dara are myeloma cells which are the most abundant CD38+ population in the BM, but later on, other CD38+ immune suppressor and effector cells can replace myeloma cells as privileged targets of Dara, both in BM and PB. In this work, we have focused on these CD38+ immune cell subpopulations. MDSC, monocytes, and NK cells were the most abundant CD38+ cell populations in both BM and PB of RRMM patients. After 3 months of D-Rd treatment, CD38 was strongly downmodulated in NK cells and weakly on MDSC and monocytes that remain targetable populations in PB.

The majority of Dara-induced immune changes occurred in the 3 months of treatment, reflecting the treatment schedule initially characterized by weekly and biweekly Dara infusions.

NK cells were the cell population showing the strongest reshuffle, mainly characterized by depletion of CD38+ NK cells and CD16+/ CD16- NK- cell subset redistribution . CD16+ NK cells decreased, whereas CD16- NK cells increased over time accounting for the recovery of total NK cell counts observed after the initial depletion (from 9 months onward). Dara also induced a significant decrease of CD16 expression levels on CD16+ NK cell subset. CD16+ and CD16- NK cells are characterized by distinct phenotype, metabolism, and functions (11). The former (also named cytotoxic NK cells) can spontaneously lyse targeted tumor cells, whereas CD16- NK cells (also named proliferative NK cells) have higher proliferative potential, and produce abundant amounts of

cytokines (such as IFN-γ, IL-2, IL-10, IL-12 and granulocyte macrophage colony stimulating factor) (12) to the expenses of cytotoxic activity (13). Based on these data, we can speculate that the Dara-induced depletion of CD38+ CD16+ NK cells is a negative on target/off tumor effect undermining the immune surveillance operated by NK cells on myeloma cells. Interestingly, *Yufeng Wang* and colleagues revealed a fratricide mechanism *via* ADCC underlying Dara-mediated CD38+ NK-cell depletion and defined CD38-/lo NK cells as more effective for eradicating myeloma (14). Deletion of CD38 through CRISPR/Cas9 induced NK cell resistance to Dara-mediated depletion and increased NK cell persistence in immune deficient mice pretreated with Dara (15). Intriguingly, surviving CD16- NK cells showed an activated phenotype, also demonstrated by Adams et al. through high-throughput immunophenotyping (16) and confirmed by high rate of expansion and cytotoxic activity observed in in vitro analysis (14). In addition to NK cell direct anti-myeloma activity, NK cell pivotal role in Dara mechanism of action is also carried out by initiating a Th1-mediated response, as demonstrated in vitro (17).

PB counts and subsets distribution of monocytes were not affected by D-Rd treatment. Since monocytes have a relevant role in Dara mechanism of action, their persistence may partially counterbalance the negative effect of Dara on NK cells. A positive correlation between monocytes and myeloma cells and susceptibility to ADCC was demonstrated (18). In vitro analysis showed that CD14+CD16+ monocyte-mediated myeloma cell killing in presence of Dara resulted in increase of CD138+CD14+CD16+ population and can be boosted by inhibiting the expression of anti-phagocytic molecule CD47 on myeloma cells (19). In addition, increased anti-myeloma activity of monocyte was observed in presence of Dara-treated NK cells *in vitro* (17). However, comparison *in vitro* showed that killing of myeloma cell line UM9 was predominantly mediated by NK cells (20). CD38 expression was significantly decreased in classical and intermediate monocytes, although the extent of the decrease was not as strong as in NK cells. Both monocytes and granulocytes were demonstrated to contribute to CD38 reduction on myeloma cells being acceptor cells of Dara–CD38 complexes through trogocytosis (20). This phenomenon contributes to reduce CDC and ADCC and can compromise the therapeutic efficacy of Dara (20).

B and T cells were also modulated by D-Rd treatment. Percentages and total counts of PB B cells progressively decreased during D-Rd treatment. D-Rd also induced a progressive differentiation of CD8+ T cells characterized by an increase of CM, EM, and TEMRA and decrease of naïve CD8+ T cells. Similar results have been reported in RRMM patients enrolled in the SIRIUS and GEN05 studies. In these patients, CD8+ T cells showed an increase in granzyme B production and CD69 and HLA DR expression after Dara monotherapy (16). An increased frequency of TCR mono- or oligo-

clonality has also been reported in CD8+ T cells suggesting that Dara can improve the frequency of tumor-reactive CD8+ cells (9,21).

Unfortunately, these potentially favorable protumor on target/off tumor effects induced by Dara can be counterbalanced by the finding that ICP expression was upregulated in CD4+ and CD8+ T cells. During D-Rd treatment, total counts of circulating exhausted CD8 and CD4 T cells were significantly increased, as demonstrated by PD-1, LAG-3 and TIGIT upregulation. Increased LAG-3 expression at the RNA level was recently demonstrated in immune cells compartment of D-Rd treated patients enrolled in POLLUX study (21). Although ICP expression is not sufficient per se to identify functional exhausted cells (22), renforced ICP expression could restrain T-cell anti-myeloma functions and limit Dara effectiveness. Preclinical data suggest that dual CD38/ICP targeting may represent a promising strategy, but phase I/II studies have not met clinical expectations (23,24).

PB Vγ9Vδ2 T-cell counts were not affected by D-Rd treatment, but a significant reduction of CD38+ Vγ9Vδ2 T cells was observed in PB of on-treatment patients. These cells are possible effector of Dara-mediated anti-myeloma functions, since they are able to exert ADCC against CD38+ cancer cell lines *in vitro* (25). However, how Dara impacts on Vγ9Vδ2 T cells is not yet known.

CD38+ immune suppressive populations are weakened by D-Rd treatment. Both lenalidomide and pomalidomide increased the percentage and the MFI of CD38 on Tregs in PBMCs from MM patients (26), suggesting that IMiDs may enhance Tregs sensitivity to Dara. Although a slow increase of Tregs was observed in PB during D-Rd treatment, a strong decline of percentage and absolute number of CD38+ Tregs occurred. Immediate and persistent decline of CD4+ CD25+CD127^{lo}CD38+ Tregs, a more immune suppressive population identified by *Krejcik and collegues* (9), was observed in PB during D-Rd treatment and similar trend was followed by CD38+ Bregs. D-Rd mediated shrinkage of these suppressive populations could contribute to enhance anti-myeloma responses.

The proportion of CD38+ Mo-MDSC was also diminished after D-Rd. However, unlike what is reported in literature (9), MDSC total counts were not affected by Dara treatment in our hands; this discrepancy could be attributable to in vitro MDSC generation and treatment (9).

Finally, we have found that some features of the baseline immune profiles of RRMM patients were correlated with the clinical response (i.e, R vs NR). Unexpectedly, CD38+ NK cells were more abundant in the PB and BM of NR compared with R patients. Since CD38 expression levels are correlated with the sensitivity to Dara at least in myeloma cells (18), we speculate that the higher CD38 expression on NK cells, associated with a lower baseline CD38 expression in myeloma cells of NR patients (data in progress) can preferentially redirect Dara towards NK cells rather than myeloma cells promoting more NK fratricide than ADCC against myeloma cells. *Margaux Lejeune* and colleagues have recently shown that this undesired side-effect can be prevented with different

strategies, from retinoic acid, interferon-α, or CD38-blocking nanobody (27). Another constraint is increased proportion of functionally exhausted CD4+ and CD8+ T cells in the PB and BM of NR patients that cannot be appropriately recruited by Dara treatment.

In conclusion, our long-term monitoring indicate that Dara-based treatments can induce long-lasting changes in the immune profiles of PB and BM cell subpopulations involved in the disease control. After myeloma cell clearance, the preferential Dara dartboard becomes the on target/off tumor CD38+ expression in immune effector and suppressor cells. Targeting CD38+ immune suppressor (i.e, Tregs, Bregs, MDSCs etc) cells can restrain the ability of residual myeloma cells to escape immune surveillance; on the other hand, targeting immune effector cells (NK cells, CD8+ T cells, Vγ9Vδ2 T cells etc) can restrain immune recognition and killing of myeloma cells. Moreover, our data indicate unveils for the first time an association between CD38+ expression in selected immune cell subsets at baseline, Dara treatment, and response to treatment.

Future studies developing novel CD38-targeted treatments should take into consideration the opportunity to tip the balance as much as possible towards on target/off tumor effects preserving and boosting immune effector functions at the expenses of protumor functions.

BIBLIOGRAPHY

1. Hill E, Morrison C, Kazandjian D. Daratumumab: A review of current indications and future directions. *Semin Oncol* (2022) 49:48–59. doi: 10.1053/j.seminoncol.2022.01.008

2. Costa F, Palma BD, Giuliani N. CD38 expression by myeloma cells and its role in the context of bone marrow microenvironment: Modulation by therapeutic agents. *Cells* (2019) 8: doi: 10.3390/cells8121632

3. Horenstein AL, Bracci C, Morandi F, Malavasi F. CD38 in adenosinergic pathways and metabolic re-programming in human multiple myeloma cells: In-tandem insights from basic science to therapy. *Front Immunol* (2019) 10:760. doi: 10.3389/fimmu.2019.00760

4. Van De Donk NWCJ, Usmani SZ. CD38 antibodies in multiple myeloma: Mechanisms of action and modes of resistance. *Front Immunol* (2018) 9: doi: 10.3389/fimmu.2018.02134

5. Nooka AK, Kaufman JL, Hofmeister CC, Joseph NS, Heffner TL, Gupta VA, et al. Daratumumab in Multiple Myeloma. *Cancer July* (2019) 15: doi: 10.1002/cncr.32065

6. Saltarella I, Desantis V, Melaccio A, Solimando AG, Lamanuzzi A, Ria R, et al. Mechanisms of resistance to anti-cd38 daratumumab in multiple myeloma. *Cells* (2020) 9:167. doi: 10.3390/cells9010167

7. Avet-Loiseau H, San-Miguel J, Casneuf T, Iida S, Lonial S, Usmani SZ, et al. Evaluation of Sustained Minimal Residual Disease Negativity With Daratumumab-Combination Regimens in Relapsed and/or Refractory Multiple Myeloma: Analysis of POLLUX and CASTOR. *J Clin Oncol* (2021) 39:1139–1149. doi: 10.1200/JCO.20

8. Castella B, Foglietta M, Sciancalepore P, Rigoni M, Coscia M, Griggio V, et al. Anergic bone marrow Vγ9Vδ2 T cells as early and long-lasting markers of PD-1-targetable microenvironment-induced immune suppression in human myeloma. *Oncoimmunology* (2015) 4:e1047580. doi: 10.1080/2162402X.2015.1047580

9. Krejcik J, Casneuf T, Nijhof IS, Verbist B, Bald J, Plesner T, et al. Daratumumab depletes CD38+ immune regulatory cells, promotes T-cell expansion, and skews T-cell repertoire in multiple myeloma. *Blood* (2016) 128:384–394. doi: 10.1182/blood-2015-12-687749

10. Glaría E, Valledor AF. Roles of CD38 in the Immune Response to Infection. *Cells* (2020) 9: doi: 10.3390/cells9010228

11. Poznanski SM, Ashkar AA. What Defines NK Cell FunctionalFate: Phenotype or Metabolism? *Metabolism? Front Immunol* (2019) 10:1414. doi: 10.3389/fimmu.2019.01414

12. Cooper MA, Fehniger TA, Turner SC, Chen KS, Ghaheri BA, Ghayur T, et al. Human natural killer cells: a unique innate immunoregulatory role for the CD56(bright) subset. *Blood* (2001) 97:3146–3151. doi: 10.1182/BLOOD.V97.10.3146

13. Caligiuri MA. Human natural killer cells. *Blood* (2008) 112:461–469. doi: 10.1182/blood-2007-09-077438

14. Wang Y, Zhang Y, Hughes T, Zhang J, Caligiuri MA, Benson DM, et al. Fratricide of NK cells in daratumumab therapy for multiple myeloma overcome by ex vivo–expanded autologous NK cells. *Clinical Cancer Research* (2018) 24:4006–4017. doi: 10.1158/1078-0432.CCR-17-3117

15. Naeimi Kararoudi M, Nagai Y, Elmas E, de Souza Fernandes Pereira M, Ali SA, Hollingshorth Imus P, et al. CD38 deletion of human primary NK cells eliminates daratumumab-induced fratricide and boosts their effector activity. *Blood* (2020) 136:

16. Adams HC, Stevenaert F, Krejcik J, Van der Borght K, Smets T, Bald J, et al. High-Parameter Mass Cytometry Evaluation of Relapsed/Refractory Multiple Myeloma Patients Treated with Daratumumab Demonstrates

Immune Modulation as a Novel Mechanism of Action. *Cytometry Part A* (2019) 95:279–289. doi: 10.1002/cyto.a.23693

17. Viola D, Dona A, Caserta E, Troadec E, Besi F, McDonald T, et al. Daratumumab induces mechanisms of immune activation through CD38+ NK cell targeting. *Leukemia* (2021) 35:189–200. doi: 10.1038/s41375-020-0810-4

18. Nijhof IS, Groen RWJ, Lokhorst HM, Van Kessel B, Bloem AC, Van Velzen J, et al. Upregulation of CD38 expression on multiple myeloma cells by all-trans retinoic acid improves the efficacy of daratumumab. *Leukemia* (2015) 29:2039–2049. doi: 10.1038/leu.2015.123

19. Storti P, Vescovini R, Costa F, Marchica V, Toscani D, Dalla Palma B, et al. CD14+CD16+ monocytes are involved in daratumumab-mediated myeloma cells killing and in anti-CD47 therapeutic strategy. *Br J Haematol* (2020) 190:430–436. doi: 10.1111/bjh.16548

20. Krejcik J, Frerichs KA, Nijhof IS, Van Kessel B, Van Velzen JF, Bloem AC, et al. Monocytes and granulocytes reduce CD38 expression levels on myeloma cells in patients treated with daratumumab. *Clinical Cancer Research* (2017) 23:7498–7511. doi: 10.1158/1078-0432.CCR-17-2027

21. Casneuf T, Adams HC, van de Donk NWCJ, Abraham Y, Bald J, Vanhoof G, et al. Deep immune profiling of patients treated with lenalidomide and dexamethasone with or without daratumumab. *Leukemia* (2021) 35:573–584. doi: 10.1038/s41375-020-0855-4

22. Blank CU, Haining WN, Held W, Hogan PG, Kallies A, Lugli E, et al. Defining 'T cell exhaustion.' *Nat Rev Immunol* (2019) 19:665–674. doi: 10.1038/s41577-019-0221-9

23. Cohen YC, Oriol A, Wu KL, Lavi N, Vlummens P, Jackson C, et al. Daratumumab With Cetrelimab, an Anti-PD-1 Monoclonal Antibody, in Relapsed/Refractory Multiple Myeloma. *Clin Lymphoma Myeloma Leuk* (2021) 21:46-54.e4. doi: 10.1016/J.CLML.2020.08.008

24. Zucali PA, Lin C-C, Carthon BC, Bauer TM, Tucci M, Italiano A, et al. Targeting CD38 and PD-1 with isatuximab plus cemiplimab in patients with advanced solid malignancies: results from a phase I/II open-label, multicenter study. *J Immunother Cancer* (2022) 10:3697. doi: 10.1136/jitc-2021-003697

25. Hoeres T, Pretscher D, Holzmann E, Smetak M, Birkmann J, Triebel J, et al. Improving Immunotherapy Against B-Cell Malignancies Using γδ T-Cell-specific Stimulation and Therapeutic Monoclonal Antibodies. *Journal of Immunotherapy* (2019) 42:331–344. doi: 10.1097/CJI.0000000000000289

26. Feng X, Zhang L, Acharya C, An G, Wen K, Qiu L, et al. Targeting CD38 suppresses induction and function of T regulatory cells to mitigate immunosuppression in multiple myeloma. *Clinical Cancer Research* (2017) 23:4290–4300. doi: 10.1158/1078-0432.CCR-16-3192

27. Lejeune M, Duray E, Peipp M, Beguin Y, Caers J. Balancing the CD38 Expression on Effector and Target Cells in Daratumumab-Mediated NK Cell ADCC against Multiple Myeloma. *Cancers (Basel)* (2021)

SUPPLEMENTAL DATA

Modulation of the immune microenvironment in multiple myeloma patients treated with Daratumumab based therapy: tumor cell-extrinsic effects of daratumumab treatment

Supplemental Table 1. *Patient characteristics*

	Dara-Rd (n=32)
Age median (range)	68 (46-80)
ISS 1 2 3 Missing	 12 (45%) 9 (33%) 6 (22%) 5
Cytogenetic risk High* Low Missing	 6 (29%) 15 (71%) 7
Prior lines median (range)	 1 (1-3)
Previous therapy ASCT IMiDs Pis	 22 (69%) 16 (50%) 32 (100%)

Supplemental Table 2. *List of antibodies used for flow cytometry*

Antigen	Fluorochrome	Catalog #	Company	clone
CD4	FITC	130-114-531	Miltenyi Biotech	REA623
CD4	PerCP	130-113-217	Miltenyi Biotech	VIT4
CD8	PerCP-Vio700	130-110-682	Miltenyi Biotech	REA734
CD3	PE	130-113-139	Miltenyi Biotech	REA613
CD3	APC	130-113-135	Miltenyi Biotech	REA613
Program death-1 (PD-1)	APC	130-117-694	Milteny Biotech	PD1.3.1.3
T-cell immunoglobulin mucin 3 (TIM-3)	APC	130-120-700	Milteny Biotech	F38-2E2
Lymphocyte-activation gene 3 (LAG-3)	APC	130-119-567	Milteny Biotech	REA351
T cell immunoreceptor with Ig and ITIM domains (TIGIT)	APC	372706	BioLegend	A15153G
CD62L	FITC	130-113-619	Miltenyi Biotech	145/15
CD45RA	APC	130-117-742	Miltenyi Biotech	REA1047
Anti-TCR Vγ9	PE	130-107-434	Miltenyi Biotech	REA470
CD56	PE	130-113-312	Miltenyi Biotech	REA196
CD14	PE	130-110-519	Miltenyi Biotech	REA599
CD14	PerCP	130-113-150	Miltenyi Biotech	TUK4
CD69	FITC	130-112-612	Miltenyi Biotech	REA824
CD127	APC	130-113-413	Miltenyi Biotech	REA614
CD25	Vio Bright FITC	130-113-283	Miltenyi Biotech	4E3
CD25	PE	130-113-286	Miltenyi Biotech	REA570
CD16	APC	130-113-389	Miltenyi Biotech	REA423
CD38 Multiepitope	FITC	CYT-38F2-R	Cytognos	Multiepitope
CD33	PE	130-111-019	Miltenyi Biotech	REA775
CD33	FITC	130-111-018	Miltenyi Biotech	REA775
CD25	APC	130-113-154	Miltenyi Biotech	BW135/80
Programmed Death-Ligand 1 (PD-L1)	PE	329706	BioLegend	29E.2A3
CD19	PE	130-113-646	Miltenyi Biotech	REA675
CD24	APC	130-112-657	Miltenyi Biotech	REA832
CD11b	APC	130-110-554	Miltenyi Biotech	REA713
FoxP3	APC	130-125-580	Miltenyi Biotech	REA1253

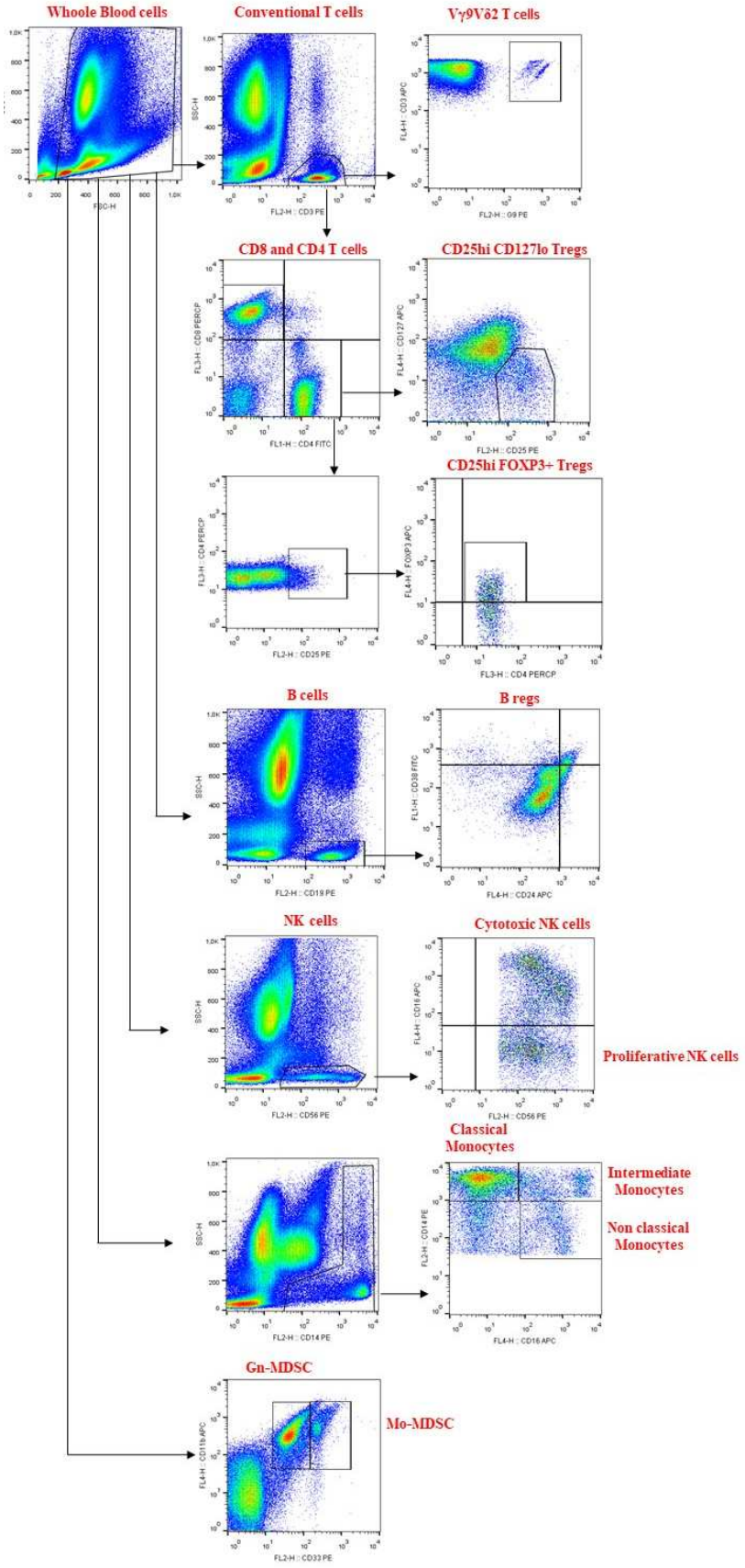

Supplemental Figure 1. Gating strategy

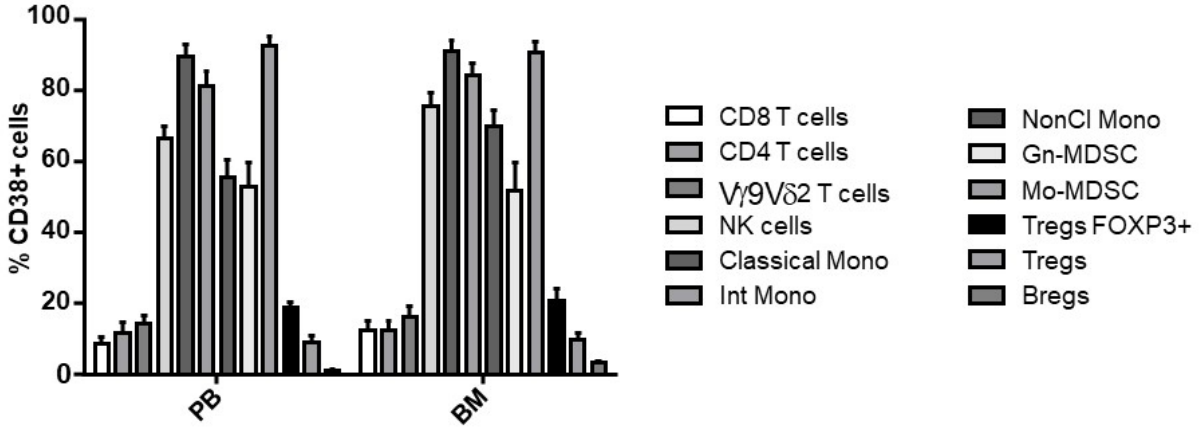

Supplemental Figure 2. CD38 expression pattern in RRMM patient. A) Proportion of CD38+ immune population in PB and BM of MM patients before D-Rd treatment. Bars represent mean values ± SEM from 9 to 35 experiments

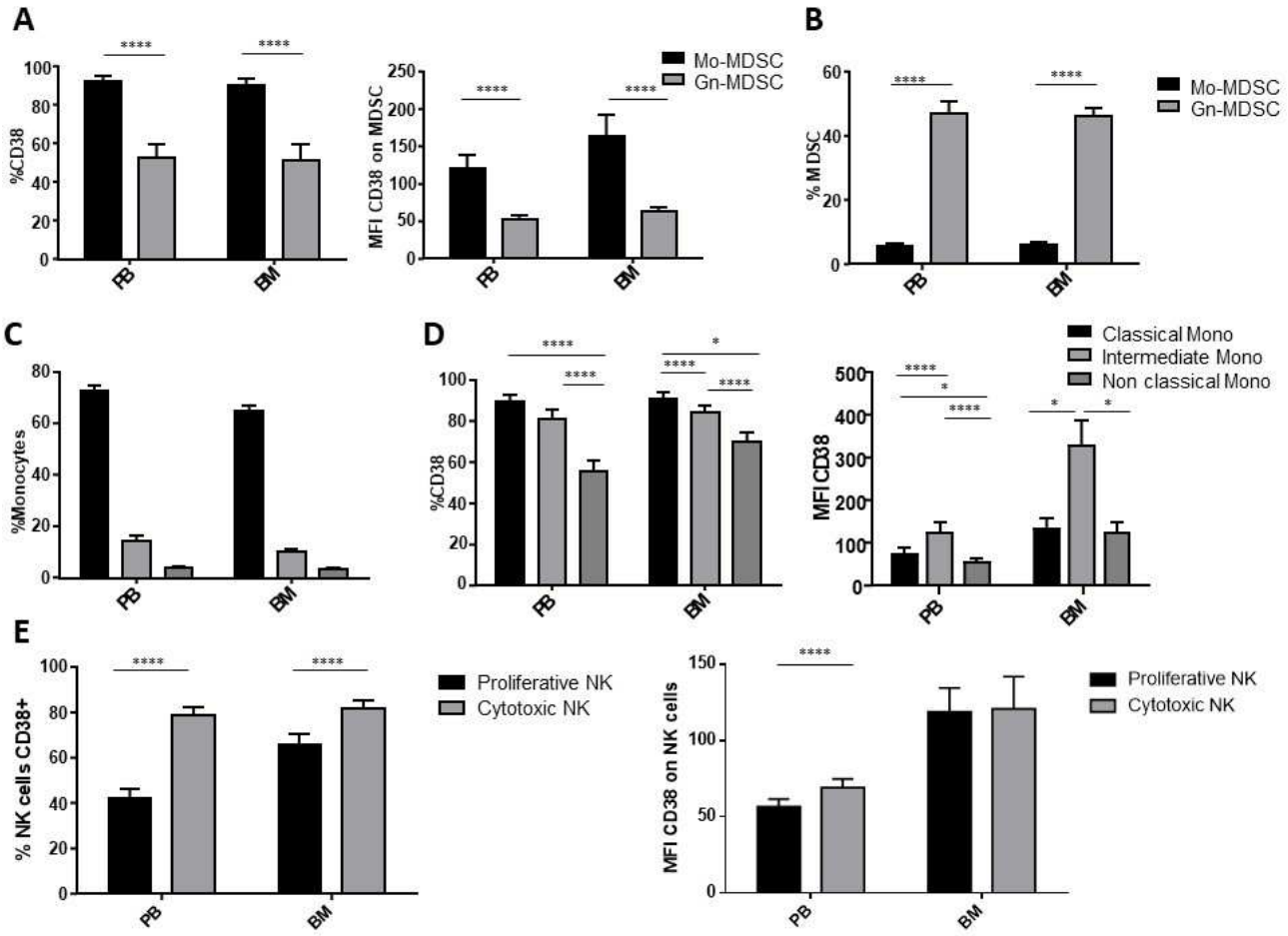

Supplemental Figure 3. **Analysis of CD38+ immune population in BM and PB of RRMM patients before DRd treatment.** (**A**) Monocyte subset distribution on BM and PB of RRMM patients before DRd treatment. Bars represent mean values ± SEM from 28 patients analyzed. (**B**) Frequency of CD38 expression and MFI on classical, intermediate and non classical monocytes of BM and PB of RRMM patients before DRd treatment. Bars represent mean values ± SEM from 28 patients analyzed. (**C**) Frequency of Mo-MDSC and Gn-MDSC on BM and PB of RRMM patients at baseline. Bars represent mean values ± SEM from 32 PB and 31 BM analysis. (**D**) CD38 expression and MFI CD38 on Mo-MDSC and Gn-MDSC from BM and PB of RRMMpatients at baseline. Bars represent

mean values ± SEM from 22 PB and 21 BM analysis. (**E**) CD38 expression and MFI CD38 on NK cell subset on BM and PB of RRMM patients before DRd treatment. Bars represent mean values ± SEM from 29 PB and 25 BM analyzed.

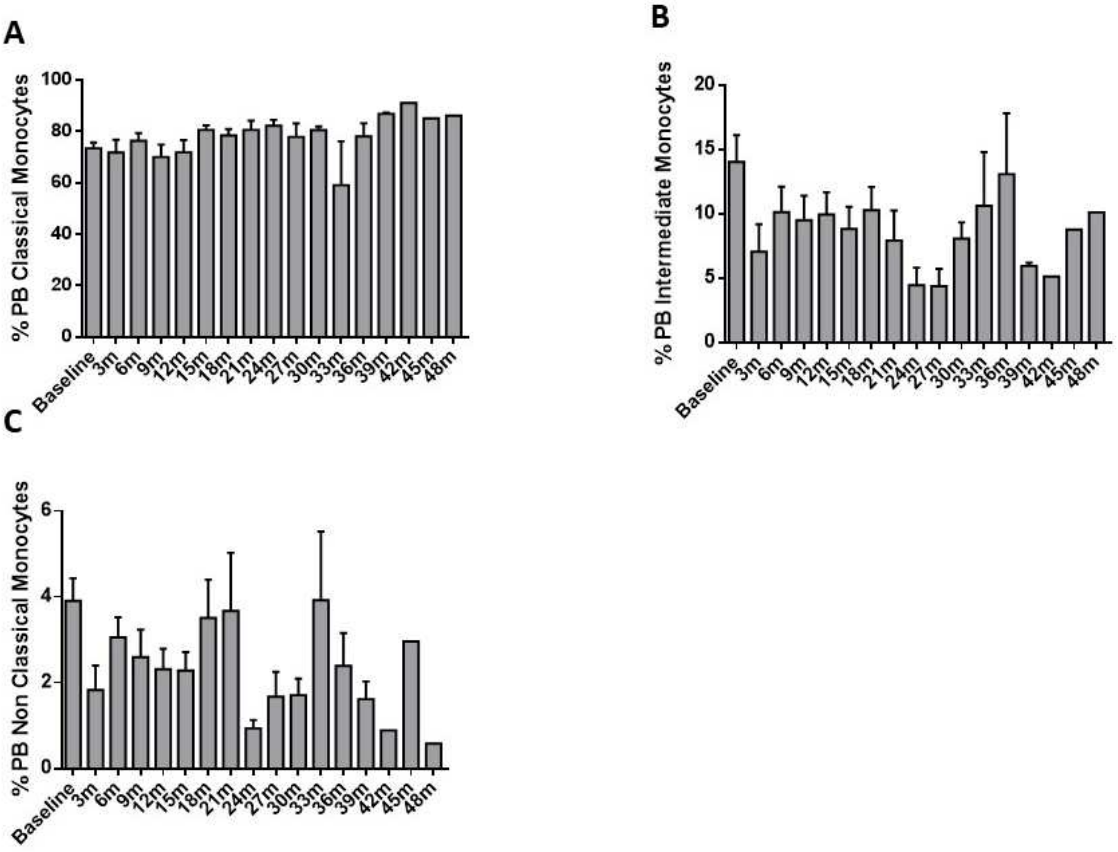

Supplemental Figure 4. D-Rd did not affect monocyte subset distribution. Frequency of (**A**) Classical Monocytes, (**B**) Intermediate monocytes, and (**C**) Non classical monocytes on PB of RRMM patients during DRd treatment. Bars represent mean values ± SEM from 28 patients analyzed.

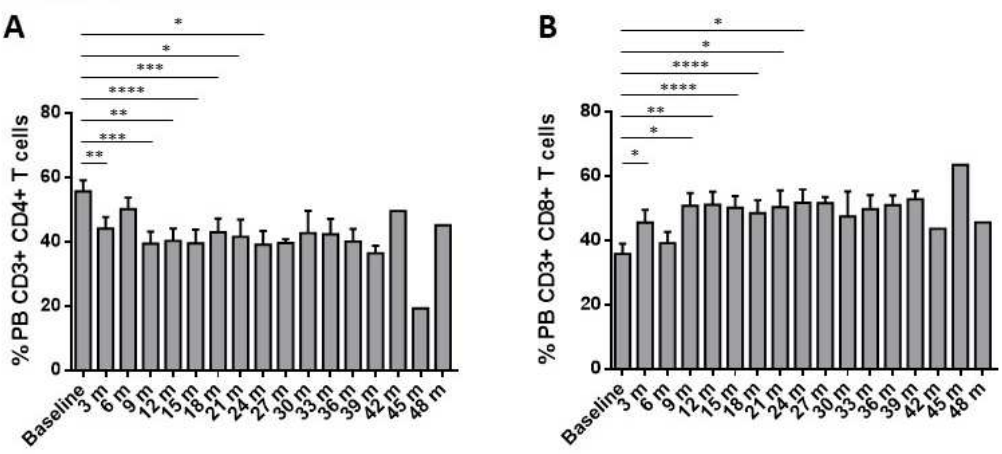

Supplemental Figure 5. T cell modulation operated by Daratumumab. Frequency of (**A**) CD4 T cells and (**B**) CD8 T cells on PB of RRMM during DRd treatment. Bars represent mean values ± SEM from 1 (42m and 48m) to 31 (Baseline) patients analyzed.

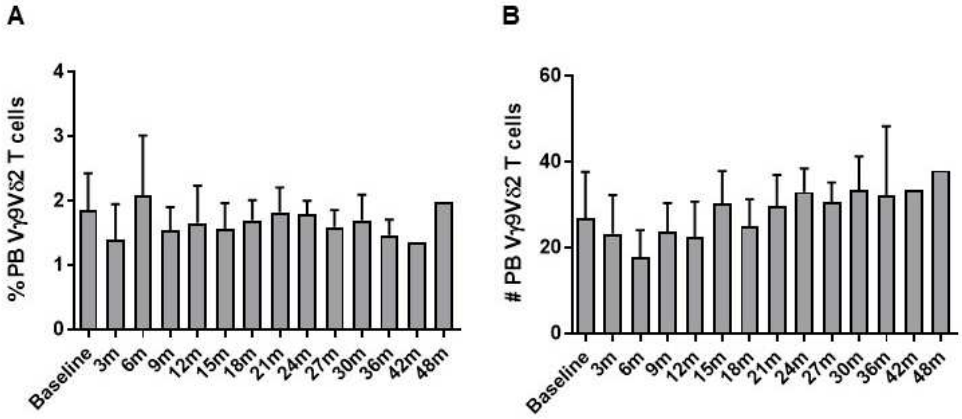

Supplemental Figure 6. Vγ9Vδ2 T-cell total counts were not affected by D-Rd (**A**) Frequency and (B) absolute counts of PB Vγ9Vδ2 T cells after D-Rd treatment. Bars represent mean values ± SEM from 1 (42m and 48m) to 18 (Baseline) patients analyzed.

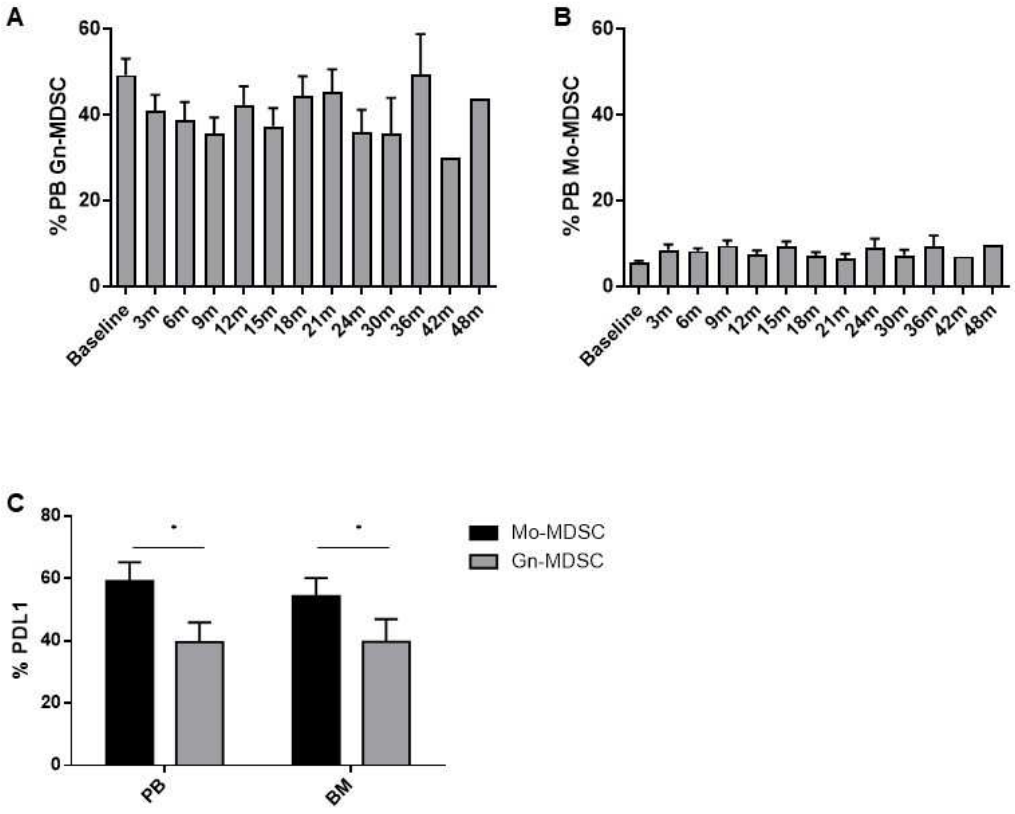

Supplemental Figure 7. MDSC total counts were not affected by D-Rd (**A**) Frequency of Gn-MDSC and (**B**) Mo-MDSC on PB of RRMM patients during D-Rd treatment. Bars represent mean values ± SEM from 1 (42m and 48m) to 25 (Baseline) patients analyzed. (**C**) Percentage of PDL-1+ MDSC in PB and BM of RRMM patients before D-Rd treatment. Bars represent mean values ± SEM from 19 patients analyzed.

The immune suppressive tumor microenvironment in multiple myeloma: the contribution of myeloid-derived suppressor cells

ABSTRACT

Myeloid derived suppressors cells (MDSC) play major roles in regulating immune homeostasis and immune responses in many conditions, including cancer. MDSC interact with cancer cells within the tumor microenvironment (TME) with direct and indirect mechanisms: production of soluble factors and cytokines, expression of surface inhibitory molecules, metabolic rewiring and exosome release. The two-way relationship between MDSC and tumor cells results in immune evasion and cancer outgrowth. In multiple myeloma (MM), MDSC play a major role in creating protumoral TME conditions. In this minireview, we will discuss the interplay between MDSC and MM TME and the possible strategies to target MDSC.

INTRODUCTION

Multiple myeloma (MM) is a paradigm disease in which progression is fueled by intrinsic alterations of myeloma cells and tumor-host interactions in the tumor microenvironment (TME) (1). Disease evolution from monoclonal gammopathy of undetermined significance (MGUS) to smoldering myeloma (SMM), and symptomatic disease is characterized by a progressive increase of myeloma cells associated with co-evolving immunological and metabolic changes making the TME unable to hold the disease in check (1). We and others have shown that immune alterations are already detectable in the very early stage of the disease (2,3) and that they persist in the remission phase (2). The immune MM TME contexture consists of effector cells (i.e, conventional T cells, unconventional T cells like NKT cells, γδ T cells, NK cells etc), professional suppressor cells [i.e, regulatory T cells (Tregs), regulatory B cells (Bregs), myeloid derived suppressor cells (MDSC)], and cells that are functionally conditioned by the TME and acquire protumoral functions like bone marrow stromal cells (BMSC), endothelial cells, osteoblasts (OB), and osteoclasts (4). Recently, BM-resident neutrophils have also been reported to contribute to the TME-induced suppressive commitment of MM patients (5). Unbalanced distribution of effector and suppressor cells already detectable in MGUS is induced by the progressive accumulation of myeloma cells driven by genetic and epigenetic drivers. The bone marrow (BM), which is where MM originates and propagates, has the capacity to physiologically host around 2-5% polyclonal plasma cells. When myeloma cell infiltration overcomes this threshold, the TME is immunologically and metabolically shaped to support myeloma cell growth, to induce drug resistance, and to suppress immune recognition. MDSC play a major role in the protumoral reset of MM TME.

We have previously shown that MDSC are significantly increased in the BM of MGUS and MM patients: granulocytic/polymorphonuclear MDSC (PMN-MDSC), and not monocytic MDSC (M-MDSC), are responsible for the increase (2). MDSC frequency is very similar in MGUS, MM at diagnosis, and MM in relapse. Unexpectedly, we have found that MDSC frequency is significantly higher in MM in remission (2), indicating that there is no correlation between the proportion of BM myeloma cells and MDSC expansion. Similar data have been reported in mouse models in which MDSC start to accumulate in the TME as early as one week after tumor inoculation when the frequency of myeloma cells is very low (<10%) as in MGUS individuals (6).

Approximately, 20-40% of MDCS express Programmed Cell Death-Ligand 1+ (PD-L1+) (2) and therefore are very well-suited to engage and suppress immune effector cells like Vg9Vd2 cells and NK cells expressing Programmed Cell Death-1 (PD-1) (2). MDSC are PD-L1+ in MGUS and MM irrespective of the disease stage, including MM in remission when most myeloma cells have been

cleared from BM (2). The persistence of PD-L1+ MDSC can hinder the immunomodulatory activity of drugs like bortezomib or lenalidomide after autologous stem cell transplantation.

In conclusion, MDSC play a major role in the establishment of the immune suppressive TME in MM. The aim of this minireview is to discuss the mechanisms exploited by MDSC in cooperation with myeloma cells, professional immune suppressor cells, and other bystander cells to promote myeloma cell growth in the BM of MM patients. We will also discuss possible interventions to dampen the immune suppression operated by MDSC and other suppressor cells and to recover the anti-myeloma activity of immune effector cells.

MDSC subsets and differentiation

MDSC play a major role in the regulation of immune homeostasis in healthy individuals, and the regulation of immune responses in infectious diseases, autoimmunity, aging, pregnancy, transplantation, and obesity (7). In cancer, the immune suppressive activity of MDSC is exploited by tumor cells to evade immune surveillance and support their survival and accumulation (7).

MDSC are derived from bone marrow hematopoietic stem cells (7). There are two major subsets of MDSC in humans: PMN-MDSC and M-MDSC. The first one are phenotypically and morphologically similar to neutrophils ($CD15^+$ and/or $CD66b^+$), whereas M-MDSC are similar to monocytes (CD14+)(7). More recently, a third subset of phenotypically distinct immature early-MDSC (e-MDSC) has been identified in cancer patients (8). In this review we will use the term MDSC to identify both PMN-MDSC and M-MDSC unless otherwise specified.

MDSC development occurs in two partially overlapping waves (9). The first one is driven by cytokines and soluble factors including granulocyte-macrophage colony-stimulating factor (GM-CSF), macrophage colony-stimulating factor (M-CSF), granulocyte colony-stimulating factor (G-CSF), interleukin 6 (IL-6), and vascular endothelial growth factor (VEGF). These cytokines and soluble factors are produced by tumor cells and/or BMSC in the TME and promote MDSC differentiation from hematopoietic progenitor cells *via* STAT3 and STAT5 activation (10–12). Mesenchymal stromal cells (MSC) also induce MDSC expansion *via* the hepatocyte growth factor (HGF), c-Met, and STAT3 phosphorylation (10). The second wave is driven by a different set of cytokines and inflammatory soluble factors like interleukin 13 (IL-13), toll-like receptor (TLR) ligands, and Prostaglandin E2 (PGE2) yielding to the functional MDSC activation *via* the STAT1 and NF-kB pathways (10,11,13). The TME is highly predisposed to drive the expansion and activation of MDSC at the expense of other myeloid-derived cells like monocytes, macrophages and dendritic cells (DC) (8).

Immunosuppressive MDSC features

The immune suppressive MDSC activity is dependent on: 1) the depletion of essential $CD8^+$ T- cell nutrients in the TME; 2) the production of immune suppressive cytokines and/or soluble factors; 3) the expression of cell surface inhibitory molecules [i.e., (PD-L1)]; 4) the protumoral metabolic TME rewiring at the expense of immune effector cells.

Amino acid depletion

MDSC express the xc- transporter and import cystine, but, unlike DC and macrophages, they are unable to export cysteine because they lack the ASC neutral amino acid transporter (14). Considering the progressive TME invasion by tumor cells and MDSC at the expense of other cells which can supply extracellular cysteine, the TME becomes depleted of cysteine jeopardizing the activation of CD8+T cells that are unable to convert cystine to cysteine to meet their metabolic requirement (14).

MDSC also deplete the TME of tryptophan *via* the enzyme indoleamine 2 3-dioxygenase (IDO) (15). T lymphocytes are very susceptible to tryptophan shortage which restrains their proliferative responses by inducing an integrated stress response and the inactivation of the mTOR pathway (16,17). Tryptophan catabolites can also induce the apoptosis of cytotoxic T cells (18,19), and the concurrent differentiation of Tregs (20). L-arginine (L-arg) is another essential amino acid which is critical for T-cell immune functions. Arginine metabolism is regulated by the inducible nitric oxide synthase (iNOS) isoenzymes, arginase (ARGI1/2) activity, and proline and polyamines synthesis. MDSC express both iNOS and Arg-1 that induce L-arg depletion in the TME leading to inhibition of CD3-ζ expression in T cells, and induction of apoptosis (7,9,21).

Cytokines and soluble factors

The production and release of suppressor cytokines and soluble factors is another mechanism exploited by MDSC to protect tumor cells from immune recognition and killing. Nitric oxide (NO), reactive oxygen species (ROS), peroxynitrite (PNT) (a short-lived product of NO reaction with ROS), interleukin 10 (IL-10), and transforming growth factor-β (TGF-β) are released by MDSC with slightly difference between PMN-MDSC and M-MDSC (7,9,22,23). The hyper-production of ROS and PNT in the TME impairs the ability of CD8 T cells to bind to peptide–major histocompatibility complexes and to respond to specific peptides (23). NO also hampers the Fc receptor-mediated effector functions of NK cells (24). IL-10 recruits Tregs in the TME and decreases CD8+ T-cell antigen sensitivity by inducing cell surface glycoprotein branching (25). TGF-β is induced by IL-13 (26) and Interferon-γ (IFN-γ) (27), and contributes to T-cell suppression through Tregs development (27). Kynurenine is another soluble immune suppressive factor that is generated in the TME as a consequence of

tryptophan catabolism by MDSC. Kynurenine can inhibit T-cell and NK cell proliferation and induce the differentiation of naïve T cells into Tregs (20).

Cell surface molecules

The cell surface expression of immune checkpoints ligands (ICP-L) like PD-L1 is another mechanism used by M-MDSC to suppress immune effector cells (2,7,9), while PMN-MDSC preferentially exploit the Fas/Fas-ligand pathway to induce T-cell depletion in the TME (28). The V-domain immunoglobulin suppressor of T cell activation (VISTA) is a novel co-inhibitory ligand/receptor highly expressed by MDSC in the TME that suppresses T-cell effector functions and contributes to acquired resistance to PD-1/PD-L1 blockade (29). Lastly, CXCR2 is another cell surface molecule that is critical in mice models and pediatric sarcoma to promote the accumulation of MDSC in the TME and hamper the efficacy of anti-PD-1 treatment (30).

Protumoral metabolic TME rewiring

The TME is a very dynamic ecosystem that is progressively molded by tumor cells to locally create protective conditions to support their growth and resistance to therapy, from conventional chemotherapy to immunotherapy (31,32). Hypoxia is a major metabolic feature of TME (32), especially in solid tumors, almost always associated with the extracellular acidification induced by lactate accumulation. Tumor cells rewire their metabolism to survive and proliferate in the TME by: 1) increasing glucose and amino acid uptake, glycolytic flux, and lactate production; 2) modifying glutamine metabolism, tricarboxylic acid cycle, and oxidative phosphorylation; 3) increasing the production of mitochondrial ROS; 4) modulating fatty acid synthesis and oxidation (FAO) (32). MDSC partially mimick the metabolic rewiring of tumor cells by adapting their lactate, glucose, and lipid metabolism to the hypoxic and acidic TME conditions (33,34) . As a result, MDSC survive in the TME, contribute to the exacerbation of the protumoral metabolic TME commitment, and maintain unaltered their immune suppressor activity (35–37).

Immune suppressive and metabolic features in MM

MM is a hematologic cancer characterized by the accumulation of malignant plasma cells (myeloma cells) in the BM. Progressive colonization of BM results in a deep remodelling of the BM niche that becomes functionally perturbated and metabolically hostile to support myeloma cell growth, immune evasion, and drug resistance (1).

MDSC play a major role in establishing the protumoral TME commitment. We have shown that MDSC accumulation in the BM is already detectable in MGUS, and their expansion persists throughout the entire period of the disease (2), including the remission phase (2). In our hands, PMN-

MDSC was the main subpopulation to be expanded in MGUS and MM (2), while other groups have reported the predominance of M-MDSC in MM at diagnosis and in relapse (38,39). Immunogenomic characterization of MM PMN-MDSC identified CD11b+CD13+CD16+ cells as the subset with strongest capacity to suppress anti-myeloma activity T-cell immune responses (40). MDSC-like suppressive activity is also exhibited MM neutrophils (5), suggesting that an accurate characterization of MDSC should be based on phenotypic markers, immunosuppressive potential, and transcriptional network.

Development and suppressor functions of MDSC are supported by myeloma cells and bystander cells via direct and indirect mechanisms. Direct mechanisms operated by myeloma cells include: 1) IL-6 production (41,42) which prevents MDSC differentiation and promotes MDSC accumulation and activation via the STAT3 signaling pathway (43); 2) the induction of Mcl-1, an anti-apoptotic protein sustaining MDSC survival (44); 3) the secretion of galectin-1 that targets CD304 on MDSC and enhances their immune suppressive capacity (45); 4) the production of chemokine ligand 5 (CCL5) and macrophage migration inhibitory factor (MIF) (46). MIF has also been reported to potentiate the immune suppressive activity of MDSC via CD84-mediated PD-L1 upregulation (47). 5) the release of exosomes that promotes MDSC growth and NO production (48).

Bystander cells in the TME also cooperate with myeloma cells in the induction and activation of immune suppressive MDSC via direct mechanisms including: 1) IL-6 release (49,50); 2) exosome release by BMSC (51); 3) production and released of immune suppressive molecules [i.e. Prostaglandin-Endoperoxide Synthase 2 (PTGS2), TGF-β, Nitric Oxide Synthase 2 (NOS2), IL-10 and IL-6)] by MSC and OB (52,53).

In addition to the direct mechanisms listed above, myeloma cells and bystander cells promote the accumulation and activation via indirect mechanisms. An example is the metabolic rewiring operated by myeloma cells and bystander cells that creates a hypoxic and nutrient-depleted TME that promotes the accumulation and activation of MDSC at the expense of immune effector cells (54–56) Lactate over-production shifts MDSC differentiation toward PMN-MDSC (57),which is the subset that we and other have shown to be increased in the peripheral blood (PB) and BM of MM patients (2,58).

The accumulation and activation of MDSC is beneficial to myeloma cells creating a very effective pro-tumoral loop (3,59). MDSC facilitate the self-renewal of myeloma stem-cells, enhance their tumorigenic potential via epigenetic regulation (60), and promote the survival of myeloma cells via AMPK phosphorylation leading to increase β-oxidation, ATP production, and increased NADPH levels (61). MDSC production of S100A9, a calcium-binding protein that promotes the release of TNF-α, IL-6, and IL-10 in autocrine pathway through TLR4 interaction, attracts myeloma cells in

the TME (62) and support myeloma cell growth via the activation of the canonical NFκB pathway (63).

Indirect mechanisms operated by MDSC to support myeloma cells are deprivation of nutrients, production of soluble factors, and the expression of cell surface inhibitory molecules. The common denominator is the impairment of anti-myeloma immune responses. In addition, PMN-MDSC are educated to express angiogenesis-related proteins to sipport tumor angiogenesis (64).

MDSC upregulate enzymes that contribute to the shortage of amino acid essential for immune effector T cells. Arginase 1 (Arg-1) expression and NO production by MDSC limits the availability of L-Arg needed for effective TCR-mediated signaling (65,66). MDSC can utilize glutamine for anaplerosis like myeloma cells (67,68) exacerbating glutamine deprivation in the TME (56).

Several soluble factors and cytokines contribute to the immune suppressor activity of MDSC in the TME, like IL-10, IL-6, TGF-β, CD40-CD40 Ligand, and IFN-γ. These cytokines tip the scales in favor of Tregs (69,70), whose number is directly correlated with MDSC expansion (58). Lastly, CD38 expression on MDSC (71) contributes to the discontinuous multicellular pathway of adenosine (Ado), an immune suppressive nucleoside highly represented in the TME of MM patients (72).

The expression of immune checkpoint (ICP)/ICP-L contributes to the impairment of anti-myeloma immune responses. We have previously demonstrated that PD-L1is expressed by BM MDSC in all disease states (2) and can contribute to hold in check anti-myeloma activity of PD1+ effector cells such as T cells, NK cells, and Vγ9Vδ2 T-cells. Recently, it has been reported in solid tumors that MDSC can boost the immune suppressive activity of Bregs against T cells via PD-1/PD-L1 axis (73,74).

Lastly, MDSC can trans-differentiate into functional osteoclasts (75) to combine immune suppressive functions and direct protumoral functions (76). In mice models, G-MDSC have also been shown to promote angiogenesis (64), another major pro-tumoral TME disruption occurring in human MM (64).

The direct and indirect mechanisms involved in the cross-talk between MDSC, myeloma cells, immune effector, immune suppressor cells, and other bystander cells in the TME of MM patients are shown in Figure 1.

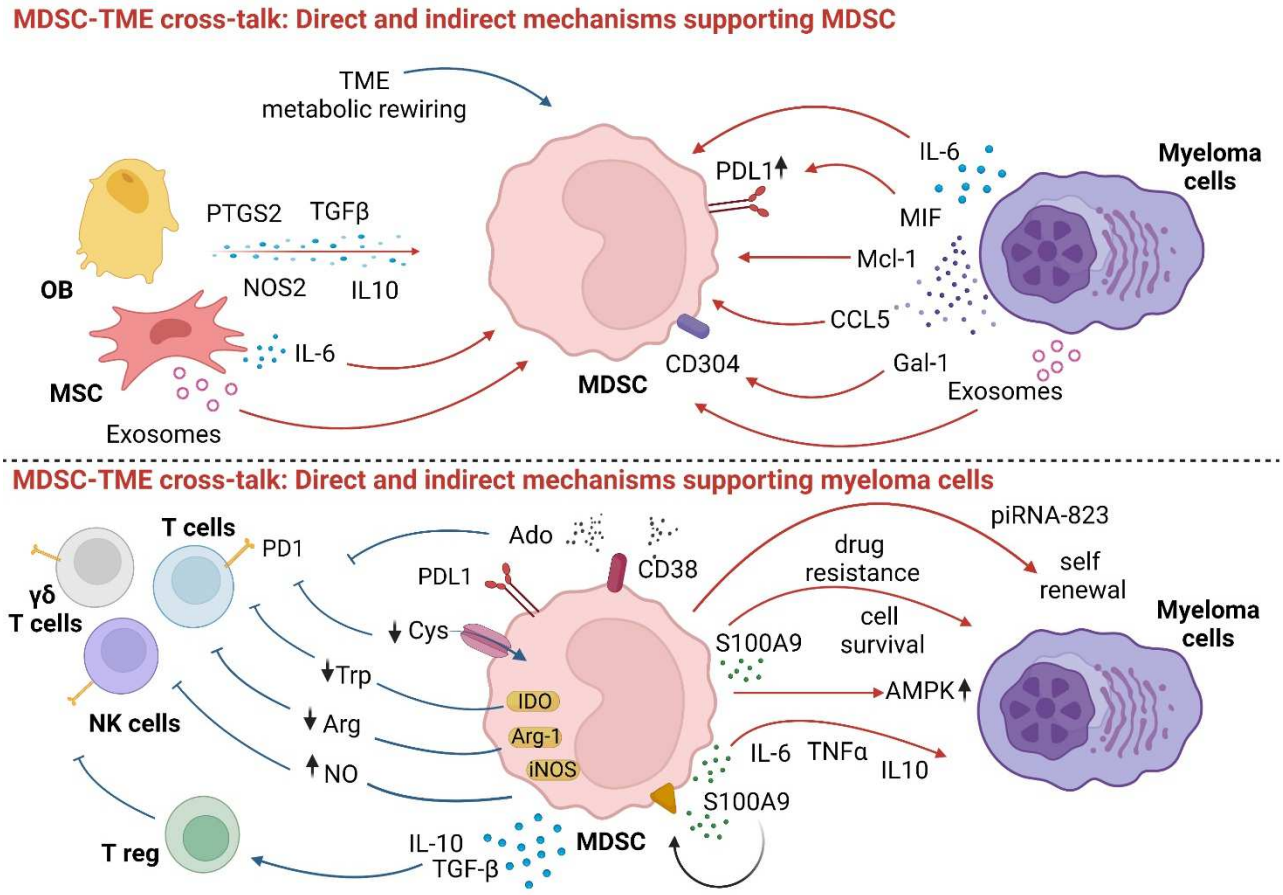

Figure 1. Myeloma cell and surrounding cells promote MDSC differentiation and suppressive functions. In turn, MDSC undermine anti-tumor immune responses and guarantee myeloma cell survival and growth. Red arrows: direct mechanisms; blue arrows: indirect mechanisms. Created by BioRender.com

Therapeutic interventions

The correlation between the frequency of MDSC and the clinical outcome identifies these cells as potential targets of immune-based therapeutic interventions (77). However, the therapeutic targeting of MDSC is not easy given their multifaceted biological functions and multiple interactions in the TME. Possible strategies are: 1) to restrain their accumulation in the PB and TME; 2) to prevent their functional activation in the TME; 3) to block their protumoral interactions with myeloma cells and bystander cells.

MDSC accumulation can be restrained by immunomodulatory drugs (IMiDs) (78) and proteasome inhibitors (PI) (61). A cereblon (CRBN)-dependent and -independent down-regulation of CCL5 and MIF is a possible mechanism of IMiDs activity on MDSC (46) that can be improved by Arg-1 inhibitors (79). Clinical data confirm the capacity of IMiDs to restrain MDSC in vivo as shown

by the decrease of PB MDSC in MM patients treated with pomalidomide, dexamethasone, and daratumumab (80). Daratumumab can also exert a favourable immune modulatory activity in the TME of MM patients by depleting CD38+ MDSC via antibody-dependent cellular cytotoxicity (ADCC) and complement-dependent cytotoxicity (CDC) (71). Data from mice models indicate that demethylating agents like decitabine (DAC), IL-18, and zoledronic acid (ZA) can also affect MDSC survival in the TME (75,81,82). ZA is currently used in MM and other solid cancers to prevent osteoclast activation and bone lesions, but this molecule is also endowed with pleiotropic immune modulatory activity (83), including the capacity in murine myeloma models to reduce the numbers of MDSC and prevent their differentiation into osteoclasts (75). Targeting CD84 and the CD304-Gal1 axis are other strategies used in myeloma mouse models to restore anti-myeloma T-cell responses by reducing MDSC accumulation and PD-L1expression (47).

The immune suppressive activity of MM MDSC has also been inhibited in vitro using ABR-238901, a small molecules able to inhibit S100A9 interactions (62), and tasquinimod (77) Anti-estrogen therapy may also restrain MDSC suppressive activity, since 17β-estradiol increases their ability to suppress T cells proliferation (84). iNOS and Arg-1 activities have been down-modulated in mice models with tadalafil (85), a PDE5 inhibitor that has been used with some evidence of clinical efficacy in relapsed/refractory MM patients in combination with lenalidomide (86). Pro-tumoral MDSC cellular interactions in the TME can also be limited by interrupting ICP/ICP-L interactions (2). Daratumumab in combination with the anti-PD1 monoclonal antibody cetrelimab has been reported to decrease the number of circulating MDSC and increase that of CD8+ T cells in the PB of MM patients in relapse (87). In acute myeloid leukemia (AML), knockdown of VISTA, a negative checkpoint regulator in the B7 family, reduced the MDSC-mediated inhibition of T cells (88). Data are not available in MM yet but VISTA up-regulation is also expected in the BM of MM given the hypoxia and low pH as reported in solid cancer (89) suggesting that this could be another ICP targetable to decrease the immune suppressive activity of MDSC.

In conclusion, understanding the mechanisms underlying the immune suppressive activity of MDSC in MM will pave the ground to the therapeutic targeting of these cells to improve the efficacy of immune-based treatments in MM.

Bibliography

1. García-Ortiz A, Rodríguez-García Y, Encinas J, Maroto-Martín E, Castellano E, Teixidó J, Martínez-López J. The role of tumor microenvironment in multiple myeloma development and progression. *Cancers (Basel)* (2021) 13:1–22. doi: 10.3390/cancers13020217

2. Castella B, Foglietta M, Sciancalepore P, Rigoni M, Coscia M, Griggio V, Vitale C, Ferracini R, Saraci E, Omedé P, et al. Anergic bone marrow Vγ9Vδ2 T cells as early and long-lasting markers of PD-1-targetable microenvironment-induced immune suppression in human myeloma. *Oncoimmunology* (2015) 4:e1047580. doi: 10.1080/2162402X.2015.1047580

3. Zavidij O, Haradhvala NJ, Mouhieddine TH, Sklavenitis-Pistofidis R, Cai S, Reidy M, Rahmat M, Flaifel A, Ferland B, Su NK, et al. Single-cell RNA sequencing reveals compromised immune microenvironment in precursor stages of multiple myeloma. *Nat Cancer* (2020) 1:493–506. doi: 10.1038/s43018-020-0053-3

4. Leone P, Solimando AG, Malerba E, Fasano R, Buonavoglia A, Pappagallo F, de Re V, Argentiero A, Silvestris N, Vacca A, et al. Actors on the scene: Immune cells in the myeloma niche. *Front Oncol* (2020) 10:1–15. doi: 10.3389/fonc.2020.599098

5. Petersson J, Askman S, Pettersson Å, Wichert S, Hellmark T, Johansson ÅCM, Hansson M. Bone Marrow Neutrophils of Multiple Myeloma Patients Exhibit Myeloid-Derived Suppressor Cell Activity. *J Immunol Res* (2021) 2021: doi: 10.1155/2021/6344344

6. Ramachandran IR, Martner A, Pisklakova A, Condamine T, Chase T, Vogl T, Roth J, Gabrilovich D, Nefedova Y. Myeloid-Derived Suppressor Cells Regulate Growth of Multiple Myeloma by Inhibiting T Cells in Bone Marrow. *The Journal of Immunology* (2013) 190:3815–3823. doi: 10.4049/jimmunol.1203373

7. Veglia F, Perego M, Gabrilovich D. Myeloid-derived suppressor cells coming of age. *Nat Immunol* (2018) 19:108–119. doi: 10.1038/s41590-017-0022-x

8. Mortezaee K. Myeloid-derived suppressor cells in cancer immunotherapy-clinical perspectives. *Life Sci* (2021) 277: doi: 10.1016/j.lfs.2021.119627

9. Veglia F, Sanseviero E, Gabrilovich DI. Myeloid-derived suppressor cells in the era of increasing myeloid cell diversity. *Nat Rev Immunol* (2021) 21:485–498. doi: 10.1038/s41577-020-00490-y

10. Yen BL, Yen ML, Hsu PJ, Liu KJ, Wang CJ, Bai CH, Sytwu HK. Multipotent human mesenchymal stromal cells mediate expansion of myeloid-derived suppressor cells via hepatocyte growth factor/c-Met and STAT3. *Stem Cell Reports* (2013) 1:139–151. doi: 10.1016/j.stemcr.2013.06.006

11. Condamine T, Gabrilovich DI. Molecular mechanisms regulating myeloid-derived suppressor cell differentiation and function. *Trends Immunol* (2011) 32:19–25. doi: 10.1016/J.IT.2010.10.002

12. Su YL, Banerjee S, White SV, Kortylewski M. STAT3 in tumor-associated myeloid cells: Multitasking to disrupt immunity. *Int J Mol Sci* (2018) 19: doi: 10.3390/ijms19061803

13. Obermajer N, Wong JL, Edwards RP, Odunsi K, Moysich K, Kalinski P. PGE2-driven induction and maintenance of cancer-associated myeloid-derived suppressor cells. *Immunol Invest* (2012) 41:635–657. doi: 10.3109/08820139.2012.695417

14. Srivastava MK, Sinha P, Clements VK, Rodriguez P, Ostrand-Rosenberg S. Myeloid-derived suppressor cells inhibit T-cell activation by depleting cystine and cysteine. *Cancer Res* (2010) 70:68–77. doi: 10.1158/0008-5472.CAN-09-2587

15. Yu J, Wang Y, Yan F, Zhang P, Li H, Zhao H, Yan C, Yan F, Ren X. Noncanonical NF-κB Activation Mediates STAT3-Stimulated IDO Upregulation in Myeloid-Derived Suppressor Cells in Breast Cancer. *The Journal of Immunology* (2014) 193:2574–2586. doi: 10.4049/jimmunol.1400833

16. Fallarino F, Grohmann U, Vacca C, Bianchi R, Orabona C, Spreca A, Fioretti MC, Puccetti P. T cell apoptosis by tryptophan catabolism. *Cell Death Differ* (2002) 9:1069–1077. doi: 10.1038/sj.cdd.4401073

17. Fallarino F, Grohmann U, You S, McGrath BC, Cavener DR, Vacca C, Orabona C, Bianchi R, Belladonna ML, Volpi C, et al. The Combined Effects of Tryptophan Starvation and Tryptophan Catabolites Down-Regulate T Cell Receptor ζ-Chain and Induce a Regulatory Phenotype in Naive T Cells. *The Journal of Immunology* (2006) 176:6752–6761. doi: 10.4049/jimmunol.176.11.6752

18. Terness P, Bauer TM, Röse L, Dufter C, Watzlik A, Simon H, Opelz G. Inhibition of allogeneic T cell proliferation by indoleamine 2,3-dioxygenase-expressing dendritic cells: Mediation of suppression by tryptophan metabolites. *Journal of Experimental Medicine* (2002) 196:447–457. doi: 10.1084/jem.20020052

19. Mezrich JD, Fechner JH, Zhang X, Johnson BP, Burlingham WJ, Bradfield CA. An Interaction between Kynurenine and the Aryl Hydrocarbon Receptor Can Generate Regulatory T Cells. *The Journal of Immunology* (2010) 185:3190–3198. doi: 10.4049/jimmunol.0903670

20. Fallarino F, Grohmann U, You S, McGrath BC, Cavener DR, Vacca C, Orabona C, Bianchi R, Belladonna ML, Volpi C, et al. The Combined Effects of Tryptophan Starvation and Tryptophan Catabolites Down-Regulate T Cell Receptor ζ-Chain and Induce a Regulatory Phenotype in Naive T Cells. *The Journal of Immunology* (2006) 176:6752–6761. doi: 10.4049/JIMMUNOL.176.11.6752

21. Matos A, Carvalho M, Bicho M, Ribeiro R. Arginine and arginases modulate metabolism, tumor microenvironment and prostate cancer progression. *Nutrients* (2021) 13: doi: 10.3390/nu13124503

22. Raber PL, Thevenot P, Sierra R, Wyczechowska D, Halle D, Ramirez ME, Ochoa AC, Fletcher M, Velasco C, Wilk A, et al. Subpopulations of myeloid-derived suppressor cells impair T cell responses through independent nitric oxide-related pathways. *Int J Cancer* (2014) 134:2853–2864. doi: 10.1002/ijc.28622

23. Nagaraj S, Gupta K, Pisarev V, Kinarsky L, Sherman S, Kang L, Herber DL, Schneck J, Gabrilovich DI. Altered recognition of antigen is a mechanism of CD8+ T cell tolerance in cancer. *Nature Medicine 2007 13:7* (2007) 13:828–835. doi: 10.1038/nm1609

24. Stiff A, Trikha P, Mundy-Bosse B, McMichael E, Mace TA, Benner B, Kendra K, Campbell A, Gautam S, Abood D, et al. Nitric oxide production by myeloid-derived suppressor cells plays a role in impairing Fc receptor–mediated natural killer cell function. *Clinical Cancer Research* (2018) 24:1891–1904. doi: 10.1158/1078-0432.CCR-17-0691

25. Smith LK, Boukhaled GM, Condotta SA, Mazouz S, Guthmiller JJ, Vijay R, Butler NS, Bruneau J, Shoukry NH, Krawczyk CM, et al. Interleukin-10 Directly Inhibits CD8+ T Cell Function by Enhancing N-Glycan Branching to Decrease Antigen Sensitivity. *Immunity* (2018) 48:299-312.e5. doi: 10.1016/j.immuni.2018.01.006

26. Irina LV, Sosunova E, Nikolaev A, Nenasheva T. Mesenchymal Stem Cells and Myeloid Derived Suppressor Cells: Common Traits in Immune Regulation. *J Immunol Res* (2016) 2016: doi: 10.1155/2016/7121580

27. Huang B, Pan PY, Li Q, Sato AI, Levy DE, Bromberg J, Divino CM, Chen SH. Gr-1+CD115+ immature myeloid suppressor cells mediate the development of tumor-induced T regulatory cells and T-cell anergy in tumor-bearing host. *Cancer Res* (2006) 66:1123–1131. doi: 10.1158/0008-5472.CAN-05-1299

28. Zhu J, Powis De Tenbossche CG, Cané S, Colau D, Van Baren N, Lurquin C, Schmitt-Verhulst AM, Liljeström P, Uyttenhove C, Van Den Eynde BJ. Resistance to cancer immunotherapy mediated by apoptosis of tumor-infiltrating lymphocytes. *Nat Commun* (2017) 8: doi: 10.1038/s41467-017-00784-1

29. Mortezaee K, Majidpoor J, Najafi S. VISTA immune regulatory effects in bypassing cancer immunotherapy: Updated. *Life Sci* (2022) 310:121083. doi: 10.1016/j.lfs.2022.121083

30. Highfill SL, Cui Y, Giles AJ, Smith JP, Zhang H, Morse E, Kaplan RN, Mackall CL. Disruption of CXCR2-mediated MDSC tumor trafficking enhances anti-PD1 efficacy. *Sci Transl Med* (2014) 6: doi: 10.1126/scitranslmed.3007974

31. Russell BL, Sooklal SA, Malindisa ST, Daka LJ, Ntwasa M. The Tumor Microenvironment Factors That Promote Resistance to Immune Checkpoint Blockade Therapy. *Front Oncol* (2021) 11:1–17. doi: 10.3389/fonc.2021.641428

32. Belisario DC, Kopecka J, Pasino M, Akman M, De Smaele E, Donadelli M, Riganti C. Hypoxia Dictates Metabolic Rewiring of Tumors: Implications for Chemoresistance. *Cells* (2020) 9: doi: 10.3390/cells9122598

33. Jian SL, Chen WW, Su YC, Su YW, Chuang TH, Hsu SC, Huang LR. Glycolysis regulates the expansion of myeloid-derived suppressor cells in tumor-bearing hosts through prevention of ROS-mediated apoptosis. *Cell Death Dis* (2017) 8: doi: 10.1038/cddis.2017.192

34. Li W, Tanikawa T, Kryczek I, Xia H, Li G, Wu K, Wei S, Zhao L, Vatan L, Wen B, et al. Aerobic Glycolysis Controls Myeloid-Derived Suppressor Cells and Tumor Immunity via a Specific CEBPB Isoform in Triple-Negative Breast Cancer. *Cell Metab* (2018) 28:87-103.e6. doi: 10.1016/j.cmet.2018.04.022

35. Fu C, Fu Z, Jiang C, Xia C, Zhang Y, Gu X, Zheng K, Zhou D, Tang S, Lyu S, et al. CD205+ polymorphonuclear myeloid-derived suppressor cells suppress antitumor immunity by overexpressing GLUT3. *Cancer Sci* (2021) 112:1011–1025. doi: 10.1111/cas.14783

36. Hossain F, Al-Khami AA, Wyczechowska D, Hernandez C, Zheng L, Reiss K, Del Valle L, Trillo-Tinoco J, Maj T, Zou W, et al. Inhibition of Fatty Acid Oxidation Modulates Immunosuppressive Functions of Myeloid-Derived Suppressor Cells and Enhances Cancer Therapies. *Cancer Immunol Res* (2015) 3:1236–1247. doi: 10.1158/2326-6066.CIR-15-0036

37. Mohammadpour H, MacDonald CR, McCarthy PL, Abrams SI, Repasky EA. β2-adrenergic receptor signaling regulates metabolic pathways critical to myeloid-derived suppressor cell function within the TME. *Cell Rep* (2021) 37: doi: 10.1016/j.celrep.2021.109883

38. Brimnes MK, Vangsted AJ, Knudsen LM, Gimsing P, Gang AO, Johnsen HE, Svane IM. Increased level of both CD4+FOXP3+ Regulatory t Cells and CD14+HLA-DR-/low myeloid-derived suppressor cells and decreased level of dendritic cells in patients with multiple myeloma. *Scand J Immunol* (2010) 72:540–547. doi: 10.1111/j.1365-3083.2010.02463.x

39. Wang Z, Zhang L, Wang H, Xiong S, Li Y, Tao Q, Xiao W, Qin H, Wang Y, Zhai Z. Tumor-induced CD14+HLA-DR−/low myeloid-derived suppressor cells correlate with tumor progression and outcome of therapy in multiple myeloma patients. *Cancer Immunology, Immunotherapy* (2015) 64:389–399. doi: 10.1007/s00262-014-1646-4

40. Perez C, Botta C, Zabaleta A, Puig N, Cedena MT, Goicoechea I, Alameda D, José-Eneriz ES, Merino J, Rodríguez-Otero P, et al. Immunogenomic identification and characterization of granulocytic myeloid-derived suppressor cells in multiple myeloma. *Blood* (2020) 136:199–209. doi: 10.1182/blood.2019004537

41. Ara T, DeClerck YA. Interleukin-6 in bone metastasis and cancer progression. *Eur J Cancer* (2010) 46:1223–1231. doi: 10.1016/j.ejca.2010.02.026

42. Harmer D, Falank C, Reagan MR. Interleukin-6 interweaves the bone marrow microenvironment, bone loss, and multiple myeloma. *Front Endocrinol (Lausanne)* (2019) 10:788. doi: 10.3389/fendo.2018.00788

43. Weber R, Groth C, Lasser S, Arkhypov I, Petrova V, Altevogt P, Utikal J, Umansky V. IL-6 as a major regulator of MDSC activity and possible target for cancer immunotherapy. *Cell Immunol* (2021) 359:104254. doi: 10.1016/j.cellimm.2020.104254

44. de Veirman K, van Ginderachter JA, Lub S, de Beule N, Thielemans K, Bautmans I, Oyajobi BO, de Bruyne E, Menu E, Lemaire M, et al. Multiple myeloma induces Mcl-1 expression and survival of myeloid-derived suppressor cells. *Oncotarget* (2015) 6:10532–10547. doi: 10.18632/oncotarget.3300

45. Lim JY, Kim TW, Ryu D Bin, Park SS, Lee SE, Kim BS, Min CK. Myeloma-secreted galectin-1 potently interacts with CD304 on monocytic myeloid-derived suppressor cells. *Cancer Immunol Res* (2021) 9:503–513. doi: 10.1158/2326-6066.CIR-20-0663

46. Kuwahara-Ota S, Shimura Y, Steinebach C, Isa R, Yamaguchi J, Nishiyama D, Fujibayashi Y, Takimoto-Shimomura T, Mizuno Y, Matsumura-Kimoto Y, et al. Lenalidomide and pomalidomide potently interfere with induction of myeloid-derived suppressor cells in multiple myeloma. *Br J Haematol* (2020) 191:784–795. doi: 10.1111/bjh.16881

47. Lewinsky H, Gunes EG, David K, Radomir L, Kramer MP, Pellegrino B, Perpinial M, Chen J, He TF, Mansour AG, et al. CD84 is a regulator of the immunosuppressive microenvironment in multiple myeloma. *JCI Insight* (2021) 6:141683. doi: 10.1172/jci.insight.141683

48. Wang J, De Veirman K, Faict S, Frassanito MA, Ribatti D, Vacca A, Menu E. Multiple myeloma exosomes establish a favourable bone marrow microenvironment with enhanced angiogenesis and immunosuppression. *Journal of Pathology* (2016) 239:162–173. doi: 10.1002/path.4712

49. Liu Z, Liu H, Li Y, Shao Q, Chen J, Song J, Fu R. Multiple myeloma-derived exosomes inhibit osteoblastic differentiation and improve IL-6 secretion of BMSCs from multiple myeloma. *Journal of Investigative Medicine* (2020) 68:45–51. doi: 10.1136/jim-2019-001010

50. Piddock RE, Marlein CR, Abdul-Aziz A, Shafat MS, Auger MJ, Bowles KM, Rushworth SA. Myeloma-derived macrophage inhibitory factor regulates bone marrow stromal cell-derived IL-6 via c-MYC. *J Hematol Oncol* (2018) 11:66. doi: 10.1186/s13045-018-0614-4

51. Wang J, De Veirman K, De Beule N, Maes K, De Bruyne E, Van Valckenborgh E, Vanderkerken K, Menu E. The bone marrow microenvironment enhances multiple myeloma progression by exosome-mediated activation of myeloid-derived suppressor cells. *Oncotarget* (2015) 6:

52. Giallongo C, Tibullo D, Parrinello NL, La Cava P, Di Rosa M, Bramanti V, Di Raimondo C, Conticello C, Chiarenza A, Palumbo GA, et al. Granulocyte-like myeloid derived suppressor cells (G-MDSC) are increased in multiple myeloma and are driven by dysfunctional mesenchymal stem cells (MSC). *Oncotarget* (2016) 7:85764–85775. doi: 10.18632/oncotarget.7969

53. Xu X, Zhang C, Trotter TN, Gowda PS, Lu Y, Ponnazhagan S, Javed A, Li J, Yang Y. Runx2 deficiency in osteoblasts promotes myeloma progression by altering the bone microenvironment at new bone sites. *Cancer Res* (2020) 80:1036–1048. doi: 10.1158/0008-5472.CAN-19-0284

54. Gavriatopoulou M, Paschou SA, Ntanasis-stathopoulos I, Dimopoulos MA. Metabolic disorders in multiple myeloma. *Int J Mol Sci* (2021) 22: doi: 10.3390/ijms222111430

55. Uckun FM. Overcoming the immunosuppressive tumor microenvironment in multiple myeloma. *Cancers (Basel)* (2021) 13: doi: 10.3390/cancers13092018

56. Castella B, Riganti C, Massaia M. Metabolic approaches to rescue antitumor Vγ9Vδ2 T-cell functions in myeloma. *Frontiers in Bioscience - Landmark* (2020) 25:69–105. doi: 10.2741/4795

57. Zhao JL, Ye YC, Gao CC, Wang L, Ren KX, Jiang R, Hu SJ, Liang SQ, Bai J, Liang JL, et al. Notch-mediated lactate metabolism regulates MDSC development through the Hes1/MCT2/c-Jun axis. *Cell Rep* (2022) 38:110451. doi: 10.1016/j.celrep.2022.110451

58. Favaloro J, Liyadipitiya T, Brown R, Yang S, Suen H, Woodland N, Nassif N, Hart D, Fromm P, Weatherburn C, et al. Myeloid derived suppressor cells are numerically, functionally and phenotypically different in patients with multiple myeloma. *Leuk Lymphoma* (2014) 55:2893–2900. doi: 10.3109/10428194.2014.904511

59. Ğoŕgun GT, Whitehill G, Anderson JL, Hideshima T, Maguire C, Laubach J, Raje N, Munshi NC, Richardson PG, Anderson KC. Tumor-promoting immune-suppressive myeloid-derived suppressor cells in the multiple myeloma microenvironment in humans. *Blood* (2013) 121:2975–2987. doi: 10.1182/blood-2012-08-448548

60. Ai L, Mu S, Sun C, Fan F, Yan H, Qin Y, Cui G, Wang Y, Guo T, Mei H, et al. Myeloid-derived suppressor cells endow stem-like qualities to multiple myeloma cells by inducing piRNA-823 expression and DNMT3B activation. *Mol Cancer* (2019) 18: doi: 10.1186/s12943-019-1011-5

61. De Veirman K, Menu E, Maes K, De Beule N, De Smedt E, Maes A, Vlummens P, Fostier K, Kassambara A, Moreaux J, et al. Myeloid-derived suppressor cells induce multiple myeloma cell survival by activating the AMPK pathway. *Cancer Lett* (2019) 442:233–241. doi: 10.1016/j.canlet.2018.11.002

62. De Veirman K, De Beule N, Maes K, Menu E, De Bruyne E, De Raeve H, Fostier K, Moreaux J, Kassambara A, Hose D, et al. Extracellular S100A9 protein in bone marrow supports multiple myeloma survival by stimulating angiogenesis and cytokine secretion. *Cancer Immunol Res* (2017) 5:839–846. doi: 10.1158/2326-6066.CIR-17-0192

63. Meng L, Tang Q, Zhao J, Wang Z, Wei L, Wei Q, Yin L, Luo S, Song J. S100A9 Derived From Myeloma Associated Myeloid Cells Promotes TNFSF13B/TNFRSF13B-Dependent Proliferation and Survival of Myeloma Cells. *Front Oncol* (2021) 11: doi: 10.3389/fonc.2021.691705

64. Binsfeld M, Muller J, Lamour V, De Veirman K, De Raeve H, Bellahcène A, Van Valckenborgh E, Baron F, Beguin Y, Caers J, et al. Granulocytic myeloid-derived suppressor cells promote angiogenesis in the context of multiple myeloma. *Oncotarget* (2016) 7:37931–37943. doi: 10.18632/oncotarget.9270

65. Grzywa TM, Sosnowska A, Matryba P, Rydzynska Z, Jasinski M, Nowis D, Golab J. Myeloid Cell-Derived Arginase in Cancer Immune Response. *Front Immunol* (2020) 11:938. doi: 10.3389/fimmu.2020.00938

66. van Valckenborgh E, Schouppe E, Movahedi K, de Bruyne E, Menu E, de Baetselier P, VanDerkerken K, van GinDerachter JA. Multiple myeloma induces the immunosuppressive capacity of distinct myeloid-Derived suppressor cell subpopulations in the bone marrow. *Leukemia* (2012) 26:2424–2428. doi: 10.1038/leu.2012.113

67. Hammami I, Chen J, Murschel F, Bronte V, De Crescenzo G, Jolicoeur M. Immunosuppressive activity enhances central carbon metabolism and bioenergetics in myeloid-derived suppressor cells in vitro models. *BMC Cell Biol* (2012) 13:1. doi: 10.1186/1471-2121-13-18

68. Wu W-C, Sun H-W, Chen J, OuYang H-Y, Yu X-J, Chen H-T, Shuang Z-Y, Shi M, Wang Z, Zheng L. Immunosuppressive Immature Myeloid Cell Generation Is Controlled by Glutamine Metabolism in Human Cancer. *Cancer Immunol Res* (2019) 7:1605–1618. doi: 10.1158/2326-6066.CIR-18-0902

69. Malek E, De Lima M, Letterio JJ, Kim B-G, Finke JH, Driscoll JJ, Giralt SA. Myeloid-derived Suppressor Cells: The Green Light for Myeloma Immune Escape. *Blood Rev* (2016) 30:341–348. doi: 10.1016/j.blre.2016.04.002

70. Kuwahara-Ota S, Shimura Y, Steinebach C, Isa R, Yamaguchi J, Nishiyama D, Fujibayashi Y, Takimoto-Shimomura T, Mizuno Y, Matsumura-Kimoto Y, et al. Lenalidomide and pomalidomide potently interfere

with induction of myeloid-derived suppressor cells in multiple myeloma. *Br J Haematol* (2020) 191:784–795. doi: 10.1111/bjh.16881

71. Krejcik J, Casneuf T, Nijhof IS, Verbist B, Bald J, Plesner T, Syed K, Liu K, Van De Donk NWCJ, Weiss BM, et al. Daratumumab depletes CD38+ immune regulatory cells, promotes T-cell expansion, and skews T-cell repertoire in multiple myeloma. *Blood* (2016) 128:384–394. doi: 10.1182/blood-2015-12-687749

72. Horenstein AL, Bracci C, Morandi F, Malavasi F. CD38 in Adenosinergic Pathways and Metabolic Re-programming in Human Multiple Myeloma Cells : In-tandem Insights From Basic Science to Therapy. *Front Immunol* (2019) 10:1–12. doi: 10.3389/fimmu.2019.00760

73. Lee-Chang C, Rashidi A, Miska J, Zhang P, Pituch KC, Hou D, Xiao T, Fischietti M, Kang SJ, Appin CL, et al. Myeloid-derived suppressive cells promote B cell-mediated immunosuppression via transfer of PD-L1 in glioblastoma. *Cancer Immunol Res* (2019) 7:1928–1943. doi: 10.1158/2326-6066.CIR-19-0240

74. Liu M, Wei F, Wang J, Yu W, Shen M, Liu T, Zhang D, Wang Y, Ren X, Sun Q. Myeloid-derived suppressor cells regulate the immunosuppressive functions of PD-1−PD-L1+ Bregs through PD-L1/PI3K/AKT/NF-κB axis in breast cancer. *Cell Death Dis* (2021) 12: doi: 10.1038/s41419-021-03745-1

75. Zhuang J, Zhang J, Lwin ST, Edwards JR, Edwards CM, Mundy GR, Yang X. Osteoclasts in Multiple Myeloma Are Derived from Gr-1+CD11b+Myeloid-Derived Suppressor Cells. *PLoS One* (2012) 7:48871. doi: 10.1371/journal.pone.0048871

76. An G, Acharya C, Feng X, Wen K, Zhong M, Zhang L, Munshi NC, Qiu L, Tai YT, Anderson KC. Osteoclasts promote immune suppressive microenvironment in multiple myeloma: Therapeutic implication. *Blood* (2016) 128:1590–1603. doi: 10.1182/blood-2016-03-707547

77. Fan R, De Beule N, Maes A, De Bruyne E, Menu E, Vanderkerken K, Maes K, Breckpot K, De Veirman K. The prognostic value and therapeutic targeting of myeloid-derived suppressor cells in hematological cancers. *Front Immunol* (2022) 13:1–16. doi: 10.3389/fimmu.2022.1016059

78. Kuwahara-Ota S, Shimura Y, Steinebach C, Isa R, Yamaguchi J, Nishiyama D, Fujibayashi Y, Takimoto-Shimomura T, Mizuno Y, Matsumura-Kimoto Y, et al. Lenalidomide and pomalidomide potently interfere with induction of myeloid-derived suppressor cells in multiple myeloma. *Br J Haematol* (2020) 191:784–795. doi: 10.1111/bjh.16881

79. Romano A, Parrinello NL, La Cava P, Tibullo D, Giallongo C, Camiolo G, Puglisi F, Parisi M, Pirosa MC, Martino E, et al. PMN-MDSC and arginase are increased in myeloma and may contribute to resistance to therapy. *Expert Rev Mol Diagn* (2018) 18:675–683. doi: 10.1080/14737159.2018.1470929

80. Pierceall WE, Amatangelo MD, Bahlis NJ, Siegel DS, Rahman A, van Oekelen O, Neri P, Young M, Chung W, Serbina N, et al. Immunomodulation in pomalidomide, dexamethasone, and daratumumab-treated patients with relapsed/ refractory multiple myeloma. *Clinical Cancer Research* (2020) 26:5895–5902. doi: 10.1158/1078-0432.CCR-20-1781

81. Zhou J, Shen Q, Lin H, Hu L, Li G, Zhang X. Decitabine shows potent anti-myeloma activity by depleting monocytic myeloid-derived suppressor cells in the myeloma microenvironment. *J Cancer Res Clin Oncol* (2019) 145:329–336. doi: 10.1007/s00432-018-2790-6

82. Nakamura K, Kassem S, Cleynen A, Avet-Loiseau H, Martinet L, Smyth Correspondence MJ. Dysregulated IL-18 Is a Key Driver of Immunosuppression and a Possible Therapeutic Target in the Multiple Myeloma Microenvironment. *Cancer Cell* (2018) 33: doi: 10.1016/j.ccell.2018.02.007

83. Castella B, Vitale C, Coscia M, Massaia M. Vγ9Vδ2 T cell-based immunotherapy in hematological malignancies: From bench to bedside. *Cellular and Molecular Life Sciences* (2011) 68:2419–2432. doi: 10.1007/s00018-011-0704-8

84. Ozerova M, Nefedova Y. Estrogen promotes multiple myeloma through enhancing the immunosuppressive activity of MDSC. *Leuk Lymphoma* (2019) 60:1557–1562. doi: 10.1080/10428194.2018.1538511

85. Serafini P, Meckel K, Kelso M, Noonan K, Califano J, Koch W, Dolcetti L, Bronte V, Borrello I. Phosphodiesterase-5 inhibition augments endogenous antitumor immunity by reducing myeloid-derived suppressor cell function. *J Exp Med* (2006) 203:2691. doi: 10.1084/JEM.20061104

86. Noonan KA, Ghosh N, Rudraraju L, Bui M, Borrello I. Targeting immune suppression with PDE5 inhibition in end-stage multiple myeloma. *Cancer Immunol Res* (2014) 2:725–731. doi: 10.1158/2326-6066.CIR-13-0213

87. Cohen YC, Oriol A, Wu KL, Lavi N, Vlummens P, Jackson C, Garvin W, Carson R, Crist W, Fu J, et al. Daratumumab With Cetrelimab, an Anti-PD-1 Monoclonal Antibody, in Relapsed/Refractory Multiple Myeloma. *Clin Lymphoma Myeloma Leuk* (2021) 21:46-54.e4. doi: 10.1016/J.CLML.2020.08.008

88. Wang L, Jia B, Claxton DF, Ehmann WC, Rybka WB, Mineishi S, Naik S, Khawaja MR, Sivik J, Han J, et al. VISTA is highly expressed on MDSCs and mediates an inhibition of T cell response in patients with AML. *Oncoimmunology* (2018) 7: doi: 10.1080/2162402X.2018.1469594

89. Deng J, Li J, Sarde A, Lines JL, Lee YC, Qian DC, Pechenick DA, Manivanh R, Le Mercier I, Lowrey CH, et al. Hypoxia-induced VISTA promotes the suppressive function of myeloid-derived suppressor cells in the tumor microenvironment. *Cancer Immunol Res* (2019) 7:1079–1090. doi: 10.1158/2326-6066.CIR-18-0507

List of publications

Giannotta C, Autino F and Massaia M Vγ9Vδ2 T cells for immunotherapy in blood cancers: ready for prime time?. Front. Immunol. *Under review*

Giannotta C, Autino F and Massaia M (2023) The immune suppressive tumor microenvironment in multiple myeloma: The contribution of myeloid-derived suppressor cells. Front. Immunol. 13:1102471. doi: 10.3389/fimmu.2022.1102471

Giannotta C, Castella B, Tripoli E, Grimaldi D, Avonto I, D'Agostino M, Larocca A, Kopecka J, Grasso M, Riganti C and Massaia M (2022) Immune dysfunctions affecting bone marrow Vγ9Vδ2 T cells in multiple myeloma: Role of immune checkpoints and disease status. Front. Immunol. 13:1073227. doi: 10.3389/fimmu.2022.1073227

Abstract (selected for oral and poster presentations)

C Giannotta, B Castella, E Saraci , G Bertuglia, S Oliva, M D'Agostino, A Larocca, M Massaia. "Immunological profiles of relapsed/refractory MM patients receiving daratumumab-based treatment". International Congress Multiple Myeloma and related malignancies, November 3-5 2022, Bari, Italy

C Giannotta, B Castella, E Tripoli, C Riganti, I C Salaroglio, M D'Agostino, M Massaia. "IMMUNE SUPPRESSION OF BONE MARROW Vγ9Vδ2 T CELLS BY BONE MARROW STROMAL CELLS (BMSC) IN MULTIPLE MYELOMA" Haematologica March 2022 107(s1): S90.

B. Castella, M. D'Agostino, C. Giannotta, S. Oliva, E. Genuardi, M. Gilestro, M. Ruggeri, P. Corradini, B. Ziccheddu, F. Maura, S. Blasi, N. Bolli, A. Larocca, M. Boccadoro, M. Massaia. "MODULATION OF THE IMMUNE MICROENVIROMENT IN MULTIPLE MYELOMA PATIENTS TREATED WITH DARATUMUMABBASED THERAPY: TUMOR CELL-EXTRINSIC EFFECTS OF DARATUMUMAB TREATMENT" Haematologica October 2020 105(s1): S35.

B Castella, C Riganti, M Foglietta, E Tripoli, C Giannotta, M Massaia. "MULTIFACETED IMMUNE CHECKPOINT EXPRESSION AND SENESCENT MARKERS IMPAIRS BONE MARROW Vγ9Vδ2 T-CELL FUNCTION IN MULTIPLE MYELOMA PATIENT". Haematologica October 2018 103: S37-38.

Oral communications at scientific meetings

"International Congress Multiple Myeloma and related malignancies" November 3-5 2022, Bari, Italy

"2nd CUNEO CITYIMMUNOTHERAPY CONFERENCE (CCITC) IMMUNOTHERAPY IN HEMATOLOGICAL MALIGNANCIES" September 29- October 2, 2021, Cuneo, Italy.

"48° CONGRESSO NAZIONALE SIE - 16° CONGRESSO NAZIONALE SIES" October 24-27 2021, Milano, Italy.

Ringraziamenti

Le persone che hanno fatto parte di questo percorso di dottorato hanno contribuito, ognuno a suo modo, alla mia crescita scientifica e personale. Per questo, voglio ringraziarle.

Ringrazio il Prof. Massaia, responsabile di questo progetto di tesi, per avermi dato la possibilità di svolgere questo dottorato e per la fiducia che ripone in me.

Ringrazio le persone la cui collaborazione fortemente arricchisce i nostri progetti di nuove idee ed entusiasmo, grazie alla Prof. Riganti, alla Prof. Ferrarini, al Dott. D'Agostino, al Dott. Bertuglia e al gruppo mielomi dell'ematologia U di Città della Salute di Torino e dell'ematologia di Cuneo, al Dott. Maura e al Dott. Ziccheddu.

Grazie al Prof. Taulli, alle Prof. Cappello e Prof. Voena e ai compagni di sventure del Cerms, per esser diventati mia nuova famiglia scientifica. A Fra, con cui ho condiviso ogni momento di questo dottorato, per rendere il Cerms un posto migliore, a Giulietta e Mavi, ad ogni caffè con Silvia, a Federica. Perché la felicità è doppia se condivisa ma anche il peso delle brutte giornate si è dimezzato con voi accanto.

Grazie a Vale, per essere mia amica prima di tutto, poi fidata compagna di facs, per tutte le volte di FL4 non visto, di eventi non acquisiti, di fluo improvvisamente senza colori e di file cancellati e mai più trovati, per tutti i prime e i clean insieme, per la disperazione condivisa, grazie per il confronto costante e il sostegno mai mancato. Grazie alla dolce Reb.

Ad Ezio, per aver riempito le mie settimane di solitudine con il suo grande affetto. Grazie per esserci stato sempre, per avermi aiutata a ritrovare nuovi equilibri. Grazie per avermi a volte tirato fuori, a volte arginato, per avermi a volte protetta, a volte spinta avanti, per volere il mio bene sempre.

A Barbara, perché nulla di tutto ciò sarebbe stato possibile senza. Grazie per essere stata stazione di partenza del mio percorso scientifico, per essere stata la mia guida e un punto fermo nonostante tutto intorno sia cambiato. Grazie per tutto ciò che mi ha trasmesso, per i momenti in lab e poi per quando il lab è diventato una chat su whatsapp, il viaggio Cuneo-Bandito o il bar del Carle. E grazie per essere anche altro, oltre che lab.

E poi grazie alla mia famiglia e al mio Gigi, il mio mago di Excel, per tutto il tempo, l'aiuto e la pazienza dedicati alle mie analisi. E soprattutto, grazie perché in questo viaggio tortuoso mi ha sempre tenuta per mano.